

---

**Misfolded proteins affect synaptic  
plasticity and network activity  
studies in mouse models of  
neurodegenerative diseases**

Sonja Blumenstock

---



München 2017



---

**Misfolded proteins affect synaptic  
plasticity and network activity  
studies in mouse models of  
neurodegenerative diseases**

**Sonja Blumenstock**

---

Dissertation

zur Erlangung des naturwissenschaftlichen Doktorgrades

an der Fakultät für Biologie

der Ludwig-Maximilians-Universität

München

vorgelegt von

Sonja Blumenstock

aus Fürth (Bay)

München, den 06.04.2017

Diese Dissertation wurde unter der Leitung von Prof. Dr. Jochen Herms am Lehrstuhl für Translationale Hirnforschung der Ludwig-Maximilians-Universität angefertigt und von Prof. Dr. Barbara Conradt an der Fakultät für Biologie vertreten.

### **Eidesstattliche Erklärung**

Ich versichere hiermit an Eides statt, dass die vorgelegte Dissertation von mir selbständig und ohne unerlaubte Hilfe angefertigt ist.

Hiermit erkläre ich, dass die Dissertation nicht ganz oder in wesentlichen Teilen einer anderen Prüfungskommission vorgelegt worden ist und ich mich anderweitig einer Doktorprüfung ohne Erfolg nicht unterzogen habe.

München, den 06.04.2017

Sonja Blumenstock

Erstgutachter:	Prof. Dr. Barbara Conradt
Zweitgutachter:	Prof. Dr. Anja Horn-Bochtler
Tag der mündlichen Prüfung:	18.10.2017

# Contents

Abbreviations	vii
List of publications	xi
Declaration	xiii
Summary	xix
<b>1 Introduction</b>	<b>1</b>
1.1 Neurodegenerative diseases . . . . .	2
1.2 Parkinson’s Disease as the most common synucleinopathy . . . . .	3
1.2.1 The alpha-synuclein protein . . . . .	7
1.3 Tauopathies by the example of Alzheimer’s Disease . . . . .	9
1.3.1 The tau protein . . . . .	11
1.4 Misfolded proteins in neurodegenerative diseases . . . . .	12
1.4.1 Contributors for the misfolding of proteins . . . . .	14
1.4.2 Cell-to-cell propagation and spreading of misfolded proteins	16
1.5 The glutamatergic synapse . . . . .	17
1.5.1 The presynapse . . . . .	18
1.5.2 The postsynapse and structural plasticity . . . . .	18
1.6 <i>In vivo</i> two-photon imaging . . . . .	21
1.6.1 Alpha-synucleinopathy and Tauopathy mouse models . . . . .	25
<b>2 Results</b>	<b>29</b>
2.1 Seeding and transgenic overexpression of alpha-synuclein triggers dendritic spine pathology in the neocortex [1] . . . . .	29

## Table of Contents

---

2.2	Impaired plasticity of cortical dendritic spines in P301S tau transgenic mice [2] . . . . .	55
2.3	<i>In vivo</i> imaging reveals reduced activity of neuronal circuits in the mouse tauopathy model. . . . .	67
<b>3</b>	<b>Discussion</b>	<b>83</b>
3.1	<i>In vivo</i> two-photon imaging in the neocortex of the mouse . . . . .	84
3.2	Seeding of pathogenic proteins . . . . .	86
3.2.1	alpha-synuclein . . . . .	86
3.2.2	Tau . . . . .	87
3.2.3	Mechanistic considerations and potential pitfalls of experimental seeding . . . . .	89
3.3	Dendritic spines in mouse models of alpha-synucleinopathy and tauopathy . . . . .	90
3.3.1	Transgenic overexpression of alpha-synuclein and mutant tau causes changes in dendritic spine plasticity . . . . .	92
3.3.2	Abnormal spine density, morphology and dendritic shape after alpha-synuclein seeding . . . . .	93
3.3.3	Proposed mechanisms for alpha-synuclein and tau-mediated spine alterations . . . . .	94
3.4	Network alterations due to aberrant expression of tau . . . . .	96
3.5	In search for toxic protein species . . . . .	97
	<b>Acknowledgements</b>	<b>119</b>

# Abbreviations

°C	degree celcius
µg	microgram
µl	microliter
µm	micrometer
α(β/γ)-syn	alpha (beta/gamma)-synuclein
A30P	point mutation in α-synuclein
A53T	point mutation in α-synuclein
Aβ	amyloid beta
AAV	adeno-associated virus
AD	Alzheimer's disease
ADAM10	a disintegrin and metalloproteinase domain-containing protein 10
ALS	amyloid lateral sclerosis
AMPA	α-amino-3-hydroxy-5-methyl-4-isoxazolepropionic acid
ANOVA	analysis of variance
AOM	acousto optical modulator
A/P	anterior/posterior
APP	amyloid precursor protein
AT8/100/180	antibodies recognizing phosphorylated tau
Az.	<i>Aktenzeichen</i>
BACE1	beta-secretase 1
BAPTA	1,2-bis( <i>o</i> -aminophenoxy)ethane-N,N,N',N'-tetraacetic acid
BSA	bovine serum albumin
C57BL/6J	wild-type mouse line
Ca <sup>2+</sup>	calcium ion
CA3	subfield of the hippocampus
CLSM	confocal laser scanning microscope
CNS	central nervous system
co	coeruleus-subcoeruleus complex
CSPα	cystein string protein α
3D	three-dimensional
D1/D2	dopamine receptor type 1/2

## Abbreviations

---

DLB	dementia with Lewy bodies
dm	dorsal motor nucleus of the glossopharyngeal and vagal nerves
dpi	days post-injection
D/V	dorsal/ventral
E46K	point mutation in $\alpha$ -synuclein
e.g.	lat. <i>exempli gratia</i> ; for example
eGFP	enhanced green fluorescent protein
ER	endoplasmic reticulum
et al.	and others
F	fluorescence
FACS	fluorescent activated cell sorting
FAD	familial Alzheimer's disease
FASS	fluorescence activated synaptosome sorting
fc	first order sensory association areas, premotor areas, primary sensory and motor fields
Fig.	Figure
FRET	Förster resonance energy transfer
fs	femtosecond
FSB	(trans,trans)-1-fluoro-2,5-bis(3-hydroxycarbonyl-4-hydroxy) styrylbenzene
FTDP-17	Frontotemporal dementia with parkinsonism-17
FUS	fused in sarcoma
g	gram
G51D	point mutation in $\alpha$ -synuclein
GABA	gamma amino butyric acid
GC	genome copies
GCaMP	GFP-based $\text{Ca}^{2+}$ probe
GECI	genetically encoded calcium indicator
GFP	green fluorescent protein
GP(i/e)	globus pallidus (interna / externa)
h	hour
hc	high order sensory association areas and prefrontal fields
<i>HD</i>	Huntington's disease (gene)
H50Q	point mutation in $\alpha$ -synuclein
h- $\alpha$ -syn	human alpha-synuclein
Hsc70	heat shock protein 70
HT7	antibody recognizing human tau
Hz	Hertz
Iba1	ionized calcium-binding adapter molecule 1
i.e.	lat. <i>id est</i> ; that is
i.p.	intraperitoneal
IPTG	isopropyl $\beta$ -D-1-thiogalactopyranoside
kDa	kilodalton



---

kg	kilogramm
KI	knock in
KO	knock out
kW	kilowatts
L	lateral
lat.	latin for
LB	Lewy body
LN	Lewy neurite
LSM	laser scanning microscope
LTD	long-term depression
LTP	long-term potentiation
M	molar
<i>MAPT</i>	microtubule associated protein tau (gene)
mc	anteromedial temporal mesocortex
mg	milligram
MHz	megahertz
min	minute
ml	milliliter
mm	millimeter
mM	millimolar
mo	month
MPTP	1-methyl-4-phenyl-1,2,3,6-tetrahydropyridine
MSA	multiple system atrophy
MT	microtubule
Munc18-1/13-1	mammalian uncoordinated-18/13
MW	molecular weight
N	number
NA	numerical aperture
NAC	non-amyloid component
NaCl	sodium chloride
NAD(P)H	nicotinamide adenine dinucleotide (phosphate)
NaHCO <sub>3</sub>	sodium bicarbonate
NFL	neurofilament light chain
NFT	neurofibrillary tangle
NGS	normal goat serum
nl	nanoliter
nm	nanometer
NMDA	N-methyl-D-aspartate
NSF	N-ethylmaleimide sensitive factor
6-OHDA	6-hydroxydopamine
P	p-value
P301S	point mutation in tau
PBS	phosphate buffered saline

## Abbreviations

---

PCR	polymerase chain reaction
PD	Parkinson's disease
PDGF $\beta$	platelet derived growth factor beta
PFA	paraformaldehyde
PFFs	preformed fibrils
PMT	photomultiplier
<i>PRNP</i>	prion protein (gene)
PRP <sup>SC</sup>	abnormal isoform of prion protein (scrapie)
PS 1/2, <i>PSEN</i>	presenilin (1/2, catalytic domain of $\gamma$ -secretase)
PSD	postsynaptic density
ROI	region of interest
rpm	revolutions per minute
s	second
S129	serine 129
SD	standard deviation
SDS	sodium dodecyl sulfate
SEM	standard error of the mean
SGT	small glutamine-rich protein
SNAP	soluble NSF adaptor protein
SNAP-25	synaptosomal associated protein of 25 kDa
SNARE	SNAP receptor
<i>SNCA</i>	alpha-synuclein (gene)
sn	substantia nigra
SNpc	substantia nigra pars compacta
SNpr	substantia nigra pars reticulata
SOD	superoxide dismutase
STN	subthalamic nucleus
t	time
Tab.	Table
<i>TARDBP</i>	TAR DNA-binding protein (gene)
TDP-43	TAR DNA-binding protein 43
Ti:Sa	lasing medium; sapphire crystal, doped with titanium ions
tg	transgene
Thy1	thymocyte antigen 1; CD90
ThS/T	Thioflavine S/T
TOR	turnover ratio
VGLUT1	vesicular glutamate transporter 1
VTA	ventral tegmental area
W	watt
WT	wild type
XFP	X (colour variable) fluorescent protein
YFP	yellow fluorescent protein

# List of publications

**Blumenstock S**, Rodrigues EF, Peters F, Blazquez L, Schmidt F, Giese A and Herms J. "Seeding and transgenic overexpression of alpha-synuclein triggers dendritic spine pathology in the neocortex." *EMBO Mol. Med.* in press

Hoffmann NA, Dorostkar MM, **Blumenstock S**, Goedert M and Herms J. "Impaired plasticity of cortical dendritic spines in P301S tau transgenic mice." *Acta Neuropathol Commun.* 2013 Dec 17;1:82.

Vonhoff F, Kuehn C, **Blumenstock S**, Sanyal S and Duch C. "Temporal coherency between receptor expression, neural activity and AP-1-dependent transcription regulates Drosophila motoneuron dendrite development." *Development* 2013 Feb 1;140(3):606-16.

## Manuscripts in preparation

Marinković P, **Blumenstock S**, Goldstein P, Korzhova V, Knebl A, Peters F, Stancu IC, Dewachter I and Herms J. *In vivo* imaging reveals reduced activity of neuronal circuits in the mouse tauopathy model.

**Blumenstock S**, Angelo MF, Peters F, Crux S, Herzog E and Herms J Local synaptic translation is reduced in tissue overexpressing alpha-synuclein.

**Blumenstock S**, Marinković P, Goldstein P, Korzhova V, Peters F, Sun F, Sgobio C and Herms J. *In vivo* imaging reveals increased activity of neuronal circuits following synuclein seeding in wild-type mice.

## Scientific talks

**Blumenstock S**, Rodrigues EF, Blazquez L, Schmidt F, Giese A and Herms J. "Seeding and transgenic overexpression of alpha-synuclein triggers dendritic spine pathology in the neocortex." SfN annual meeting, 2016, San Diego, USA.

## Scientific poster presentations

**Blumenstock S**, Rodrigues EF and Herms J. "Long-term *in vivo* imaging of dendritic spine dynamics in a mouse model of Parkinson's disease" Alzheimer's & Parkinson's Diseases Congress - AD/PD<sup>TM</sup>, 2015, Nice, France.

**Blumenstock S**, Rodrigues EF and Herms J. "Long-term *in vivo* imaging of dendritic spine dynamics in a mouse model of Parkinson's disease" Neurowoche München, 2014, Munich, Germany.

# Declaration

All work included in this thesis was performed at the Ludwig-Maximilians-Universität under the supervision of Prof. Dr. Jochen Herms.

For the publication by Hoffmann et al., co-author Sonja Blumenstock provided technical support, which included immunohistochemistry and confocal microscopy, as used in figures 3 and 4 of the publication. She also performed all experimental procedures for the revision of the manuscript, which further included quantitative biochemical methods such as protein detection in synaptosomal and PSD fractions.

For the manuscript by Marinković et al., co-author Sonja Blumenstock performed experiments including the seeding of tau, immunohistochemistry, confocal microscopy as well as window implantation and training of experimental animals for *in vivo* two-photon imaging. She further contributed to manuscript writing and manuscript assembly.

I confirm that these statements about the contribution of Sonja Blumenstock as co-author are accurate.

Munich, 6. April 2017

Prof. Dr. Jochen Herms

---

# List of Figures

1.1	The Parkinson's Disease brain . . . . .	6
1.2	Structure of $\alpha$ -synuclein . . . . .	7
1.3	The Alzheimer's Disease brain . . . . .	10
1.4	Structure of tau . . . . .	12
1.5	Misfolded proteins in neurodegenerative diseases . . . . .	13
1.6	The glutamatergic synapse . . . . .	20
1.7	Principles of one- and two-photon microscopy . . . . .	23
2.1	[1] Fig 1. $\alpha$ -Synuclein overexpression alters spine density and dynamics <i>in vivo</i> . . . . .	32
2.2	[1] Fig 2. $\alpha$ -Synuclein overexpression alters spine density, dynamics, and morphology differently depending on age. . . . .	33
2.3	[1] Fig 3. Injection of PFFs into the dorsal striatum triggers cortical $\alpha$ -synuclein aggregation. . . . .	35
2.4	[1] Fig 4. The presence of accumulated $\alpha$ -synuclein induced by seeding 5 months prior to analysis causes spine loss and malformation in layer V apical dendrites. . . . .	37
2.5	[1] Fig 5. Cortical $\alpha$ -synuclein accumulation and long-term <i>in vivo</i> imaging of PDGF-h- $\alpha$ -syn GFP-M mice. . . . .	39
2.6	[1] Fig S1. Spine morphology changes in $\alpha$ -syn transgenic mice. . . . .	49
2.7	[1] Fig S2. Distribution of phosphorylated $\alpha$ -syn aggregates in the mouse brain. . . . .	50
2.8	[1] Fig S3. Templated misfolding of $\alpha$ -synuclein. . . . .	51
2.9	[1] Fig S4. Presence of microglia in the neocortex. . . . .	52
2.10	[1] Fig S5. Spine morphology changes in PFF-seeded mice (5 mo post-injection). . . . .	53
2.11	[1] Fig S6. Presynaptic glutamatergic bouton density does not differ in seeded or transgenic mice. . . . .	54

## List of Figures

---

2.12 [2] Fig 1. Decreased dendritic spine density and impaired spine kinetics in P301S Tau mice. . . . .	58
2.13 [2] Fig 2. Tau transgene expression affects dendritic spine morphology. . . . .	61
2.14 [2] Fig 3. YFP-expressing layer V neurons are free of hyperphosphorylated tau. . . . .	61
2.15 [2] Fig 4. Failure to detect tau in cortical dendritic spines by means of immunohistochemistry. . . . .	63
2.16 Seeding of Tau PFFs causes local formation of NFTs. . . . .	74
2.17 Chronic two-photon calcium imaging in the tauopathy model. . .	75
2.18 Recording of neuronal activity in awake mice. . . . .	77
2.19 Neuronal activity is reduced in P301S mice independently of NFT presence . . . . .	78



# List of Tables

1.1	Neurodegenerative diseases grouped by the deposition of aggregated proteins . . . . .	3
2.1	[1] Appendix Table S1. Antibodies used in this study . . . . .	48

## List of Tables

---

# Summary

Neurodegenerative diseases are common causes of dementia, which is defined as a general decline in mental abilities severe enough to interfere with daily life. The most common form of dementia is Alzheimer's disease (AD), the most common neurodegenerative movement disorder – also frequently accompanied by dementia – is Parkinson's disease (PD). Being age-related, progressive and up to date incurable disorders, the global rise in life expectancy entails a strong rise in case numbers, bringing along an enormous economical and emotional burden for patients, their families and health systems.

On a molecular level, the cause for AD, PD and other neurodegenerative diseases is reflected in the misfolding and aggregation of certain usually monomeric proteins of the brain. Two examples of such proteins, described in detail in this work are  $\alpha$ -synuclein, a small presynaptic protein and tau, a group of proteins involved in cytoskeleton dynamics. Several extrinsic and intrinsic factors can contribute to the conformational templating of these proteins, leading to progressive aggregation, inflammatory reactions, cellular transport deficits, synaptic dysfunction and ultimately to cell death, the structural basis of symptoms in neurodegenerative diseases.

Apart from transgenic mouse models, which have been used widely for the study of neurodegeneration, a recent development involves the injection of pathogenic protein aggregates directly into (brain) tissue, termed seeding and triggers the molecular cascade of conformational templating and progressive protein aggregation.

In the present work, two publications and one unpublished manuscript are included which investigate the role of the pathogenic proteins  $\alpha$ -synuclein and tau in the light of structural brain plasticity and network function. The primary method used was *in vivo* two-photon microscopy that enabled the chronic follow-up of small neuronal structures like dendritic spines or the activity of single neurons in the brain network over prolonged periods of time in living mice.

The recently published study by Blumenstock et al. investigated the effects of  $\alpha$ -syn overexpression and  $\alpha$ -syn seeding on dendritic spines, which are small protrusions from neuronal dendrites corresponding to the postsynaptic compartment of glutamatergic synapses. Chronic *in vivo* two-photon microscopy and *ex vivo* confocal laser scanning microscopy was performed in mice expressing transgenic eGFP in a subset of neurons of the neocortex. In one part of the study, dendritic spines on apical dendrites of the somatosensory cortex were analyzed *in vivo* in mice overexpressing human  $\alpha$ -synuclein. Compared to controls, these mice showed reduced spine density, altered spine morphology and changes in spine dynamics in an age-dependent manner. After progressive spine loss due to a decreased fraction of gained spines in young mice, older mice showed no further net spine loss over time at an overall reduced spine density compared to mice expressing endogenous levels of  $\alpha$ -syn. Spine morphology was found to be changed accordingly. Another part of this study investigated for the first time the impact of  $\alpha$ -syn seeding on dendritic structures. The histochemical properties of  $\alpha$ -syn inclusions developing predominantly in layer IV of the cortex after seeding were found to resemble Lewy inclusions, as they were phosphorylated, ubiquitinated and amyloid. Five months after intracerebral inoculation with preformed fibrils, spine density was reduced on layer V apical dendrites of the somatosensory cortex and spine morphology was changed towards relatively less thin spines. Apical tuft dendrites were furthermore found to develop dystrophic swellings following  $\alpha$ -syn seeding. Summarized, these results provide new insights about the dynamic changes in synaptic plasticity linked to the pathologic accumulation of  $\alpha$ -synuclein.

The study published by Hoffmann et al. investigated the impact of the tau protein, which is implicated in several neurodegenerative tauopathies, including Alzheimer's disease and frontotemporal dementia (FTD). Mice overexpressing human tau carrying the FTDP-17-linked mutation P301S were subjected to chronic *in vivo* microscopy. The experiments revealed a reduced spine density compared to controls, which was due to a decrease in the formation of new spines. Spines showed morphological changes like an increased spine head volume, which could represent a compensatory mechanism for spine loss to strengthen the remaining synaptic contacts. Moreover, the absence of detectable amounts of tau

in dendritic spines indicate that axonal pathology and local network dysfunction might cause spine impairments.

In the study by Marinković et al., the functional consequences of different species of tau protein were investigated. As the exact nature of tau species causing neuronal malfunction and degeneration are still not known, tau seeding was used to induce the formation of neurofibrillary tangles in a portion of cortical neurons of P301S mice that normally don't show prominent fibrillary tau aggregation. By using chronic *in vivo* two photon microscopy, network activity was measured in transgenic P301S mice with and without neurofibrillary tangles formed after seeding. This approach also enabled intrinsically comparing the activity of tangle-bearing neurons with the activity of their tangle-free neighbors. It was shown that P301S cortical neurons are less active than WT neurons and that this effect is independent of NFT presence.

In conclusion, the studies combined in this thesis provide new insights into toxic role of misfolded, hyperphosphorylated and aggregated protein species that are linked to the progression of neurodegenerative diseases. Dendritic spine loss was demonstrated in two mouse models expressing high levels of soluble  $\alpha$ -syn or Lewy Body-like structures. Both studies on tau indicate that soluble oligomeric species of tau are most likely linked to the malfunction and structural degeneration of neurons. The chronic studies on synaptic plasticity furthermore add important knowledge on synapse dynamics in  $\alpha$ -synuclein and tau related disorders, as they provide a link to the pathophysiology underlying dementia.



# Introduction

### 1.1 Neurodegenerative diseases

Speaking in terms of global health, mankind in the 21. century has benefited from growing wealth, improved hygiene and advanced medical care, all of which contributes to population growth and the rise in life expectancy — especially in developing countries [3]. On the other hand stands a considerable increase in cases of neurodegenerative diseases like Alzheimer’s Disease (AD) and Parkinson’s Disease (PD), for which advanced age is the major risk factor. Pathological changes of the nervous system lead to a certain dissociation of body and mind in form of motor and mental impairments and present great personal hardship for affected individuals and their families. Medical treatment is frequently hampered by the lack of a correct diagnosis and even if such exists, only symptomatic treatments are available on the market up to date. In order to regulate the enormous financial, societal and emotional burden of these brain disorders, the thorough scientific understanding of neurodegenerative diseases is of utmost importance for the development of preventive measures and curative therapies.

Neurodegenerative diseases are commonly sporadic and, less frequently, genetic pathological events which can affect a population of neuronal cells or the entire central nervous system (CNS). The slow progressive loss of neuronal function ranges from initial synaptic dysfunction to extensive neuron death with resulting brain atrophy and the according implications for the patient. This heterogeneous group of disorders can be roughly categorized according to their symptoms into dementias and movement disorders or alternatively according to their molecular biology into proteinopathies like  $\alpha$ -synucleinopathies, tauopathies,  $A\beta$  proteinopathies, polyglutamine repeat diseases, TDP-43 proteinopathies, and prion diseases, as outlined in Table 1.1 (adapted from [4]).



## 1.2 Parkinson's Disease as the most common synucleinopathy

Toxic protein	Protein deposit	Familial disease	Linked gene	Sporadic disease	Genetic risk factor
$\alpha$ -synuclein	Lewy bodies	Familial PD	<i>SNCA</i>	PD	<i>SNCA</i> polymorphism
	Lewy neurites			DLB	<i>MAPT</i> haplotype
	Glial cytoplasmic inclusions	Not identified	Not applicable	MSA	Not identified
Tau	Neuronal and glial inclusions	FTDP-17	<i>MAPT</i>	AD and tauopathies	<i>MAPT</i> haplotype
$\beta$ -amyloid ( $A\beta$ )	Senile plaques	Familial AD	<i>APP</i> <i>PS1</i> <i>PS2</i>	AD	<i>ApoE4</i>
Polyglutamine repeat expansion	Nuclear and cytoplasmic inclusions	Huntington's Disease	<i>HD</i>	Not applicable	Not identified
TDP-43	TDP-43 inclusions	Autosomal dominant	<i>TARDBP</i>	Sporadic	Not identified
SOD	Hyaline inclusions		<i>SOD1</i>	ALS	
FUS	FUS inclusions	familial ALS	<i>FUS</i>		
PrP <sup>SC</sup>	Protease-resistant PrP <sup>e</sup>	Familial prion protein disease	<i>PRNP</i>	Sporadic prion protein disease	<i>PRNP</i> polymorphism

**Table 1.1. Neurodegenerative diseases grouped by the deposition of aggregated proteins**

## 1.2 Parkinson's Disease as the most common synucleinopathy

200 years after James Parkinson's essay on the shaking palsy [5], which was the initial formal description of the disorder now bearing his name, Parkinson's Disease (PD) has received an enormous and increasing amount of attention. Together with dementia with Lewy Bodies (DLB) and multiple system atrophy (MSA), these diseases are classified as synucleinopathies. Today, PD is the second most common neurodegenerative disorder [6] after Alzheimer's disease, affecting over 1.5% of the world population over 65 years of age (reviewed by [7]). The predominant sporadic form of PD also called idiopathic PD usually commences at an age between 50 and 60 years and is foreshadowed by a considerable preclinical period, estimated to last 5 up to 20 years before the first onset of motor symptoms [8, 9, 10]. In contrast, the rarer genetic forms of PD make up 2-3% of the late-onset cases and about 50% of the early-onset cases (reviewed

## 1. Introduction

---

by [11, 12]).

In his essay based on the study of six cases, James Parkinson described the major motor symptoms characterizing this disease [5], including rest tremor, slowness of movement (bradykinesia), rigidity, postural and gait impairment, festination, falls, soft speech, dysphagia and saliva trickling from the mouth. As motor networks are not the only parts of the brain affected by the progressive neurodegeneration, there is a great spectrum of non-motor symptoms [13] as well, including sleep disturbances [14], olfactory dysfunction [15], psychiatric disorders [16] and digestive disturbances [17]. Cognitive dysfunction is also a very common occurrence, its severity ranging from mild cognitive impairment to dementia. In fact, dementia is a frequent symptom in the terminal stages of PD [18]. One of the largest prospectively followed PD autopsy series found that 80% of patients with PD develop dementia after 20 years [19].

After Parkinsons initial description, it took 150 years until the underlying biochemical changes in the brain – the loss of striatal and nigral dopamine – were identified [20, 21] and the first effective treatment, i.e. the introduction of high-dosage levodopa, was developed [22]. The cellular basis of the dopamine neurotransmitter deficiency was determined to be the loss of neurons in the basal ganglia and more precisely, in the substantia nigra pars compacta (SNpc) [23, 24] (Figure 1.1 A). Apart from SNpc neuron loss, the gold standard for the *post mortem* diagnosis of many synucleinopathies is the presence of dense proteinaceous aggregates called Lewy bodies. They consist of abnormal accumulations of the protein alpha-synuclein ( $\alpha$ -syn), neurofilament, ubiquitin and other proteins and form round cytoplasmic inclusions (Lewy bodies, LBs) and elongated neuritic inclusions (Lewy neurites, LNs) [25, 26] (Figure 1.1 B-D). The ultrastructure of these intracellular accumulations with a dense eosinophilic center and a pale halo was described as early as 1865 by Duffy and Tennyson; the connection to PD, however, originates from the German neurophatologist Friedrich Lewy [27]. LBs display a dense network of fibrillary, amyloid polymers with a typical  $\beta$ -sheet protein structure, which can be stained specifically with congo red derivatives and Thioflavin S and are resistant against proteinaceous digestion [28, 29]. Additionally, pale bodies are considered precursors of LBs and represent another neuropathological hallmark in PD brains. They are pallid cy-

toplasmic inclusions with a less eosinophilic structure than LBs and are without a halo [30].

Dopaminergic neuron loss has functional consequences on two efferent networks which control the fine tuning of motor function (see Figure 1.1 E, reviewed by [31]) and this gives rise to the motor symptoms: (1) the direct pathway via the internal globus pallidus, facilitating movement and (2) the indirect pathway via the external globus pallidus and the subthalamic nucleus, which repress motor action. Dopamine release in a healthy individual increases the contribution of the direct over the indirect pathway, thereby facilitating movement. The balance between the two efferences was thought to be controlled through feedback from the SNpc and the ventral tegmental area to the striatum via differential expression of dopaminergic receptors of the D1 or the D2 type. The degeneration of dopaminergic neurons in the SNpc leads to a superfluous inhibitory contribution of the basal ganglia to the thalamus, which in turn causes a diminished thalamic activation of neocortical motor neurons. Their reduced activity finally results in the attenuated motoric abilities (hypokinesia) [32]. The precise reasons for the increased vulnerability and selective loss of dopaminergic neurons are not entirely clear, but there is reason to believe that oxidative stress and toxic protein aggregation are mechanisms that lead to neuronal damage and, ultimately, neuronal death [33, 34, 35].

Based on the topographical extent of lesions in the brains from PD patients, the course of pathology can be traced and categorized into six stages according to Braak et al. and is illustrated in Figure 1.1 F. The stages describe the histological state of the brain from incidental to symptomatic PD. Lesions initially occur in the brainstem, the anterior olfactory nucleus and in the enteric nervous system, during the pre-symptomatic phase of the disease. The spread of pathology gradually follows an ascending course to the midbrain in stage 3 where it gives rise to the prominent motor phenotype and later involves associative cortical regions [38]. In the recent years, evidence has pointed out that the presence of LBs might likely just be the tip of the iceberg rather than the cause of neurodegeneration. In fact, Kramer and Schulz-Schäffer showed that presynaptic  $\alpha$ -syn oligomers and micro-aggregates might be responsible for neurodegeneration as well as for synapse loss observed in post-mortem DLB brains rather than LBs,

## 1. Introduction

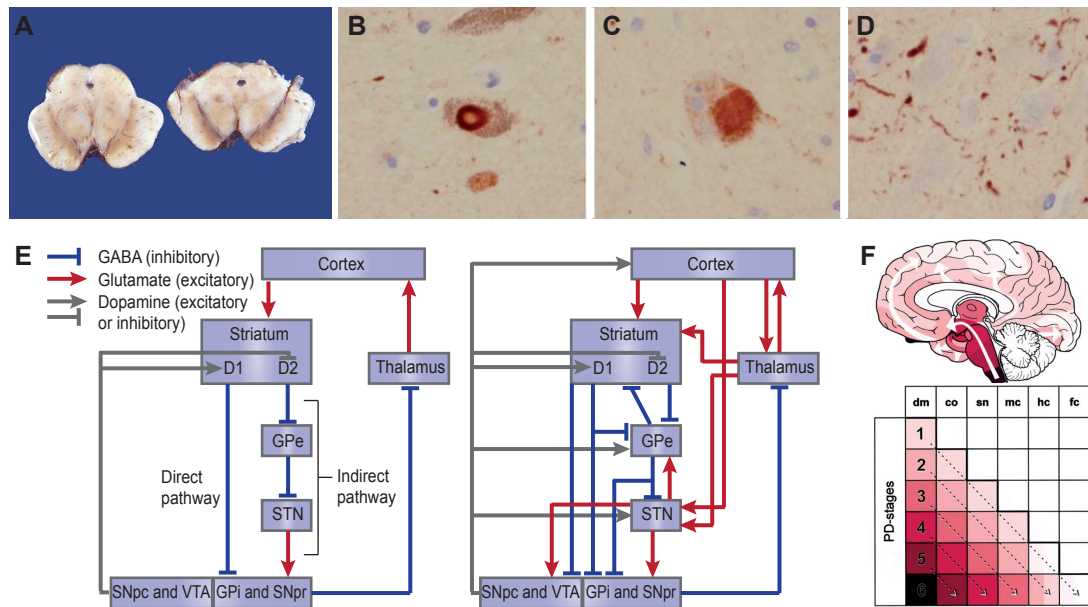


**Figure 1.1. The Parkinson's Disease brain.** **A.** The midbrain from a PD patient (left) shows depigmentation due to the loss of melanin-containing neurons in the substantia nigra pars compacta compared to a healthy control (right) [36]. **B-D.** The typical microscopic pathology in PD brains contains Lewy Bodies (B), pale bodies (C) and Lewy neurites (D) [37]. **E.** Left: The input from two efferent pathways determines the output of the basal ganglia and the fine-tuning of movement. Right: Recent anatomical studies have drawn a more complex picture of connections in the midbrain, which complicates the prediction of how the transformation of inputs generates outputs. GPe/i, globus pallidus externa/interna; SNpc/r, substantia nigra pars compacta/reticulata; STN, subthalamic nucleus (adapted from [31]). **F.** The staging of Parkinson's Disease according to Braak [38]. dm, dorsal motor nucleus of the glossopharyngeal and vagal nerves; co, coeruleus-subcoeruleus complex; sn, substantia nigra; mc, anteromedial temporal mesocortex; hc, high order sensory association areas and prefrontal fields; fc, first order sensory association areas, premotor areas, primary sensory and motor fields.

which might represent a protective mechanism to sequester smaller and more toxic  $\alpha$ -syn aggregates [39].

With the latest addition from 2016 [40], 23 so-called PARK loci have been identified that have been shown to be related to genetically linked parkinsonism. Mutations and deletions in these genes can lead to dysfunctions of synapses, mitochondria, intracellular signal cascades or lysosomal or proteasomal degradation mechanisms, thereby paving the way for synaptic and neuronal degeneration (reviewed by [41]).

### 1.2.1 The alpha-synuclein protein

The *SNCA* gene encodes for the 140 amino acid alpha-synuclein ( $\alpha$ -syn) protein, which is highly conserved in the central nervous system. Along with its discovery in the pacific electric ray (*Torpedo californica*) [42],  $\alpha$ -synuclein was named after its presence at both the *synapse* and *nucleus* [43, 44].

The protein sequence of  $\alpha$ -syn can be divided into three overlapping regions: (1) the N-terminal region (aa 1 – 95) comprises seven imperfect 11 amino acid repeats (XKTKEGVXXXX) which can form an amphiphatic alpha-helix for membrane interaction, (2) the central hydrophobic NAC domain (non-amyloid beta component of AD amyloid plaques, aa 61 – 95) which confers the beta-sheet potential and (3) the acidic and amphiphatic C-terminal region (aa 96 – 140) with an unfolded conformation (reviewed by [45, 46]). The  $\alpha$ -syn protein sequence subdivision is illustrated in Figure 1.2. Among the three identified members of the synuclein family (alpha, beta and gamma-synuclein),  $\alpha$ -syn structurally stands out by its NAC domain. Apart from that, all three synucleins are neuronal proteins that localize preferentially to presynaptic terminals [43, 47].

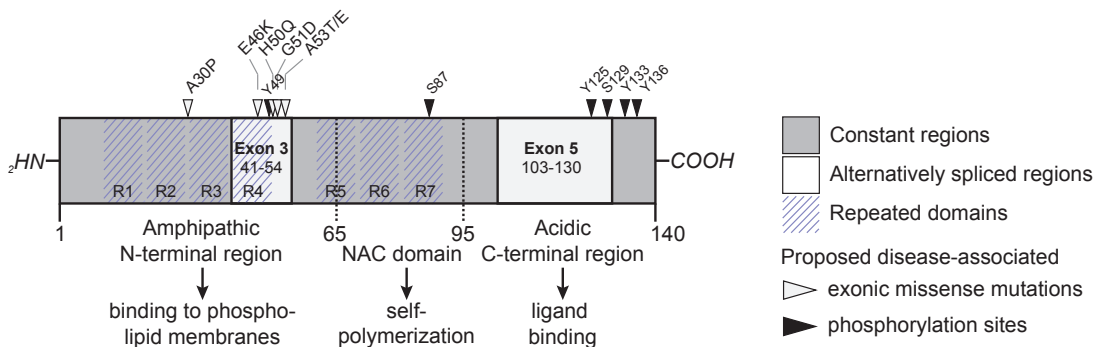


**Figure 1.2. Structure of  $\alpha$ -synuclein.**  $\alpha$ -syn is a 140 amino acid, 14.5 kDa protein divided into three domains: the amphipathic N-terminal region; the hydrophobic and aggregation-prone NAC domain; and the acidic C-terminal region. All pathogenic missense mutations described up to date are localized to the N-terminal region, while most disease-related phosphorylation sites are in the C-terminal region. Both mutations and posttranslational modifications may interfere with the physiological conformation of  $\alpha$ -syn and facilitate fibrillization. Adapted from [48].

$\alpha$ -syn can adopt a great variety of conformations, exhibiting dynamic changes depending on its environment. In solution,  $\alpha$ -syn is present as a natively unfolded monomer, lacking a uniform tertiary structure [49]. In the presence of acidic lipid

## 1. Introduction

---

membranes [50] or membranes with a high curvature [51], the N-terminal domain of  $\alpha$ -syn folds into an  $\alpha$ -helical structure for membrane interaction. Therefore, it seems that  $\alpha$ -syn conforms to its physiological structure and function primarily in the presence of its molecular interacting partners. Beyond that,  $\alpha$ -syn can interact with other  $\alpha$ -syn molecules to form multimers. It is currently controversially debated whether  $\alpha$ -syn physiologically also exists as a tetramer [52] and whether this conformation might represent a molecular strategy for "safe" storage prior to its biological functions. Moreover — and relevant for the pathologic state — there is  $\alpha$ -syn self-assembly into  $\beta$ -pleated sheets and the formation of insoluble aggregates [53]. The aspects of protein aggregation are introduced in detail in section 1.4

Around the turn of the millenium, studies led to the notion that  $\alpha$ -syn functions as a modulator of synaptic transmission. The expression of the protein is induced during development and lags behind proteins involved in the establishment of synaptic structure [54, 55]. Furthermore,  $\alpha$ -synuclein expression levels are changed in conditions with altered synaptic plasticity or neuronal injury [56, 47]. In the presynaptic terminal,  $\alpha$ -syn was shown to move away from vesicles upon repeated neuronal firing, to gradually return later. It was therefore suggested that  $\alpha$ -syn acts as a negative regulator for neurotransmitter release [57] through transient binding to synaptic vesicles [58] and regulating the readily releasable synaptic vesicle pool [59]. Other studies suggest a direct interaction between  $\alpha$ -syn and SNARE (soluble NSNF attachment protein receptor) proteins. These receptors are — together with Sec1/Munc-18-like proteins — crucial for controlling the membrane fusion mechanism during neurotransmitter release [60]. The role of  $\alpha$ -syn includes vesicular trafficking to, and docking with, the presynaptic membrane [61, 62], as well as vesicular endocytosis [63]. It is believed that  $\alpha$ -syn acts in synergy with CSP $\alpha$  in a chaperone-like fashion for SNARE-complex assembly [64] and that this process involves its binding to synaptobrevin-2 [61]. These functional aspects are illustrated in Figure 1.6. The interaction of  $\alpha$ -syn with a vast number of proteins involved in dopamine biosynthesis and handling furthermore strongly suggests a specialized role of  $\alpha$ -syn in the dopaminergic synapse (reviewed by [65]).

## 1.3 Tauopathies by the example of Alzheimer's Disease

Most prominent among this heterogenous group of dementias — which are termed tauopathies — stands Alzheimer's Disease (AD), being diagnosed in 50-75% of patients. Another 5-10% of dementia patients suffer from Frontotemporal lobar dementia (FTLD), but many other diseases may also be accompanied by tauopathy, including Down Syndrome, Pick's Disease, ALS and parkinsonism linked to chromosome 17 (FTDP-17) (reviewed by [66, 67]).

The recognition of Alzheimer's Disease as a disorder originates back to the German psychiatrist and neuropathologist Alois Alzheimer and his patient Auguste Deter, who presented herself with cognitive impairment and disorientation in time and space [68]. Today we know that dementia associated with Morbus Alzheimer typically starts as mild cognitive impairment slowly progresses over several years, making patients dependent on care in the late stages [69]. After Auguste Deter's death at 55, Alzheimer was also the first to describe the two neuropathological characteristics found in the brains of AD patients: amyloid plaques and neurofibrillary tangles (NFTs) (Figure 1.3 A-D). Plaques consist mainly of aggregated  $A\beta$  amyloid peptides being cleavage products of the amyloid precursor protein (APP). NFTs are intracellular aggregates of the microtubule-associated protein tau, which is hyper-phosphorylated and forms so-called paired helical filaments. NFTs are also typical for other tauopathies, including Down's syndrome, progressive supranuclear palsy, Pick's disease and several disorders with parkinsonism [70].

Furthermore, the loss of neurons and synapses can be observed in the AD brain. In combination with the degeneration of neurites, these pathogenic processes are responsible for the macroscopic brain atrophy present in AD (reviewed by [72]). Neurons of the hippocampus, the connected entorhinal cortex and the frontal, parietal and temporal neocortex degenerate in particularly great measure [73, 74, 75]. Accordingly, synaptic loss can be observed both for the presynaptic and the postsynaptic compartments in AD brains and highly correlates with the severity of cognitive impairment [76, 77].

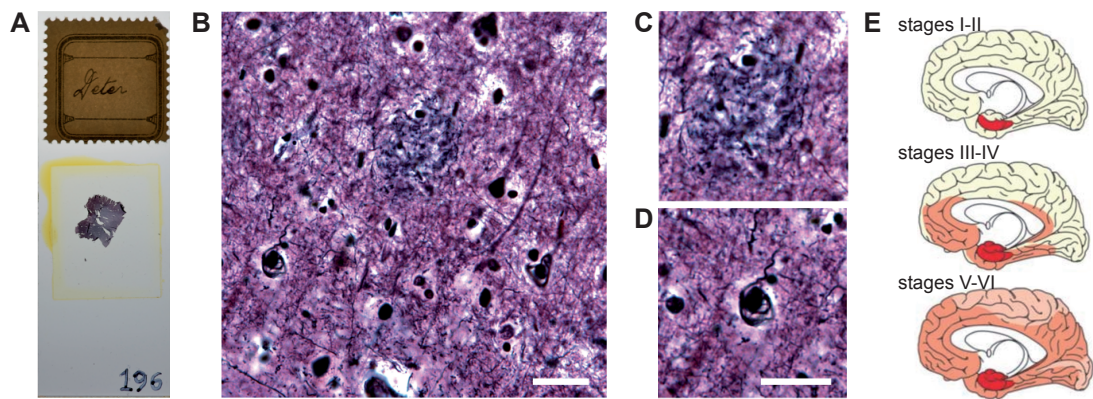


**Figure 1.3. The Alzheimer's Disease brain.** **A.** Histological brain section from Auguste Deter, which was kindly provided by Prof. Dr. h.c. Hans Kretschmar for microscopic imaging, as depicted in B-D at the Center for Neuropathology and Prion Research. **B.** Bielschowsky silver staining to show the neuropathological characteristics in AD brains. **C.** Amyloid plaques and **D.** Neurofibrillary tangles. **E.** The staging of AD according to Braak. Adapted from [71].

The sequence of events which lead to the deposition of  $A\beta$  amyloid plaques and tau NFTs can be summarized with the amyloid cascade hypothesis. At its beginning stands the proteolytic processing of the amyloid precursor protein (APP), which is an ubiquitously expressed integral membrane protein and can be cleaved in one of two pathways. Non-amyloidogenic cleavage involves the metalloprotease ADAM10 (a disintegrin and metalloprotease 10) and  $\gamma$ -secretase and produces the APP intracellular domain and a short extracellular fragment called p3. The amyloidogenic pathway in contrast involves cleavage by the  $\beta$ -secretase BACE1 ( $\beta$ -site APP cleaving enzyme 1) followed by  $\gamma$ -secretase and yields the APP intracellular domain and the longer extracellular  $A\beta$  peptide. Especially the 42-amino-acid long  $A\beta_{42}$  peptide is prone for aggregation, if produced excessively (reviewed by [78, 79]). Successive  $A\beta$  aggregation over time can then cause synapse damage, immune reaction in form microglial and astrocytic activation and phosphorylation of tau, which in turn aggregates over several toxic intermediate forms to finally form NFTs [80, 81].

Similar to the staging of Parkinson's disease, the tau pathology follows a defined pattern of spatial development across brain regions which are grouped into six Braak Stages. The first tau aggregates are formed in the entorhinal and trans-entorhinal cortex (stages I and II), followed by the hippocampus (stages III and



IV) and the neocortex (stages V and VI), as illustrated in Figure 1.3 E [82, 83]. The involvement of tau in the onset and the progression of Alzheimer's disease is not entirely clarified. Nevertheless, there is strong evidence of a causative relation between insoluble tau aggregates and neurodegeneration (reviewed by [84]). The extent of tau pathology usually correlates better to cognitive decline than the extent of amyloid plaque deposition (reviewed by [85]). This is the reason why tau pathology is routinely assessed for staging in *post mortem* AD brains.

### 1.3.1 The tau protein

Tau (from: tubulin associated unit) is a microtubule (MT)-binding protein and localized particularly to axons of the CNS [86]. Alternative splicing of the *MAPT* gene (from: microtubule associated protein tau [87]) localized on chromosome 17q21 and containing 16 exons results in 6 isoforms of the tau protein [88]. These consist of 3 or 4 C-terminal repeat regions for MT binding (3/4R tau) and a certain number of N-terminal regions (0/1/2N tau), as shown in Figure 1.4. The adult human brain expresses all six isoforms at approximately a one-to-one ratio of 4R to 3R tau [89]. Natively unfolded tau protein binds to MTs through interaction between amino acids within its repeat domains and  $\alpha$ - and  $\beta$ -tubulin molecules. This interplay promotes MT formation and stability [90]. Consequently, 4R tau has a higher affinity for binding to microtubules than 3R tau, owing to the additional repeat domain [91].

The MT-binding ability of tau is also regulated by posttranslational modifications, primarily through phosphorylation, but other modifications of tau have been reported as well (reviewed by [92]). Phosphorylation of tau leads to its detachment from MTs and is controlled by a balance in phosphatase and kinase activities. Although tau-binding stabilizes MTs and is essential for their integrity, it also represents a physical obstacle for vesicles and other forms of cargo transported along the MT. Therefore, frequent cycles of tau phosphorylation, leading to its detachment from the MT and dephosphorylation, and, promoting its binding, occur to enable efficient cellular transport and rearrangement of MTs (reviewed by [93]). Particularly when detached from MTs, tau can also

## 1. Introduction

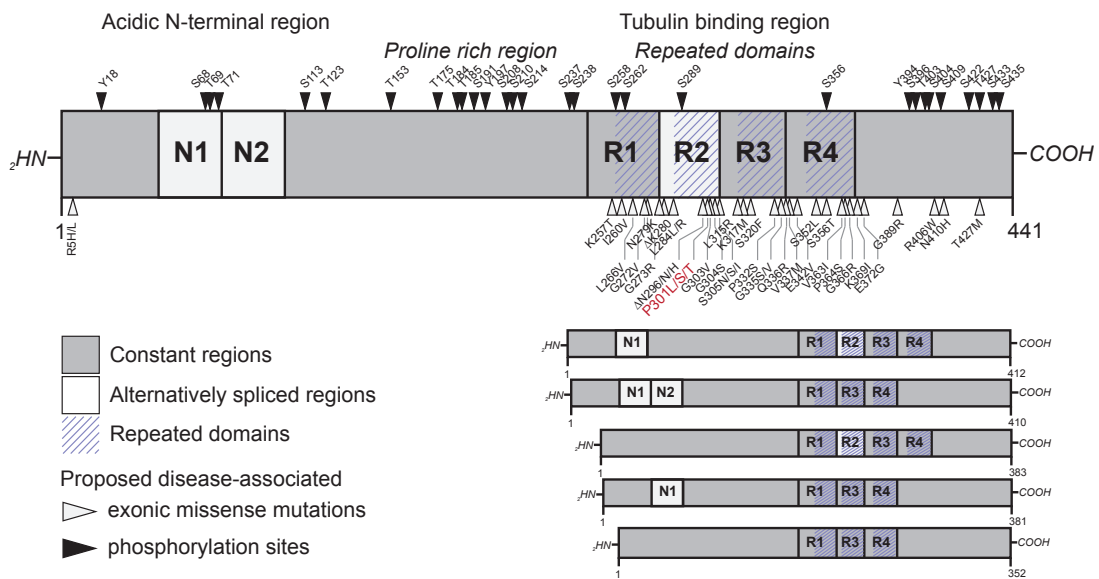


**Figure 1.4. Structure of tau.** Alternative splicing of the N1, N2 and R2 regions yields 6 different tau isoforms, which contain an acidic N-terminal region and a tubulin binding region. The majority of disease-related exonic missense mutations localize to the C-terminal and tubulin binding region. Adapted from [48, 67].

bind to a heterogeneous population of other structures and enzymes, including RNA, presenilin 1 (PS1) and the plasma membrane [94, 95, 96] which ultimately might lead to protein misfolding and aggregation [97].

With its ability to modulate MT-dynamics, tau therefore directly or indirectly contributes to cellular structure and function. *In vitro* experiments have shown that tau-mediated axonal transport is necessary for synapse maintenance as the mislocalization of tau to the somatodendritic compartment causes synapse degeneration [98, 99].

## 1.4 Misfolded proteins in neurodegenerative diseases

Growing evidence reveals a common pathogenic mechanism underlying many neurodegenerative disorders: the misfolding of distinct proteins and their aggregation and deposition in nervous tissue is associated with progressive CNS amyloidosis. Generally speaking, soluble or natively unfolded proteins change their

conformation, adopt a  $\beta$ -sheet-rich structure and form growing disease-specific fibrillar aggregates which are deposited extracellularly, in the cytoplasm, in the nucleus or in neurites (Figure 1.5). In most cases, this process develops over an entire lifetime and doesn't manifest clinically before middle or late life. In healthy individuals, refined cellular quality-control measures like molecular chaperones promote proper protein folding and the ubiquitin-proteasome system or the autophagy-lysosomal system degrade any proteins that remain misfolded [100]. It is still not entirely understood what ultimately causes the defect of these control measures, but mutations in certain disease-related genes can speed up the process of protein aggregation, by directly facilitating the propensity of resulting proteins to aggregate or by interfering with the physiological processing of amyloidogenic proteins.

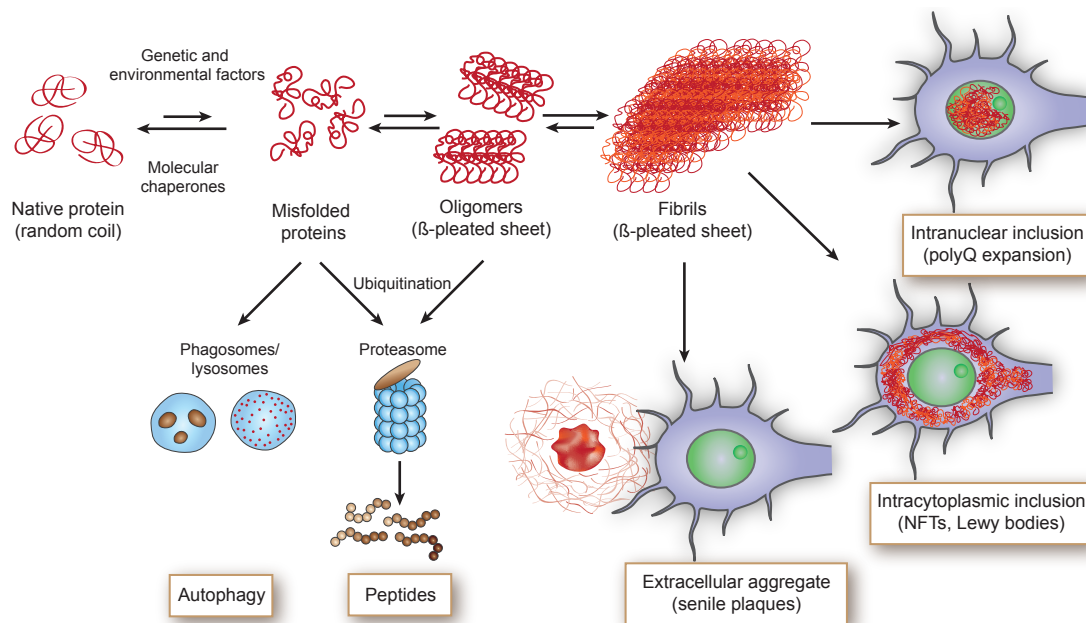


**Figure 1.5. Misfolded proteins in neurodegenerative diseases.** Native proteins can misfold, aggregate and fibrillize, leading to the formation of protein aggregates in the nucleus, the cytoplasm or the extracellular space. Genetic and environmental factors may facilitate this process, whereas cellular quality-control measures like molecular chaperones, autophagy or the ubiquitin-proteasome system act as a counterbalance and limit the accumulation of misfolded protein. Adapted from [4].

### 1.4.1 Contributors for the misfolding of proteins

Familial forms of parkinsonism can be caused by point mutations in the *SNCA* gene that lead to pathogenic amino acid substitutions in the protein (A30P, E46K, H50Q, G51D, A53E or A53T) [101, 102, 103, 104, 105, 106] (see 1.2). Duplication or triplication of the *SNCA* gene [107, 108] can also result in PD or DLB, which indicates that a 50 % increase in protein expression suffices to trigger the disease [109]. This is consistent with the notion described above that the conformational templating of  $\alpha$ -syn is initially an energetically unfavorable process with a long lag-phase, which can be however overcome by a higher abundance of  $\alpha$ -syn leading to a greater stochastic formation of aggregates.  $\alpha$ -syn protein with the A30P, A53T, H50Q and E46K mutations have been reported to increase the rate of aggregation and to more readily form protofibrils and fibrils than the WT protein [28, 110, 111]. The A30P mutation has also been shown to directly disrupt the association of  $\alpha$ -syn with membranes as well as its synaptic localization [112]. Furthermore, environmental factors such as the exposure to the complex I inhibitor rotenone induces oxidative stress, which causes nigrostriatal dopaminergic degeneration and promotes the formation of Lewy bodies [113]. On the contrary, both the A53E and G51D mutations were described to reduce the intrinsic propensity of  $\alpha$ -syn to aggregate [114, 115], despite still causing early-onset PD with  $\alpha$ -syn pathology [104, 106].

The neuropathology of AD is characterized by two types of lesions. NFTs form in the cytoplasm and consist of aberrantly phosphorylated tau, whereas senile plaques are extracellular depositions consisting largely of  $\beta$ -amyloid ( $A\beta$ ). Mutations of both the amyloid precursor protein (APP) and presenilin (PS1 or PS2) ultimately lead to an increased production of the amyloidogenic  $A\beta_{42}$  cleavage product of APP, which readily fibrillizes to gradually form senile plaques, as outlined in the amyloid cascade hypothesis of AD [81].

The number of pathogenic mutations known for tau are somewhat larger than for the  $\alpha$ -syn protein. Although the deposition of tau is secondary after  $A\beta$  accumulation in the amyloid cascade, it has a stronger causal relationship to neurodegeneration [84]. Under pathologic conditions, the balance of the MT-tau protein binding is disturbed, leading to an increase in the level of unbound

tau, which is prone to aggregate with further tau molecules and other proteins. This significantly affects the control of MT-dynamics and impairs axonal transport. Tau hyperphosphorylation, misfolding and progressive aggregation can be triggered by several pathogenic events, including over 30 known mutations in the *MAPT* gene (see Figure 1.4). A direct relationship between splice-site and missense mutations such as G272V, P301L and R406W and filamentous, hyper-phosphorylated tau inclusions were initially reported for cases of FTD with parkinsonism linked to chromosome-17 (FTDP-17) [116, 117]. Mutations in exon 10 also often perturb the balanced one-to-one ratio of the 4R and 3R tau isoforms, favoring the expression of the 4R isoform in most cases and thereby affecting MT-binding affinities and increasing the propensity to aggregate [89]. Finally, the ability of many cofactors promoting the misfolding and fibrillization of tau may explain in part the presence of tau deposits in many different neurodegenerative diseases.

Despite their clinically distinct features, there is increasing evidence for the considerable overlap of synucleinopathies and tauopathies, which might share a mechanistic link. On the one hand, 50-60 % of AD patients with NFTs also have  $\alpha$ -syn-containing Lewy bodies [118, 119, 120]. Moreover, 50 % of AD patients displaying extrapyramidal signs show considerable co-localization of  $\alpha$ -syn and phospho-tau pathology in the substantia nigra [121, 122]. On the other hand, a co-staining of phospho-tau with  $\alpha$ -syn has been observed in 30-40 % of the Lewy bodies in the nucleus basalis of Meynert and the locus coeruleus [123], and in 10-30 % of LBs in the medulla [124] of PD and DLB patients. Other studies showed the overlap of phospho-tau with  $\alpha$ -syn pathology in FTL and progressive aphasia [125], in the Parkinsonism-Dementia complex of Guam [29] and in PD patients with the A53T  $\alpha$ -syn mutation [126]. Furthermore, axonal deficits are not a unique feature of tauopathies, but have been described in numerous neurodegenerative diseases including synucleinopathies (reviewed by [127]). So there is ample reason to believe that no simplistic linear pathways lead to the one or the other neurodegenerative disorder, but that multiple intrinsic and extrinsic factors contribute to the individual disease process of patients. In fact, a regression model considering cortical  $A\beta$ , tau and  $\alpha$ -syn pathologies more accurately predicted dementia than any one of the single markers alone [128].

### 1.4.2 Cell-to-cell propagation and spreading of misfolded proteins

The spatiotemporal sequence of LB and NFT pathology in PD and AD has led to the hypothesis that progression is related to the cell-to-cell propagation of pathogenic proteins like  $\alpha$ -syn and tau and their templated misfolding. Support for this idea came from observations in patients with PD who received implants of fetal graft neurons into the striatum to compensate for the degenerated dopaminergic neurons of the SNpc [129]. The *post mortem* analysis of these brains showed  $\alpha$ -syn pathology in the transplanted neurons, which indicated a spread of pathology from other neurons. Furthermore, the ascending distribution of  $\alpha$ -syn and tau pathology in patient brains as described by Braak [38, 82] can be interpreted as representing the dissemination of  $\alpha$ -syn and tau across connected brain regions. Further support comes from the case of a woman who died from AD at the age of 85 and whose cortex was partly disconnected from the rest of the brain during surgery 20 years earlier [130]. In contrast to other brain areas, this isolated brain region contained no amyloid plaques or NFTs, which highlights that the spread of pathology requires connection.

The cell-to-cell propagation hypothesis was experimentally challenged in a number of cell culture studies. Using transfection reagents driving membrane permeability, the addition of a small amount of exogenous  $\alpha$ -syn preformed fibrils (PFFs) provokes cells expressing endogenous  $\alpha$ -syn to develop amyloid inclusions [131, 132, 133]. Thereafter, a study on  $\alpha$ -syn demonstrated that the sole addition of PFFs to primary neurons is sufficient to induce inclusion formation [134]. The first cellular experiments on the influence of extracellular tau on intracellular tau exposed human fetal cortical cultures to brain extracts from AD patients to show that the cells developed inclusions similar to paired helical filaments (PHFs) [135]. Later, cultured cells were described to take up aggregated, but not monomeric, tau and to develop intracellular fibrils, which in turn were competent to seed fibril formation *in vitro* [136]. Intracellular tau inclusions were furthermore demonstrated to molecularly resemble tau in human NFTs [137] and also that pathologic inclusions can be nucleated by PFFs in primary neurons [138]. Apart from cellular models, animal models are widely used to study

the spreading of  $\alpha$ -syn and tau pathology and are outlined in section 1.6.1.

Although the misfolded proteins characteristic of neurodegenerative diseases do not reach the infectiousness of prions, they share some features and molecular modes of behavior. On top of being able to propagate, there is increasing evidence for the existence of strains. This implicates that pathologic aggregates featuring specific molecular traits can be recovered from host cells or organisms and reintroduced into naïve cells where they re-establish identical pathology.  $\alpha$ -synuclein, for instance, was shown to adopt distinct conformations producing characteristic fibril shapes depending on the physical conditions during fibril production [139]. Injected into rat brains, these strains display differential seeding capacities and cause distinct histopathological phenotypes [140]. In a recent study from the tauopathy field, tau aggregates from 5 different human tauopathies were also associated with different sets of strains. The introduction of these strains into cells bearing aggregation-prone mutated tau lead to the formation of inclusions with unique morphologies, which could also be successfully passaged over 6 months [141]. From this evidence it is tempting to believe that the unique conformations of  $\alpha$ -syn or the tau proteins might also be responsible for the varied types of synucleinopathies and tauopathies, but this remains the subject of further study.

## 1.5 The glutamatergic synapse

The human brain is one of the most complex structures known and it contains almost one hundred billion neurons and an estimated hundred trillion ( $10^{14}$ ) specialized junctions called synapses (reviewed by [142, 143]). Synapses are local sites for signal transduction and plasticity within the brain and the majority form at contacts between presynaptic axons and postsynaptic dendrites and use glutamate as neurotransmitter, making glutamatergic neurons the principal excitatory system in the brain. The architecture of glutamatergic synapses comprises a presynaptic compartment, the synaptic cleft, and a postsynaptic compartment, typically a dendritic spine. The structure and function of a glutamatergic synapse and the involvement of tau and  $\alpha$ -syn proteins is illustrated in Figure 1.6.

### 1.5.1 The presynapse

The presynapse is the point of arrival for action potentials originating in the neuronal cell body and traveling along the axon. It contains mitochondria and numerous synaptic vesicles, often bound to the presynaptic cytoskeleton. Their life-cycle at the synapse includes various proteins that mediate their transport, interaction with the cytoskeleton, uptake and storage of neurotransmitter, regulated interaction and fusion with the plasma membrane at the presynaptic active zone and finally their recycling (reviewed by [144]). In functionally mature glutamatergic synapses, the presynaptic compartments are enriched with glutamate-filled synaptic vesicles and specialized active zones that reinforce the release of glutamate into the synaptic cleft (reviewed by [145]). Glutamate is released from the presynaptic terminal upon the arrival of an action potential. The opening of voltage-gated  $\text{Ca}^{2+}$  channels cause a local increase of  $\text{Ca}^{2+}$  ions in the presynapse, leading to a cascade of events that finally cause vesicles of the presynaptic active zone carrying glutamate to fuse with the presynaptic membrane and release glutamate into the synaptic cleft. At the postsynaptic membrane, glutamate acts upon postsynaptic glutamate receptor channels, mainly of the AMPA ( $\alpha$ -amino-3-hydroxy-5-methyl-4-isoxazole propionic acid) and NMDA (N-methyl-D-aspartate) type (reviewed by [145]).

Parallel pre- and postsynaptic intracellular signaling cascades can trigger protein synthesis and simultaneous control of synaptic plasticity. The isolation and molecular analysis of the synaptic compartment has naturally been of great interest for researchers. Half a century of research using subcellular fractionation of brain tissue and protein identification has led to a certain understanding of the synaptic proteome [144].

### 1.5.2 The postsynapse and structural plasticity

”...the surface...appears bristling with points or short spines” [146]. These words from 1888 by the legendary spanish neuroanatomist Ramón y Cajal refer to the first description of dendritic spines on a Purkinje neuron. Since then, technical advances have broadened our knowledge of the structure and function of these small protrusions from the dendritic shaft. Today we know that most excitatory



synapses in the mature mammalian brain occur on dendritic spines and that a spine head typically contains the input of a single synapse. Dendritic spines protrude from the dendritic shaft and are typically 0.5 – 3  $\mu\text{m}$  in length and up to 0.8  $\mu\text{m}^3$  in volume (reviewed by [147]).

On the ultrastructural level, an electron-dense structure called the postsynaptic density (PSD) is associated with the spine membrane facing the synaptic cleft. It consists of structural proteins, neurotransmitter receptors of the AMPA and NMDA types and proteins for signal transduction. Additionally, spines contain a cytoskeleton, polyribosomes and smooth endoplasmatic reticulum which can fold into a structure known as the spine apparatus [148, 147]. Spine morphology displays great heterogeneity; apparent even on single dendrites [151, 152]. Based on detailed anatomical analysis of fixed tissue, the morphological subtypes mushroom, stubby and thin have been defined [153, 154]. Mushroom spines have a large, bulbous head that is connected to the dendrite through a narrow spine neck, whereas thin spines have a smaller head. Stubby spines lack the spine neck and appear as round elevations from the dendritic shaft. In addition, filopodia are very long and thin structures that lack a spine head. They are considered precursors of dendritic spines and are the most dynamic of dendritic structures, which protrude and retract rapidly from the dendritic shaft and only sometimes develop into one of the other spine types [152, 155]. Importantly, dendritic spine density, shape and size are remarkably dynamic and known as structural plasticity. Changes occur over timescales ranging from seconds to minutes and from hours to days [156] but tend to become increasingly stable in mature neurons [157]. Morphological changes of spines are also tightly linked to their content of organelles and specific molecules. As the size of the spine head correlates with the size of the PSD, it also correlates with the amount of postsynaptic receptors [158], the number of docked presynaptic vesicles [159] and therefore the strength of synaptic transmission.

The spine head represents a biochemically and electrically isolated compartment, in which reactions and electric potentials occur. *Ex vivo* studies have shown that high-frequency stimulation of the presynapse inducing long-term potentiation (LTP) leads to an increase in spine volume [160, 161] as well as to the *de novo* formation of spines [162, 163, 164]. 15-19 hours after LTP, newly formed

# 1. Introduction

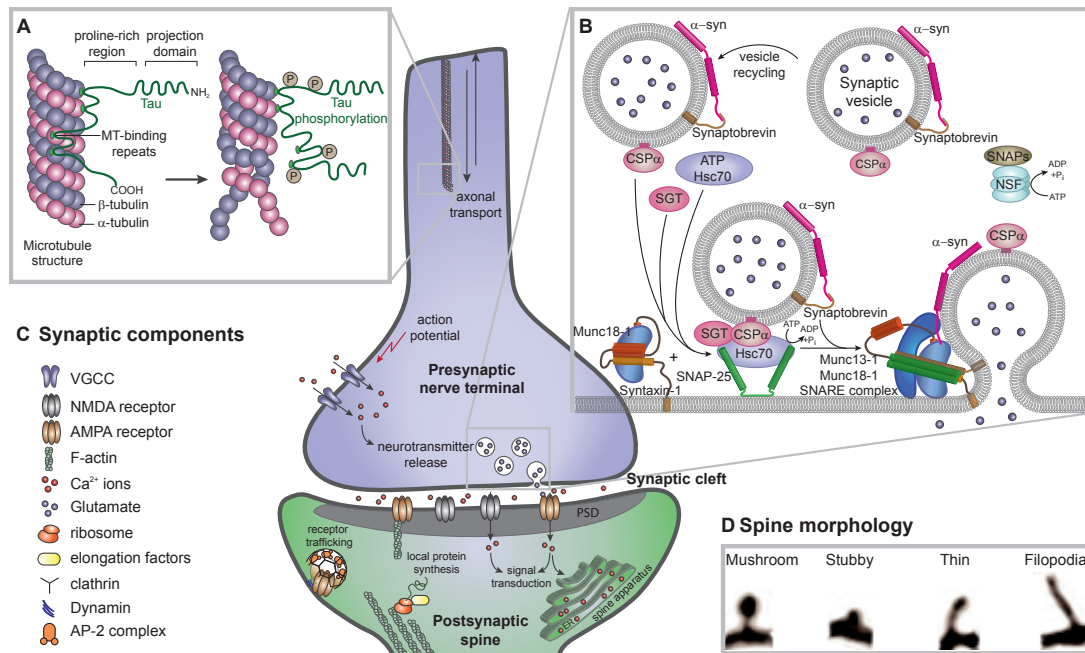


**Figure 1.6. The glutamatergic synapse.** **A.** Microtubules are composed of  $\alpha$ - and  $\beta$ -tubulin arranged into cylindrical polymers and provide structural support to neurons. The protein tau can bind to MTs via its tubulin-binding motifs in the 3 or 4 repeat domains. Phosphorylation of Tau by kinases at a number of serine or threonine residues attenuates its binding to microtubules as well as its stability. Adapted from [93]. **B.** Overview of the function of  $\alpha$ -syn on synaptic vesicles. Munc18-1 is bound in a closed conformation to the membrane-anchored syntaxin-1. SNAP-25 remains in a state competent for membrane fusion by interacting with its co-chaperones CSP $\alpha$ , Hsc70 and SGT. Upon vesicle fusion with the plasma membrane, the full SNARE complex is assembled, which is orchestrated in parts by the Munc proteins and assisted by  $\alpha$ -syn through yet to be determined interactions. After fusion, the SNARE complex is disassembled by SNAPs and NSF and synaptobrevin is recycled back to vesicle membranes. CSP, cysteine string protein; NSF, N-ethylmaleimide sensitive factor; SGT, small glutamine-rich protein; SNAPs, soluble NSF adaptor proteins; SNARE, SNAP receptor; SNAP-25 synaptosomal associated protein of 25 kDa. Adapted from [149]. **C.** Synaptic components important for signal transmission and plasticity. Action potentials arriving at the presynaptic terminal cause Ca<sup>2+</sup> influx through voltage-gated calcium channels, which mediates glutamate release. At the postsynaptic side, ionotropic AMPA receptors anchored in the structural support of the PSD convert the chemical glutamatergic signal back to an electric signal, activating NMDA receptors and causing postsynaptic Ca<sup>2+</sup> influx. This activates signal cascades enabling the synapse to adapt its reactivity and plasticity in the long term. This is also mediated by local translation and dynamic trafficking of receptors to and from the membrane facing the synaptic cleft. Adapted from [150]. **D.** Spine morphology classes as seen with confocal microscopy.

spines also have developed ultrastructural features of mature synapses, such as an attached and vesicle filled presynaptic bouton and a synaptic cleft [165]. In contrast, low-frequency presynaptic stimulation inducing long-term depression (LTD) results in spine shrinkage [166, 161] and reduced neuronal activity causes a loss of spines [162]. Being the first postsynaptic element encountered by the excitatory neurotransmitter, spines play a pivotal role in the integration of synaptic input and by their plasticity in learning and memory [167]. In disorders like PD or AD, in which synapses degenerate with and even before neurons [168, 169], the study of synaptic plasticity can therefore give important insights about the pathophysiology of these diseases.

## 1.6 *In vivo* two-photon imaging

As life is inherently dynamic, the microscopy of living tissue (*in vivo*) enabling the detailed description of cells, tissues and biological processes in their natural surrounding has enormous value for the understanding of organisms in health and disease. Unfortunately, the optical properties of living tissue make it ill-suited for direct microscopic measurements by itself, owing to the scattering of visible light and its light-protective mechanisms to prevent photodamage by sunlight. Fluorescence microscopy techniques were developed to enable the specific and selective detection of molecules at low concentration and with a high signal-to-noise ratio (reviewed by [170]). One drawback with conventional fluorescence microscopy, however, is the restriction on its use to thin samples, as the entire sample is excited indiscriminately of the focal plane. In order to avoid the obscuration of the image by out-of-focus light, confocal laser scanning microscopes (CLSM) [171, 172] prevent it from reaching the detector using a pinhole and thus enable optical sectioning of specimens. At the same time, the rejection of out-of-focus light means the rejection of a large proportion of emitted photons. Increasing excitation increases the emission signal but also can induce photodamage and photobleaching, which can be considered the Achilles heel of this otherwise superior technique [170].

Two developments of the last two decades have revolutionized fluorescence microscopy: the introduction of genetically encoded fluorophores like the green

## 1. Introduction

---

fluorescent protein (GFP) [173, 174] and the invention of two-photon microscopes [175]. Unlike traditional optical microscopy techniques including confocal microscopy, which use linear (one-photon) excitation, nonlinear absorption requires two photons for the excitation of a fluorophore. The nonlinear optical effect was originally proposed by the physicist Maria Göppert-Mayer in 1931 and states that a fluorophore can be stimulated by effectively simultaneous absorption of two photons, if the sum of their energies equals the required energy of excitation [176, 177]. The probability of excitation under nonlinear conditions is extremely low, but increases proportionally to the square of light intensity [178]. The development of ultrafast lasers [179] allowed the efficient multiphoton excitation of fluorescence, which requires extremely short pulses and high repetition frequencies (typically 100-fs pulses at 100 MHz) of mode-locked lasers and generates extremely high photon densities (several kW/cm<sup>3</sup>) [175, 178, 180]. The light source of choice most commonly has been the Ti:sapphire laser [181], which can be tuned to wavelengths between 670 and 1070 nm. The principles of one- and two-photon microscopy are illustrated in Figure 1.7.

Nonlinear excitation holds a number of advantages over linear excitation for the imaging of biological specimens [182]: (1) the infrared light used for excitation is absorbed and reflected to a lesser extent by tissue, which increases the penetration of light into the tissue and enables the examination of fluorophores deep (up to 1 mm) in living samples; (2) as the nonlinear optical effect is dependent on a high local concentration of photons, excitation essentially only occurs at the focal point, leading to an inherent optical sectioning. Without any out-of-focus excitation, photodamage and photobleaching are likewise reduced. (3) Especially deep in tissue, the efficiency of detection is substantially higher, as emitted fluorescence scattered by tissue also contributes to the signal, as long as they reach the detector.

For *in vivo* studies using 2-photon-microscopy, the biological structures of interest have to fluoresce. Some metabolic products like NAD(P)H [nicotinamide adenine dinucleotide (phosphate)] [183], flavines [184] and indolamines [185] have an intrinsic fluorescence which can be used to measure the metabolic state of a cell. In addition, second harmonic generation (SHG) enables direct imaging of anisotropic biological structures which can be hyperpolarized, such as

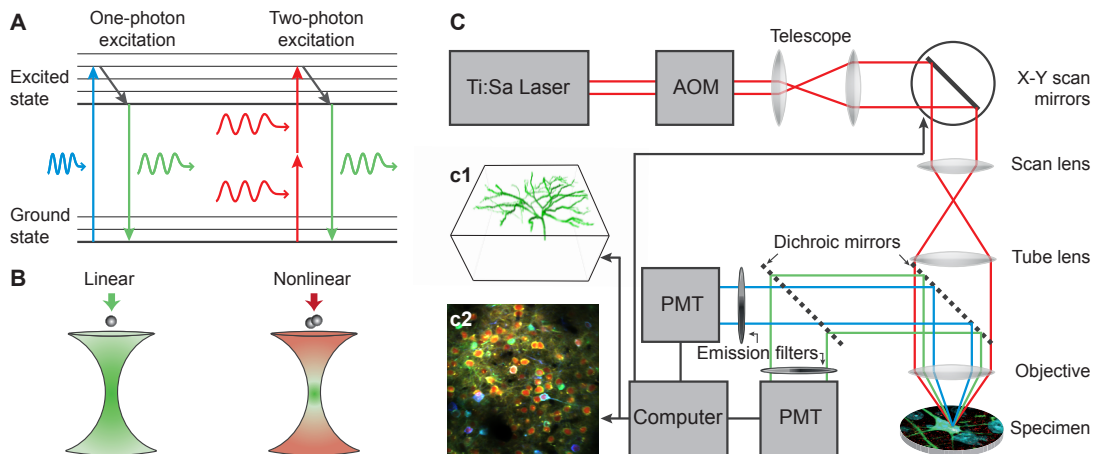


**Figure 1.7. Principles of one- and two-photon microscopy.** **A.** Simplified Jablonski-diagram to illustrate linear one-photon (blue) and nonlinear two-photon (red) excitation. Valence electrons of a fluorophore can be excited to an energetically higher state by the absorbance of one or two photons. Relaxation to the ground state can occur through non-radiative transitions or through emission of light — shown here as green fluorescence. **B.** One-photon linear excitation generates an entire cone of fluorescent light, whereas two-photon nonlinear excitation creates spatially confined signal in the vicinity of the focal spot. **C.** Schematic of a two-photon microscope and the generation of three-dimensional image stacks. A Ti:Sa laser generates photon pulses in femtosecond-cycles and can be tuned to wavelengths between 670 and 1070 nm. An acousto-optic modulator (AOM) regulates light intensity and a telescope increases the light ray width. A system of X-Y scan mirrors and an array of lenses guide the focused beam of light grid-type across the specimen. The emitted fluorescence wavelengths are separated using dichroic mirrors. Photomultiplier tubes (PMTs) convert the arriving photons into electric signal, which is processed using imaging software. Combining optical sectioning with X-Y scanning enables the creation of three-dimensional image stacks or videos longitudinally over time. Shown here exemplarily are the reconstruction of a dendritic tree from a cortical neuron (c1) and an activity profile of layer II cortical neurons (c2). Adapted from [180].

collagen [186, 187, 188]. Another approach involves the direct injection of fluorophores. Angiography visualizes the vasculature [189] whereas fluorophores able to cross the blood-brain-barrier can be used to label certain structures within the brain tissue. Thioflavin S [190] and FSB [191] [(trans,trans)-1-fluoro-2,5-bis(3-hydroxycarbonyl-4-hydroxy)styrylbenzene] are two examples of amyloid-binding fluorophores that can be used to label neurofibrillary tangles *in vivo*.

As mentioned above, genetically encoded fluorophores are a very elegant way to visualize structures of interest. GFP is a naturally fluorescent protein originally isolated in 1962 by biochemist Osamu Shimomura et al. [192] from the jellyfish, *Aequoria Victoria*. It can be expressed fused to a protein of interest

## 1. Introduction

---

in a specific tissue and in any species in which genetic engineering is possible [173, 193]. Spectral color variants (XFPs) have been generated by introducing mutations into the GFP gene and create great experimental flexibility for the microscopist [194]. For *in vivo* imaging of neuronal structure including dendrites and spines, transgenic mice expressing XFPs under the control of the pan-neuronal promoter Thy1.2 have been generated. GFP-M and the YFP-H are two examples of mouse lines in which the random expression of the Thy1.2 promoter drives sparse labeling including a subset of pyramidal neurons in the neocortex [195], making them and their dendritic trees optically distinguishable and depictable.

The use of fluorophores to pick up neuronal function on the cellular level is among the great advances in neuroscience of the last few decades. Calcium indicators respond to the binding of calcium ions ( $\text{Ca}^{2+}$ ) by changing their fluorescent properties and consequently give an immediate measure of neuronal activity. Here one can distinguish between bioluminescent proteins, chemical and genetically encoded calcium indicators (reviewed by [196]). Bioluminescent proteins like aequorin were the first  $\text{Ca}^{2+}$  indicators [192] rely on oxidation for the emission of photons, whereas chemical  $\text{Ca}^{2+}$  indicators like fura-2 [197] or Oregon Green 488 BAPTA-1 (1,2-bis(*o*-aminophenoxy)ethane-*N,N,N',N'*-tetraacetic acid) [198] change their fluorescence upon the chelation of  $\text{Ca}^{2+}$  ions. Genetically encoded  $\text{Ca}^{2+}$  indicators (GECI) come in two flavors. FRET-based indicators use the conformational change of a protein upon  $\text{Ca}^{2+}$  binding to induce Förster resonance energy transfer (FRET), leading to a shift in the primarily emitted fluorescence wavelength [199]. Single-fluorophore GECIs increase their emitted fluorescence upon  $\text{Ca}^{2+}$  binding due to intramolecular conformational changes. Prime representatives from this family, which experience frequent use in *in vivo* conditions and were also used for this work are the GCaMP indicators, which consist of an enhanced GFP protein, flanked by the  $\text{Ca}^{2+}$  binding protein calmodulin and the calmodulin-binding peptide M13 on the other side [200].

The *in vivo* imaging of neuronal structures requires optical access to the brain. In order to achieve this, two approaches have been described and used: (1) the open skull preparation and (2) the thinned skull preparation. The open skull preparation implicates the removal of a typically round piece of skull with

a diameter of 3 to 8 mm [201, 202]. In the case of a chronic experiment, it is replaced by a round piece of glass of the same size that is fixed permanently to the skull. Applying this approach, the experimenter profits of a large and optical perfectly transparent area to study and allows imaging up to 800  $\mu\text{m}$  deep into the tissue. Depending on the skill of the surgeon and biological factors (such as bone regrowth), this preparation can stay optically accessible for weeks up to months and enables any desired number of imaging time points. It has to be noted that the invasive nature of this type of surgery provokes an immune reaction of glial cells, which however subsides during a recovery period of three to four weeks [201]. The thinned skull preparation is less invasive, as the bone is not fully perforated but thinned down to a 20  $\mu\text{m}$  transparent layer [203, 204, 205]. The superior transparency of a glass window cannot be reached by this approach, which limits the penetration depth of the 2-photon laser and enables imaging only in superficial tissue. Moreover, with a diameter of about 200  $\mu\text{m}$ , the accessible area is significantly smaller than in the open skull preparation. Repetitive imaging is possible, but bone regrowth requires a new preparation if imaging time points are further apart than 24 h which is typically successful only three to four times. An advantage of this method is that very long time periods between imaging sessions can be used. Overall, both preparations have their benefits and depend on an experienced surgeon for an optimal result.

### 1.6.1 Alpha-synucleinopathy and Tauopathy mouse models

The study of human neurodegenerative diseases is complicated by several factors. Patient studies are subject to multitudinous restrictions and due to a continuing lack of safe and reliable biomarkers, the definite diagnosis into a disease category can commonly only be made *post mortem*. Brain tissue is often not available until hours after the time of death, and is thus unsuitable for sensitive biochemical analysis and in any case only gives information about the pathological state at that time point, but not about the pathogenesis or the etiology. Histological analysis of brain tissue extracted through biopsy is possible only in rare cases. The heterogeneity across patient groups is large due to the presence of concomi-

## 1. Introduction

---

tant diseases, which diminishes the ability to make generally valid statements. Along with the major efforts in medical research to develop symptomatic and reversible treatments, the intervention in the early pre-clinical stages to prevent disease could be crucial (reviewed by [206]).

Complementary to human studies, animal models constitute a great potential in modern neuroscience. The utilized model organisms range from invertebrates like nematodes (*Caenorhabditis elegans*) or fruit flies (*Drosophila melanogaster*), which are widely used to investigate molecular pathways, over zebra fish (*Danio rerio*) to mammals like mice (*Mus musculus*) or rats (*Rattus norvegicus forma domestica*) and less commonly primates. Several reasons make mice one of the most widely used model organisms. They are relatively easy to breed and to house, their genome has a great similarity with the human genome, and there are refined tools for genetic modifications (reviewed by [207]). The introduction of transgenes, for instance, allows the expression of genes like the mutant human *MAPT*- or *SNCA* genes. Promoters that drive expression in the brain can be selected to be cell-type- or tissue-specific and drug-based genetic switches enable the temporal conditional expression of a transgene (reviewed by [208]). One can also knock in (KI) discrete mutations by homologous recombination or knock out (KO) a gene to abolish its expression altogether [209]. Furthermore, the availability of inbred strains with a common genetic background facilitate the comparison between cohorts and the life span of around 2 years enables studies over prolonged periods of time [210].

There is a great variety in available transgenic mouse lines for the study of  $\alpha$ -synucleinopathies and tauopathies, which are extensively reviewed elsewhere [210, 211, 207]. Here, the focus shall be on two lines in which *in vivo* experiments were performed — one for modeling tauopathy and one for modeling synucleinopathy. PDGF-h- $\alpha$ -syn mice express wild-type human  $\alpha$ -syn under the control of the pan-neuronal platelet-derived growth factor- $\beta$  (PDGF $\beta$ ) promotor. In the brain of these mice, granular inclusions of  $\alpha$ -syn in neuronal cell bodies and neurites can be found chiefly in the cortex, the hippocampus and the olfactory bulb. A slight reduction in the density of dopaminergic terminals can be observed in the striatum and aged transgenic mice display mild motor impairments [212].

The P301S mouse model expresses the shortest human four-repeat isoform of



tau (0N4R) with the P301S mutation. In humans, this mutation causes FTDP-17 and is associated with early-onset dementia with parkinsonism [213]. The Thy1.2 promoter drives expression in CNS-neurons, leading to intraneuronal inclusions of hyper-phosphorylated tau and to age-dependent neuron loss in the cortex and the spinal cord [214]. As a consequence, a pronounced motor phenotype including muscle weakness, tremor and hindlimb paraparesis is present in 5-month-old homozygous P301S mice.

In order to study the induction and spread of  $\alpha$ -syn and tau inclusion pathology, more options than transgenic mouse models are available. The method of injecting pre-existing proteinaceous aggregates (the "seed") into the brain, which have the ability to induce further misfolding among endogenous protein and propagate from cell to cell, has become known as seeding. The induction of  $\alpha$ -syn pathology has been achieved in several ways: (1) the intracerebral injection of brain lysates from aged, motor-impaired transgenic mice or human MSA patients can induce pathology in  $\alpha$ -syn overexpressing mice [215, 216]; (2) the intracerebral injection of *in vitro* preformed fibrils (PFFs) of  $\alpha$ -syn into transgenic  $\alpha$ -syn mice causes a similar phenotype, providing more direct evidence that the induction and spread of pathology is specifically caused by misfolded  $\alpha$ -syn and not by other potential inducers — like glial factors or cellular injury response activators — present in brain extracts [217, 218, 219]; (3) the peripheral injection of PFFs into the hindlimb muscle [220] of PD mouse models was sufficient to induce  $\alpha$ -syn pathology; (4) for  $\alpha$ -syn there is also evidence for seeded conformational templating in WT mice. The injection of LB-enriched extracts from the SNpc from *post mortem* PD or DLB brains into WT mice or monkeys resulted in progressive nigrostriatal neurodegeneration and  $\alpha$ -syn inclusion formation [221, 222]. Finally, the intracerebral injection of  $\alpha$ -syn PFFs also induces LB-like pathology in WT mice [223].

The first evidence that tau propagates *in vivo* was provided in 2009 using the ALZ17 mouse line expressing the wild-type human 2N4R tau isoform under the control of the Thy1.2 promoter. Brain extracts were prepared from the P301S mice described above [214], which develop abundant tau pathology primarily in the brainstem and the spinal cord by 6 months of age. Injection of brain extracts containing 0N4R P301S tau aggregates into the hippocampus and cortex

## 1. Introduction


---

of ALZ17 mice resulted in fibrillary hippocampal inclusions that included the 2N4R tau isoform, indicating that at least some of the tau within the inclusions was recruited from wild-type tau protein expressed in the ALZ17 mice [224]. Since then, several other studies have shown the seeding and spreading abilities of tau with preparations from human tauopathies [225, 226] and PFFs [227, 228, 229].

# Results

## 2.1 Seeding and transgenic overexpression of alpha-synuclein triggers dendritic spine pathology in the neocortex [1]

# Seeding and transgenic overexpression of alpha-synuclein triggers dendritic spine pathology in the neocortex

Sonja Blumenstock<sup>1,2,3</sup> , Eva F Rodrigues<sup>2</sup>, Finn Peters<sup>2</sup> , Lidia Blazquez-Llorca<sup>4</sup> , Felix Schmidt<sup>1,5</sup>, Armin Giese<sup>1</sup>  & Jochen Herms<sup>1,2,3,\*</sup> 

## Abstract

Although misfolded and aggregated  $\alpha$ -synuclein ( $\alpha$ -syn) is recognized in the disease progression of synucleinopathies, its role in the impairment of cortical circuitries and synaptic plasticity remains incompletely understood. We investigated how  $\alpha$ -synuclein accumulation affects synaptic plasticity in the mouse somatosensory cortex using two distinct approaches. Long-term *in vivo* imaging of apical dendrites was performed in mice overexpressing wild-type human  $\alpha$ -synuclein. Additionally, intracranial injection of preformed  $\alpha$ -synuclein fibrils was performed to induce cortical  $\alpha$ -syn pathology. We find that  $\alpha$ -synuclein overexpressing mice show decreased spine density and abnormalities in spine dynamics in an age-dependent manner. We also provide evidence for the detrimental effects of seeded  $\alpha$ -synuclein aggregates on dendritic architecture. We observed spine loss as well as dystrophic deformation of dendritic shafts in layer V pyramidal neurons. Our results provide a link to the pathophysiology underlying dementia associated with synucleinopathies and may enable the evaluation of potential drug candidates on dendritic spine pathology *in vivo*.

**Keywords** alpha-synuclein; dendritic spines; *in vivo* imaging; seeding; synucleinopathies

**Subject Category** Neuroscience

**DOI** 10.15252/emmm.201607305 | Received 7 November 2016 | Revised 27 February 2017 | Accepted 2 March 2017

## Introduction

The mammalian brain contains a complex network of billions of neurons communicating through different types of synapses that can be severely and irreversibly disturbed by neurodegeneration. In

synucleinopathies like Parkinson's disease (PD) or dementia with Lewy bodies (DLB), progressive neurodegeneration is linked to misfolding and intracellular aggregation of the synaptic protein  $\alpha$ -synuclein ( $\alpha$ -syn; Clayton & George, 1999; Lücking & Brice, 2000) and leads to motor as well as cognitive deficits and ultimately to dementia (Spillantini *et al*, 1997; Burn, 2004; Aarsland *et al*, 2008). Familial cases of PD or DLB can be caused by mutations in the  $\alpha$ -syn gene (Polymeropoulos *et al*, 1997; Krüger *et al*, 1998; Zarranz *et al*, 2004) or overexpression of  $\alpha$ -syn (Simón-Sánchez *et al*, 2009) and strengthen the association between protein load/aggregation and the onset of disease. Although the filamentous, cytosolic  $\alpha$ -syn inclusions called Lewy bodies (Spillantini *et al*, 1998) are a prerequisite for the histopathological diagnosis of PD and DLB, only an imperfect correlation between the Lewy body load and severity of cognitive impairment is known (Hughes *et al*, 1992; Parkkinen *et al*, 2005). Several studies rather support synaptic failure as the predominant pathophysiological mechanism. Presynaptic neurotransmitter release has been proven to be unbalanced in PD (Nikolaus *et al*, 2009). Moreover, presynaptic  $\alpha$ -syn oligomers and micro-aggregates are thought to be responsible for neurodegeneration as well as for dendritic spine loss observed in postmortem DLB brains (Kramer & Schulz-Schaeffer, 2007).

Over the past few years, an increasing body of evidence supports the concept of the propagation of misfolded  $\alpha$ -syn species from neuron to neuron, where they are transported along axons and trigger the conversion of endogenous  $\alpha$ -syn into a pathologic form in culture and *in vivo* (Luk *et al*, 2012a,b). Aspects of progressive  $\alpha$ -syn aggregation—namely the spread along synaptically connected brain regions and the maturing of Lewy-like inclusions—can be recapitulated in model systems by exogenous introduction of *in vitro*-generated, preformed fibrils (PFFs) of  $\alpha$ -syn, which under certain conditions is even possible in non-transgenic animals (Luk *et al*, 2012a,b; Masuda-Suzukake *et al*, 2013; Osterberg *et al*, 2015).

Dendritic spines are small protrusions from the dendritic shaft which are highly regulated and have been shown to be altered in

1 Center for Neuropathology and Prion Research, Ludwig-Maximilians University, Munich, Germany

2 German Center for Neurodegenerative Diseases (DZNE), Munich, Germany

3 Munich Cluster of Systems Neurology (SyNergy), Munich, Germany

4 Departamento de Psicobiología, Universidad Nacional de Educación a Distancia (UNED), Madrid, Spain

5 Department of Neurology, Ludwig-Maximilians University, Munich, Germany

\*Corresponding author. Tel: +49 89 4400 46427; Fax: +49 89 4400 46429; E-mail: jochen.herms@med.uni-muenchen.de

several neurological disorders including neurodegenerative diseases (Fiala *et al*, 2002; Penzes *et al*, 2011; Murmu *et al*, 2013). Various studies in the field of  $\alpha$ -syn-related disorders have addressed the impairment of dendritic spines in brain areas like the striatum (McNeill *et al*, 1988; Day *et al*, 2006; Zaja-Milatovic *et al*, 2006; Finkelstein *et al*, 2016), the hippocampus (Winner *et al*, 2012), the olfactory bulb (Neuner *et al*, 2014), and naturally the substantia nigra (Patt *et al*, 1991). However, chronic effects of cortical  $\alpha$ -syn have not been studied extensively, even though it is becoming more and more evident that the cortical involvement in the pathophysiology of PD and DLB cannot be neglected.

This study aims to extend the understanding of the structural consequences of neocortical  $\alpha$ -syn accumulation on dendritic spines in a time-resolved manner. To address this question, we used chronic two-photon *in vivo* imaging to monitor spine dynamics over time, in young and aged transgenic mice overexpressing human wild-type  $\alpha$ -synuclein (PDGF-h- $\alpha$ -syn) (Masliah, 2000). Furthermore, we used PFFs as a tool to induce cortical  $\alpha$ -syn accumulation in mice expressing only the reporter transgene eGFP in order to study the structural consequences of  $\alpha$ -syn seeding on dendritic architecture and spines.

Here, we report detrimental effects on dendrites and dendritic spines due to  $\alpha$ -syn overexpression as well as seeding. Accumulation of  $\alpha$ -syn in the neocortex triggers the loss of dendritic spines, interferes with spine dynamics, and leads to dystrophic malformation of dendritic branches. Our combination of a transgenic and a PFF-seeding mouse model provides new insights on the  $\alpha$ -syn-dependent mechanisms that lead to dendritic spine decay in the cortex and therefore might create a better understanding of cognitive decline in synucleinopathies.

## Results

### Overexpression of wild-type human $\alpha$ -synuclein leads to changes in dendritic spine density and dynamics in aged mice

*In vivo* two-photon imaging was performed in three age groups of mice (3, 6, and 12 months), which were chosen according to previously published data on the progression of  $\alpha$ -syn accumulation and its corresponding behavioral phenotype (Masliah, 2000; Rockenstein *et al*, 2002; Amschl *et al*, 2013). We consider the 3-month-old cohort as “presymptomatic”, whereas the 6- and 12-month-old cohorts show a developing and fully fledged phenotype, respectively.

Previous long-term *in vivo* imaging studies have shown that spines are highly dynamic structural elements and can be classified accordingly: Persistent spines are long lasting and stable for weeks up to the entire life span, whereas transient spines are newly formed and lost within days (Grutzendler *et al*, 2002; Trachtenberg *et al*, 2002; Holtmaat *et al*, 2005). In both h- $\alpha$ -syn transgenic and control mice, dendritic images were analyzed for spine density and dynamics. Newly appeared and disappeared spines relative to the previous imaging session were marked as “gained” or “lost”, respectively. Spines that were gained at a certain time point and persisted for < 7 days were considered as being “transient” (Fig 1A).

Our image analysis in the 6- and 12-month-old cohorts revealed that the number of spines per  $\mu$ m was significantly lowered in mice

overexpressing h- $\alpha$ -syn. The ANOVA genotype main factor was significantly changed (6 M:  $F_{(1,7)} = 27.11$ ;  $P = 0.0012$  and 12 M:  $F_{(1,7)} = 55.78$ ;  $P = 0.0001$ ), denoting that h- $\alpha$ -syn mice exhibit considerably less ( $\approx 30\%$ ) dendritic spines on apical tuft dendrites but show no increase or decrease in spine density over the imaging time period relative to controls (Fig 1B).

Concerning spine dynamics, the fractions of both gained and lost spines were found to be elevated; however, only the comparison of the lost fractions reached statistical significance (6 M:  $F_{(1,7)} = 5.85$ ;  $P = 0.0461$  and 12 M:  $F_{(1,7)} = 8.86$ ;  $P = 0.0206$ ). As newly gained spines were disproportionately more often lost again, the fraction of transient spines showed a significant increase in both 6- and 12-month-old h- $\alpha$ -syn mice (6 M:  $F_{(1,7)} = 7.19$ ;  $P = 0.0315$  and 12 M:  $F_{(1,7)} = 24.25$ ;  $P = 0.0017$ ; Fig 1C).

As a consequence of the change in spine dynamics, the daily turnover ratios were found to be significantly elevated in h- $\alpha$ -syn mice (6 M:  $F_{(1,7)} = 5.65$ ;  $P = 0.0491$  and 12 M:  $F_{(1,7)} = 6.93$ ;  $P = 0.0338$ ; Fig 1D). In summary, we could show that spine density is significantly reduced and does not further change over the imaging interval of 35 days. Moreover, parameters of spine dynamics were profoundly changed in mice overexpressing  $\alpha$ -syn compared to controls. The significant increase in transient spine fraction both in 6 and 12 months of age indicates that compensatory mechanisms may take place. Since there are no significant differences between 6 and 12 months of age, spine pathology does not further progress after 6 months of age but has reached a stable equilibrium.

### Young adult $\alpha$ -synuclein overexpressing mice exhibit a different dynamic phenotype than aged mice

In order to reveal when the spine loss starts leading to reduced spine density in 6- and 12-month-old h- $\alpha$ -syn mice, we analyzed a 3-month-old cohort over 6 weeks. Different to the older cohort, we observed a progressive decrease in spine density, with a significant interaction between genotype and time in Bonferroni’s *post hoc* test ( $F_{(5,30)} = 15.18$ ;  $P < 0.001$ ). Compared to controls, spine density in h- $\alpha$ -syn mice was reduced 12% on average at the first imaging time point (age of mice: 3 months) and 30% at the last imaging time point (age of mice: 4.5 months; Fig 2A).

Moreover, the dynamic fractions of spines show a somewhat contradictory picture compared to the 6- and 12-month-old mice. Our data revealed a significant impairment in the formation of new spines in h- $\alpha$ -syn mice ( $F_{(1,6)} = 8.71$ ;  $P = 0.0256$ ), while the fraction of lost spines was unaffected, which accounts for the progressive decrease in spine density. By implication, stable spines represent a significantly larger fraction in these mice ( $F_{(1,6)} = 8.71$ ;  $P = 0.0256$ ), while the fraction of transient spines is not significantly different from controls (Fig 2B). We also observed no significant change of the daily turnover ratio (TOR) between the groups at 3 months of age (Fig 2C).

Our results demonstrate that overexpression of human  $\alpha$ -syn leads to structural alterations of dendritic spines in the cerebral cortex. The alterations develop already in young adults at the age of 3–4.5 months, significantly before behavioral or motoric phenotypes become apparent (Amschl *et al*, 2013), but reach a state of dynamic equilibrium later and do not progress further until 12 months of age.

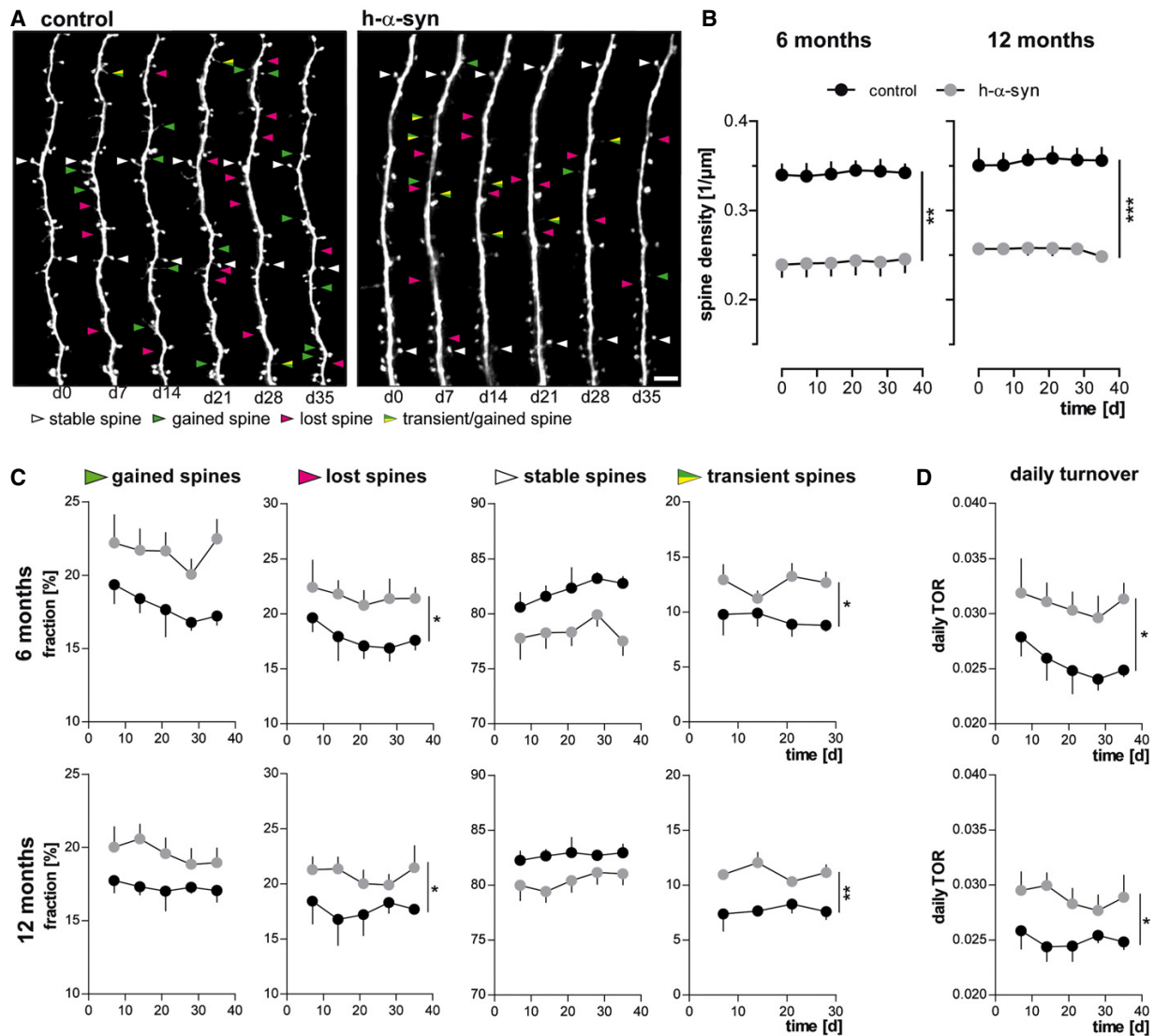


**Figure 1.**  $\alpha$ -Synuclein overexpression alters spine density and dynamics *in vivo*.

A Representative *in vivo* two-photon recordings of eGFP-labeled apical tuft dendrites in the somatosensory cortex in h- $\alpha$ -syn and control animals. Arrowheads mark representative spines that were stable (white, present > 7 days), newly formed (green), or lost (magenta). Gained spines that do not stabilize (yellow/green, present < 7 days) are defined as transient. Scale bar, 5  $\mu$ m.

B Spine density is reduced in both 6- (\*\* $P$  = 0.0012) and 12-month-old (\*\*\* $P$  = 0.0001) h- $\alpha$ -syn animals.

C The fractions of both gained ( $P_{6\text{ months}} = 0.0527$ ;  $P_{12\text{ months}} = 0.0678$ ) and lost spines ( $*P_{6\text{ months}} = 0.0461$ ;  $*P_{12\text{ months}} = 0.0206$ ) are elevated in h- $\alpha$ -syn mice compared to controls; the fraction of transient spines is significantly higher ( $*P_{6\text{ months}} = 0.0315$ ;  $**P_{12\text{ months}} = 0.0017$ ).

D Consequently, the daily turnover ratio (TOR) is significantly increased in both 6- and 12-month-old h- $\alpha$ -syn mice ( $*P_{6\text{ months}} = 0.0491$ ;  $*P_{12\text{ months}} = 0.0338$ ).

Data information:  $n = 5$  (h- $\alpha$ -syn),  $n = 4$  (control) animals, mean with s.e.m.; two-way ANOVA genotype main factor,  $*P < 0.05$ ,  $**P < 0.01$ ,  $***P < 0.001$ .

### Alterations in spine density and morphology in young adult and aged PDGF-h- $\alpha$ -syn mice

The progressive decrease in spine density seen in young adult mice could be monitored *in vivo* between 3 and 4.5 months of age. Extrapolation of the data curve (Fig 2A) of  $\alpha$ -syn overexpressing

animals to an earlier age would yield a time point at which no difference in synaptic spine densities between the groups is present. As chronic *in vivo* imaging in younger mice is technically not possible (bone growth in mice until 6–8 weeks of age, 4 weeks postsurgery necessary for chronic window clearing/healing), we addressed this question with a single time point *ex vivo* approach. Confocal

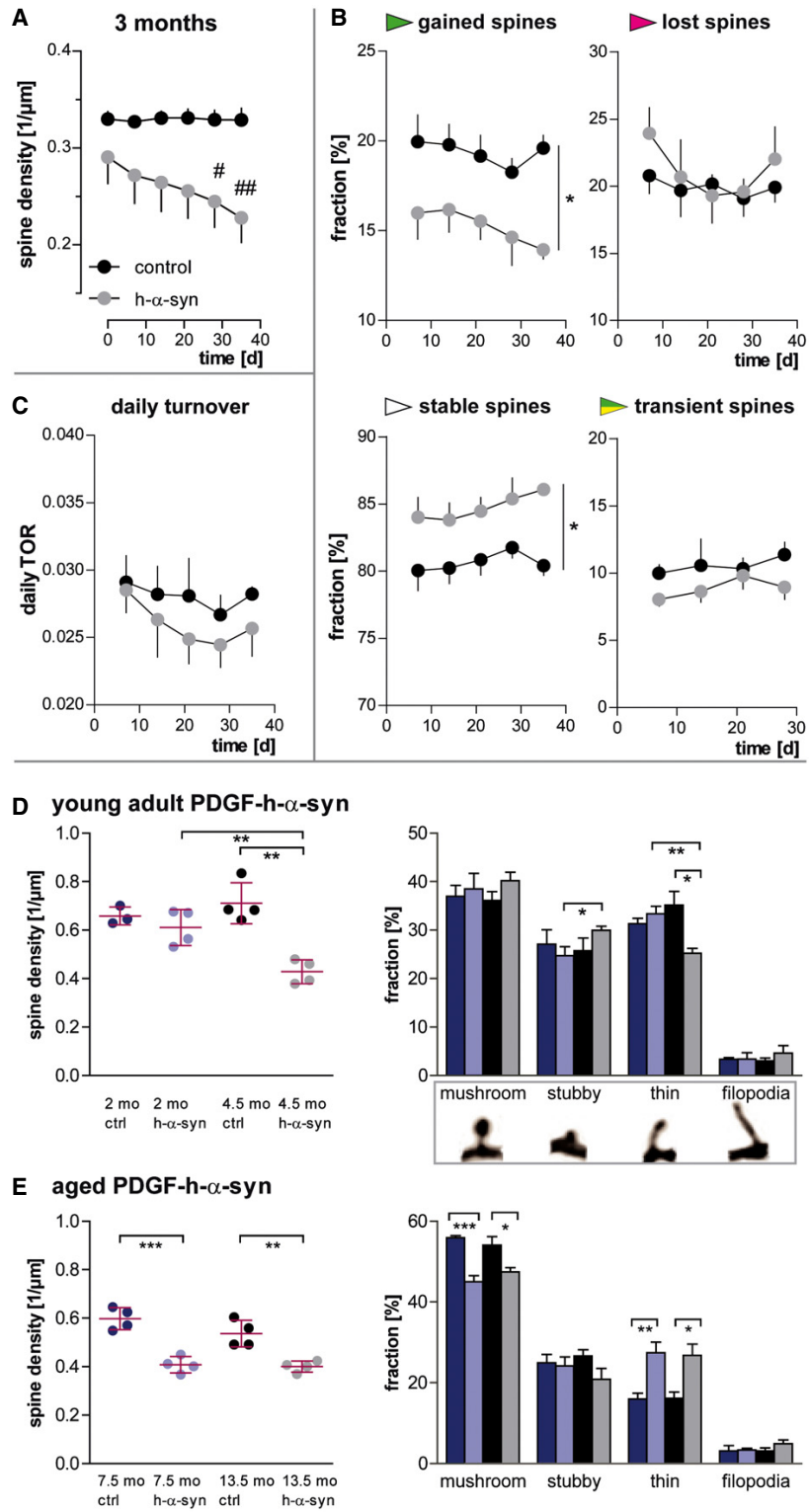


Figure 2.

**Figure 2.  $\alpha$ -Synuclein overexpression alters spine density, dynamics, and morphology differently depending on age.**

- A In young, 3-month-old h- $\alpha$ -syn mice, progressive decrease in spine density is observed *in vivo*.  
 B The loss of spines in young h- $\alpha$ -syn animals is driven by a reduced fraction of newly gained spines, while the fraction of lost spines remains unchanged and the fraction of stable spines is increased (\* $P_{\text{gained/stable}} = 0.0256$ ).  
 C The daily turnover of spines shows no significant difference between groups ( $P = 0.4062$ ).  
 D *Ex vivo* confocal data in young mice confirm synapse loss in h- $\alpha$ -syn mice between 2 and 4.5 months of age (\*\* $P_{\text{syn 2/4.5 months}} = 0.0064$ ; \*\* $P_{\text{ctrl/syn 4.5 months}} = 0.0012$ ) and show a shift in spine morphology toward relatively more stubby (\* $P_{\text{stubby}} = 0.0418$ ) and less thin spines (\*\* $P_{\text{h-}\alpha\text{-syn 2/4.5 months}} = 0.0044$ ; \* $P_{\text{ctrl/syn 4.5 months}} = 0.0155$ ).  
 E *Ex vivo* confocal data in aged h- $\alpha$ -syn mice show a decrease in total spine density (\*\*\* $P_{7.5 \text{ months}} = 0.0005$ ; \*\* $P_{13.5 \text{ months}} = 0.0039$ ) as well as in the fraction of mushroom spines (\*\*\* $P_{7.5 \text{ months}} = 0.0004$ ; \* $P_{13.5 \text{ months}} = 0.0298$ ), whereas the fraction of thin spines is increased (\*\* $P_{7.5 \text{ months}} = 0.0097$ ; \* $P_{13.5 \text{ months}} = 0.0155$ ).
- Data information: (A–C)  $n = 4$  animals per group; (D, E)  $n = 3–4$  animals per group as illustrated; mean with s.e.m.; Bonferroni's *post hoc* test (A): \* $P < 0.05$ , \*\* $P < 0.01$ , \*\*\* $P < 0.001$ ; two-way ANOVA genotype main factor (B, C): \* $P < 0.05$ , \*\* $P < 0.01$ , \*\*\* $P < 0.001$ ; Student's *t*-test (D, E): \* $P < 0.05$ , \*\* $P < 0.01$ , \*\*\* $P < 0.001$ .

imaging of apical tuft dendrites (layer I) was performed in brain slices of control as well as h- $\alpha$ -syn mice that were 2 and 4.5 months old. Note that the higher resolution of confocal microscopy in brain slices leads to an overall increased detection of spine density and a better ability to judge spine morphology. Two remarkable differences concerning the age and the genotype of the animal were observed. Firstly, at 2 months of age, there was no difference in spine density between control and transgenic animals, whereas at 4.5 months, spine density in h- $\alpha$ -syn mice showed a ~40% decrease ( $t_{(6)} = 5.770$ ;  $P = 0.0012$ ) relative to age-matched controls. Secondly, there was a significant difference in the spine densities of the h- $\alpha$ -syn mice ( $t_{(6)} = 4.097$ ;  $P = 0.0064$ ; ~30% reduction at 4.5 months) depending on their age, whereas this had no impact on the spine densities of control animals (Fig 2D).

In order to clarify whether the progressive spine loss in h- $\alpha$ -syn mice is reflected by changes in spine morphology, we furthermore analyzed spine shape for which three morphological subtypes have been defined (Rocheffort & Konnerth, 2012). Thin spines have an elongated appearance, with a long neck and a small spine head. Mushroom spines have the largest, round head, while stubby spines are devoid of a neck and appear as round elevation from the dendritic shaft. In addition, filopodia are very long and thin structures that lack a spine head and are considered the most dynamic of dendritic structures, which appear and disappear rapidly and only sometimes develop into one of the other spine types. In the morphological analysis of our confocal data, the absolute numbers (Appendix Fig S1A) as well as the fractions of mushroom, stubby and thin spines as well as filopodia, were comparable in 2-month-old mice independent of the expression of human  $\alpha$ -syn (Fig 2D).

In 4.5-month-old h- $\alpha$ -syn mice, the density of all morphological spine types is decreased (Appendix Fig S1A); however, not all types are lost to the same extent. The normalized fractions reveal a slight increase in the fraction of stubby spines ( $t_{(6)} = 2.579$ ;  $P = 0.0418$ ), whereas thin spines clearly represent a smaller fraction compared both to age-matched controls ( $t_{(6)} = 3.346$ ;  $P = 0.0155$ ) and to younger h- $\alpha$ -syn mice ( $t_{(6)} = 4.443$ ;  $P = 0.0044$ ) (Fig 2D).

The confocal imaging data from aged mice confirmed the reduction in spine density of ~30% in both 7.5- and 13.5-month-old h- $\alpha$ -syn brains. Compared to controls, the fractions of mushroom spines were decreased, while the fractions of thin spines were increased (Fig 2E and Appendix Fig S1B).

Taken together, our data confirmed our hypothesis that structural changes of dendritic spines develop within a certain time frame in young  $\alpha$ -syn overexpressing mice. This time frame was determined to be approximately between 2 and 4.5 months of age.

Before, the dendritic appearance in these mice is indistinguishable from healthy controls. Later,  $\alpha$ -syn overexpression causes changes in dendritic spines toward an overall lower spine density and a shift in spine morphology.

#### Intrastriatal injection of preformed $\alpha$ -synuclein fibrils triggers a progressive spread of endogenous protein aggregation

$\alpha$ -syn pathology can be induced in wild-type mice by injecting preformed fibrils (PFFs) (Luk *et al*, 2012a). Using this as a tool to investigate whether seeded pathology of disease-associated  $\alpha$ -syn will lead to structural alterations in synapses, we injected healthy 2-month-old GFP-M mice with PFFs prepared *in vitro*. Prior to injection, the quality of the injection material was controlled. The amyloid nature of PFFs was confirmed in a thioflavin T (ThT) assay, as ThT changes its fluorescent properties upon binding to amyloid  $\beta$ -sheet structures (Fig 3A). Differential centrifugation through a sucrose gradient confirmed the strongly increased sedimentation coefficient and thus the increased molecular density of PFFs compared to  $\alpha$ -syn monomers (Fig 3B). Finally, an electron micrograph visualized the fibrillary structure of PFFs (Fig 3C).

Sonicated PFFs were stereotactically injected into the striatum (Fig 3D), an area which contains extensive efferent and afferent projections to other brain regions and is affected in PD (Shepherd, 2013). As cortical neurons are the targets of interest in this study, the time-course and extent of  $\alpha$ -syn pathology progression into different layers of the neocortex was monitored at different days postinjection (dpi). The phosphorylation of  $\alpha$ -syn at S129 (pS129) is widely considered as a pathologic posttranslational modification (Tenreiro *et al*, 2014; Oueslati, 2016) and was used in this study to identify pathologic inclusions.

Striatal injection of PFFs resulted in intraneuronal aggregation of phosphorylated  $\alpha$ -syn (pS129-immunopositive) in the neocortex, at first confined to layer IV and V neurons (30–150 dpi), developing later to spread over all cortical layers (9 months postinjection; Fig 3E). pS129- $\alpha$ -syn inclusions appeared as cytoplasmic fibrillary forms (Fig 3F), which could also be stained by anti-ubiquitin (Fig 3G) and thioflavin S (Fig 3H and I), thereby presenting Lewy-body-like traits. Inclusions were also observed in the contralateral cortex relative to the injection site and the amygdala (Appendix Fig S2B). Due to a reported cross-reactivity between the pS129 antibody and phosphorylated neurofilament subunit L (NFL; Sacino *et al*, 2014b), we confirmed the presence of phosphorylated  $\alpha$ -synuclein inclusions with a costaining for NFL (Appendix Fig S2B and C). The



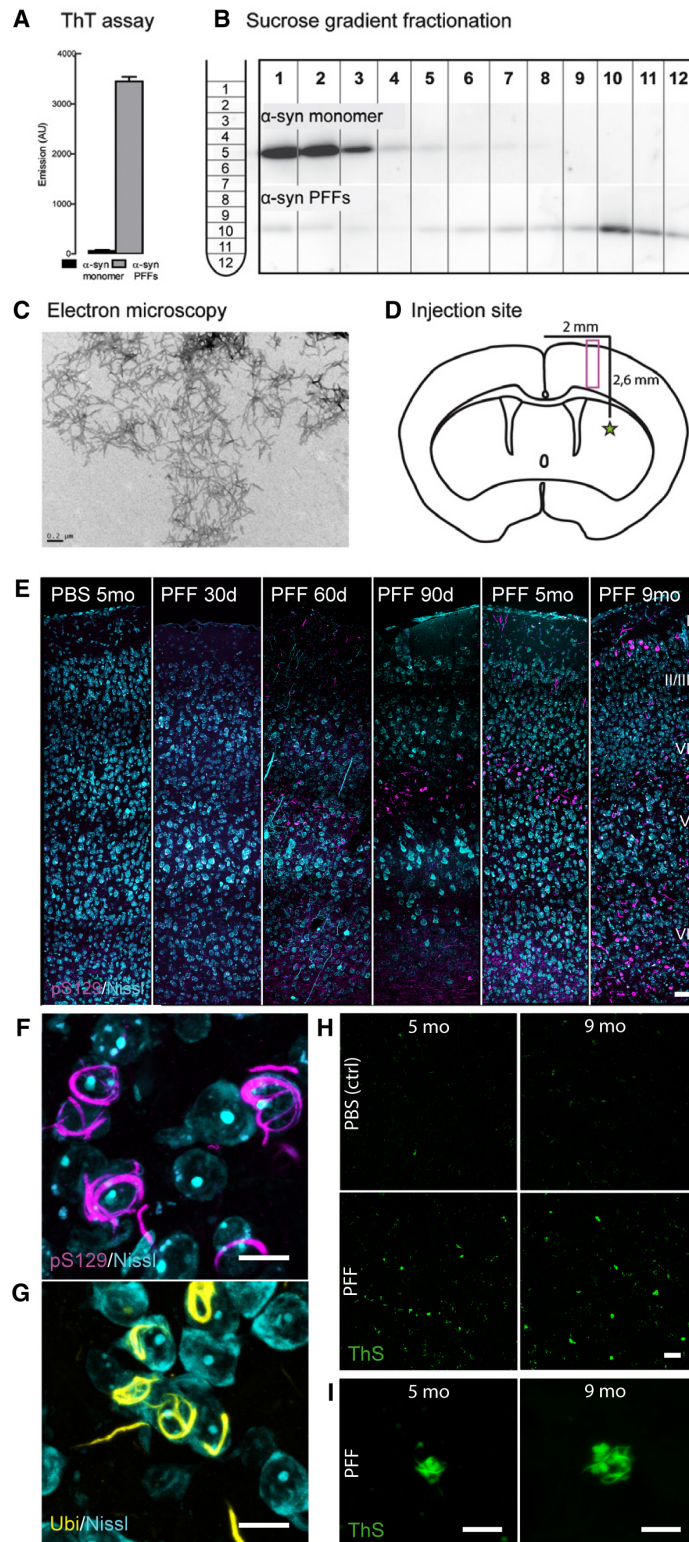


Figure 3.

**Figure 3. Injection of PFFs into the dorsal striatum triggers cortical  $\alpha$ -synuclein aggregation.**

A–C The quality of the injection material was verified using ThT fluorescence assay (A), sucrose-gradient fractionation (B), and electron microscopy (C). Scale bar: 0.2  $\mu$ m.

D Injection site, 0.2 mm anterior of the bregma (star) and imaging area (box) as depicted in (E).

E–I Representative images of the cortical layers I–VI in the somatosensory cortex of mice at different time points postinjection. Controls were injected with sterile PBS. Neurons in the layers IV and V of the somatosensory cortex contain aggregates of  $\alpha$ -synuclein phosphorylated at S129 (F), which are ubiquitin-positive (G) as well as thioflavin S-positive (H, I). Image stacks (E–I) are depicted as maximum intensity projections. Scale bars: 50  $\mu$ m (E), 10  $\mu$ m (F, G), 20  $\mu$ m (H), 5  $\mu$ m (I).

presence of pS129- $\alpha$ -syn inclusions across different brain regions is shown in Appendix Fig S2D.

Control brains injected with PBS did not show comparable immunopositive inclusions (Fig 3E). Importantly, also monomeric  $\alpha$ -syn injected into GFP-M mice as well as PFFs injected into  $\alpha$ -syn knock-out mice (SNCA KO) failed to induce the phenotype as observed after injection of PFFs (Appendix Fig S2E).

In order to further examine whether the effect can be attributed to templated conversion of endogenous mouse  $\alpha$ -syn into misfolded and aggregated species rather than just the uptake of PFFs by cells, control injections of fluorescently labeled PFFs into the striatum were performed. Twenty-four hours after the injection, the injection material was prominently detectable in the striatum, corpus callosum, and the injection canal (Appendix Fig S3B and C). At 6 dpi, however, the fluorescent material was removed from the injection site (Appendix Fig S3D) and later showed very little colocalization with developing pS129- $\alpha$ -syn-positive aggregates at 30 dpi (Appendix Fig S3E and F). We therefore conclude that the spreading of intracellular  $\alpha$ -syn aggregation in our model is dependent on the introduction of fibrillary  $\alpha$ -syn as a molecular template on top of endogenous  $\alpha$ -syn expression and not simply due to a cellular uptake of injected PFFs.

Considering inflammation as a contributor in neurodegenerative diseases (Perry *et al*, 2010) and synaptic plasticity (Morris *et al*, 2013) and as PFF-induced  $\alpha$ -syn accumulations have been associated with microglia (Sacino *et al*, 2014a), we assessed the presence and activation of microglia in the neocortex with two markers. Anti-Iba-1 marks all microglial cells including their processes, CD68 is a marker associated with active phagocytosis. We find that at the time point of spine analysis (5 months postinjection), the cortical area covered by microglia shows a tendency toward higher coverage, especially in layer IV (Appendix Fig S4A and B). We also observed a tendency for an increase in the coverage with activated microglia (Appendix Fig S4C and D) as well as occasional colocalization of CD8-positive microglia and pS129-positive aggregates (Appendix Fig S4E). However, variation between samples is high and the effect is not significant.

#### Seeded $\alpha$ -synuclein aggregates have detrimental effects on dendrites and spines

Advantageous to other mouse models, the seeding model does not require a disease-related transgene to induce a pathologic phenotype. In this way, we wanted to investigate structural alterations that might be the consequence of dose- and time-controlled molecular templating of  $\alpha$ -syn aggregates. Five months after the injection of PFFs or PBS (control) into the dorsal striatum, brain slices were stained for pS129-positive  $\alpha$ -syn aggregates, which were most abundant in layer IV and upper layer V of the cortex, including pyramidal

eGFP-expressing neurons (Appendix Fig S3A). In order to study whether structural changes might be solely attributed to a local effect of intracellular aggregates on neighboring dendrites or due to a more global disturbance in the synaptic network, we imaged apical dendrites located in two different layers (Fig 4A). Dendrites imaged in layer IV or V were spatially close to cells bearing an intraneuronal  $\alpha$ -syn accumulation, while tuft dendrites of layer I were distal to these cells (Fig 4B).

Indeed, we found alterations in spine density irrespective of the cortical location of the dendrites. In both layer IV/V ( $t_{(11)} = 3.628$ ;  $P = 0.004$ ) and layer I ( $t_{(11)} = 3.838$ ;  $P = 0.0028$ ), spine density was found to be lowered in brains which had been injected with PFFs and contained  $\alpha$ -syn aggregates (Fig 4C).

We next investigated how vulnerable the morphological spine types are in response to seeded  $\alpha$ -syn. In the layer IV/V dendrites, all types were lost to the same extent, leaving the fractions of mushroom, stubby, and thin spines comparable in controls and seeded animals (Appendix Fig S5B and Fig 4C). Contrarily, in apical tuft dendrites (layer I), thin spines proved to be more and stubby spines less vulnerable to seeded  $\alpha$ -syn. The fraction of thin spines was therefore decreased ( $t_{(11)} = 2.350$ ;  $P = 0.0385$ ), while the fraction of stubby spines was increased ( $t_{(11)} = 2.599$ ;  $P = 0.0247$ ) (Appendix Fig S5A and Fig 4C). This phenotype was already observed in our *ex vivo* spine data of young transgenic h- $\alpha$ -syn mice (see Fig 2) and could be reproduced here. On the presynaptic side, no overt change in the density of excitatory boutons could be detected in both the transgenic and the seeding mouse model (Appendix Fig S6I–L).

The irregular form of the tuft dendritic shafts in PFF-seeded brains was an additional observation. In controls, injected only with PBS, the diameter of dendritic shafts was found to be relatively uniform. In contrast, apical tuft dendrites of PFF-seeded mice showed an irregular appearance of the dendritic shaft. Over the length of the dendrites, large swellings could be observed as well as segments with an extremely narrow diameter (Fig 4D). In a histogram plotting the frequency of diameter values, dendritic shaft diameters follow a normal distribution ( $R^2 = 0.9263$ ) for the control animals. For the seeded mice, the variety of values is broader and the values are best described with two distributions: one at very low dendritic diameter ( $R^2 = 0.9250$ ) and one comparable to the control distribution ( $R^2 = 0.9664$ ), with the exception of the presence of abnormally high values (Fig 4E). As a consequence of the high variation, the mean standard deviation of the dendritic shaft diameter was found to be significantly increased ( $t_{(11)} = 3.054$ ;  $P = 0.011$ ) in mice that were seeded with  $\alpha$ -syn PFFs (Fig 4F). Note that this phenotype was only observed in our seeding, but not in the transgenic model.

With our approach, we could show that the introduction of  $\alpha$ -synuclein seeds and the consecutive accumulation in the cerebral

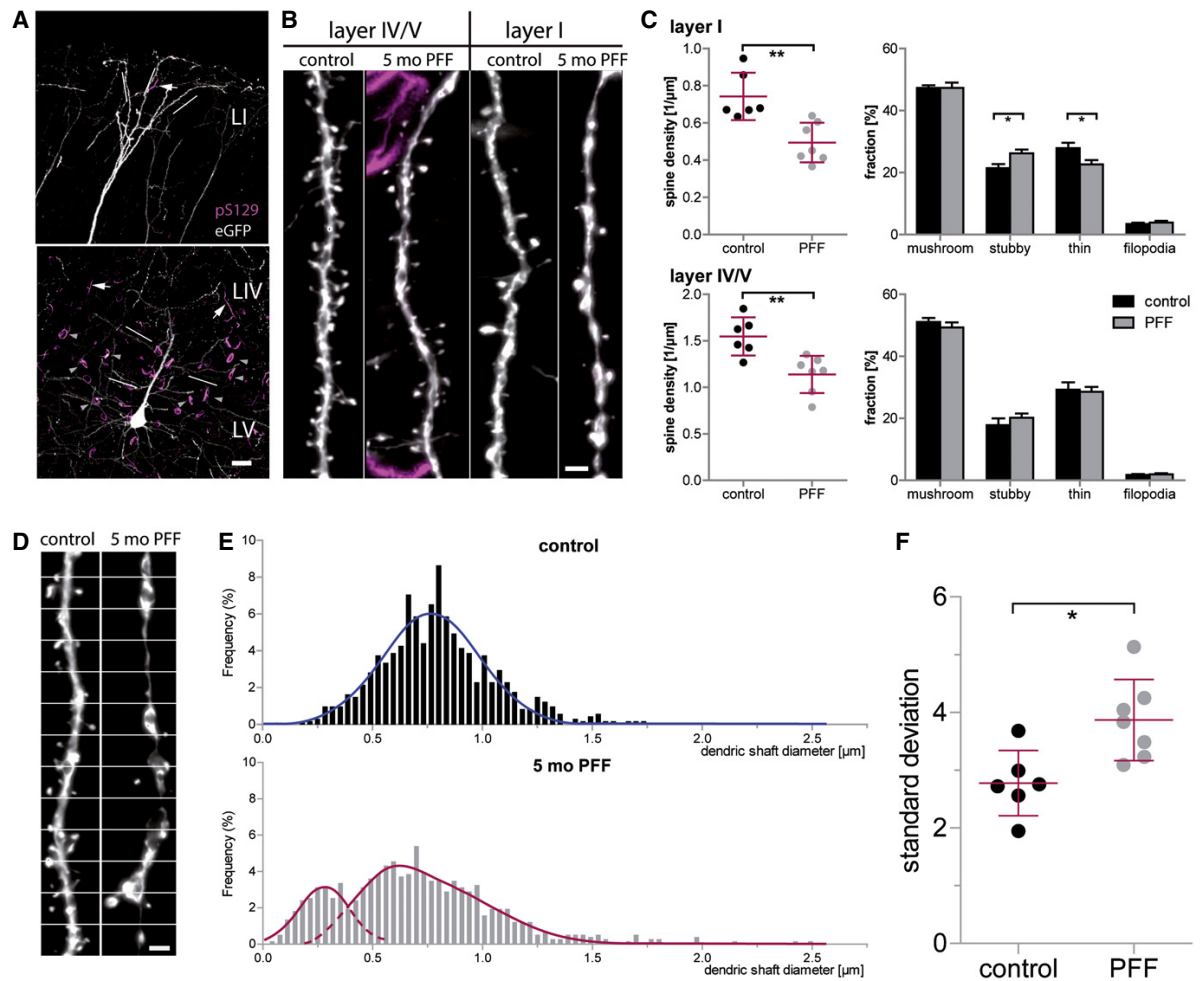


**Figure 4.** The presence of accumulated  $\alpha$ -synuclein induced by seeding 5 months prior to analysis causes spine loss and malformation in layer V apical dendrites.

- A  $\alpha$ -Synuclein aggregates occur as intrasomal (arrowheads) and neuritic (arrows) accumulations and are present predominantly in upper layer V and layer IV of the cortex. In layer I, pS129-positive structures are much less dense. Lines exemplarily mark dendrites used for analysis.
- B Spine analysis was performed on apical dendrites located in the cortical layers IV/V and I.
- C In layer I, spine density is reduced relative to PBS-injected controls (\*\* $P = 0.0028$ ), with the fraction of stubby spines being increased (\* $P = 0.0247$ ) and the fraction of thin spines being decreased (\* $P = 0.0385$ ). In layer IV/V, spine density is reduced as well (\*\* $P = 0.004$ ), without a significant effect on spine morphology.
- D In apical tuft dendrites of PFF-injected mice, dendrites display dystrophic swellings and parts of very small diameter; white lines: measurement positions.
- E Histograms of the dendritic shaft diameter.
- F Variation in the diameter of single dendrites in seeded mice compared to controls (\* $P = 0.011$ ).

Data information:  $n = 6$  (control),  $n = 7$  (PFF) animals, mean with s.e.m.; Student's  $t$ -test: \* $P < 0.05$ , \*\* $P < 0.01$ . Scale bars: 20  $\mu\text{m}$  (A), 2  $\mu\text{m}$  (B, D).

cortex triggers structural changes both at the level of the dendritic spine and the dendritic shaft.

## Discussion

This study presents converging evidence from two distinct approaches for the adverse effects of  $\alpha$ -syn accumulation for the density and structural plasticity of dendritic spines in the cerebral

cortex. Dendritic spines are excitatory postsynapses, and their loss has been described repeatedly as a structural correlate for cognitive impairment and dementia (Terry *et al*, 1991; Dickson *et al*, 1995; Bellucci *et al*, 2012; Picconi *et al*, 2012). Moreover, the effects of mutated and accumulated  $\alpha$ -syn have been studied in several brain regions. Striatal spine loss has been reported in various animal models of PD and in PD and DLB patients (McNeill *et al*, 1988; Zaja-Milatovic *et al*, 2006). In a mouse model overexpressing the human A53T  $\alpha$ -syn mutation, spine loss has been observed in the

striatum and in the hippocampus (Finkelstein *et al*, 2016). Some authors report that D2R striatopallidal neurons in reserpine and 6-OHDA-treated mice selectively lose spines (Day *et al*, 2006), while others found spine loss on both direct and indirect pathway neurons in 6-OHDA- or MPTP-treated models (Suárez *et al*, 2014). In contrast, another study failed to detect striatal spine loss in A53T mice, despite a decrease in the number of SNpc neurons (Oaks *et al*, 2013).  $\alpha$ -syn was also demonstrated to have negative impact on newly generated neurons of the hippocampus (Winner *et al*, 2012) and the olfactory bulb (Neuner *et al*, 2014), particularly on their dendrite outgrowth and spine development.

In our current study, we aimed to extend this knowledge with a chronic examination of spines in the cortex. As the chronic effects of  $\alpha$ -syn on cortical spine plasticity remain incompletely understood, we used two different mouse models which exhibit  $\alpha$ -syn accumulation in the cortex. In our transgenic model, wild-type human  $\alpha$ -syn was expressed under the PDGF promoter, leading to neocortical accumulation of mostly soluble protein located as inclusions in neuronal cell bodies as well as synaptic terminals (Masliah, 2000; Rockenstein *et al*, 2002; Amschl *et al*, 2013). Our seeding model was based on the striatal injection of preformed wild-type mouse  $\alpha$ -syn fibrils and caused a slowly progressing phenotype of phosphorylated  $\alpha$ -syn-positive neuronal inclusions, which first developed in the deeper layers of the neocortex and condensed over time to mature into fibrillary Lewy-like inclusions.

Our study also provides *in vivo* evidence that accumulation of wild-type  $\alpha$ -syn interferes with cortical spine plasticity and spine density which declined in young adult mice starting from about 3 months of age and stabilized at a reduced overall density in older mice ( $\approx 30\%$ ). This spine loss occurs well before behavioral impairments become apparent in these mice (Masliah, 2000; Amschl *et al*, 2013) and may be the result of a presymptomatic change in pre- and postsynaptic function.

While numerous studies have made great effort to unravel the molecular mechanism behind  $\alpha$ -syn toxicity, it remains to be clarified whether a toxic gain-of-function or a loss-of-function or both is responsible for synapse and cell loss. Among the toxic gain-of-function effects of  $\alpha$ -syn are the impairment of lysosomal and proteasomal protein degradation, induction of endoplasmic reticulum (ER) stress, Golgi fragmentation, and active formation of pores on cellular membranes (reviewed by Cookson & van der Brug, 2008). For instance, it was shown that the acute application of  $\alpha$ -synuclein oligomers onto autaptic hippocampal cultures as well as onto hippocampal slices significantly enhances basal NMDA receptor activation and the amplitude of AMPA-receptor-mediated synaptic currents (Hüls *et al*, 2011; Diogenes *et al*, 2012). This augmented excitatory transmission could be explained by (i)  $\alpha$ -syn oligomer-mediated pore formation in the postsynaptic membrane (Volles *et al*, 2001; Furukawa *et al*, 2006; Schmidt *et al*, 2012), (ii) enhancement of voltage-operated  $\text{Ca}^{2+}$  channel activity (Hettiarachchi *et al*, 2009), or (iii) inefficient membrane repolarization (Shrivastava *et al*, 2015), all causing increased calcium influx which in turn results in AMPA-receptor recruitment to the dendritic spine membrane (Byth, 2014). The resulting postsynapse is saturated with receptors and therefore unable to recruit extra AMPA receptors upon theta-burst stimulation which causes a long-term potentiation (LTP) decline and overall excitotoxicity (Yuste & Bonhoeffer, 2001; Diogenes *et al*, 2012). On the long term—as we

analyzed the structural impact of transgenic and seeded  $\alpha$ -synuclein during and after several months—this proposed mechanism based on a slightly but chronically enhanced calcium influx may disturb the tightly controlled, calcium-dependent machinery of synaptic plasticity. Likewise, a primary presynaptic pathology might alter synaptic vesicle release which as a long-term consequence may alter dendritic spine plasticity. Excessive  $\alpha$ -synuclein has been shown to inhibit neurotransmitter release via specifically reducing the size of the synaptic vesicle recycling pool (Nemani *et al*, 2010) as well as to regulate SNARE-driven membrane fusion (Garcia-Reitböck *et al*, 2010; Burre *et al*, 2015). A study in DLB brain tissue showed massive deposits of diffuse aggregates in the cortical and subcortical gray matter, which were located at synaptic terminals and were linked to dendritic spine loss. This suggests that the subcellular presynaptic location of  $\alpha$ -syn is important for its neurodegenerative effect (Kramer & Schulz-Schaeffer, 2007) and although our models show no overt presynaptic loss, an alteration in function seems likely. The functional roles of  $\alpha$ -synuclein, in conjunction with regulating actin dynamics and chaperoning the polymerization of microtubule-associated proteins (Sousa *et al*, 2009), would certainly impair spine stability and dendritic plasticity (Tsaneva-Atanasova *et al*, 2009).

The  $\alpha$ -syn loss-of-function hypothesis comprises that with progressing aggregation, endogenous  $\alpha$ -syn becomes sequestered into inclusions; be they oligomers, protofibrils, or mature LBs and LNs, leaving less functional protein to perform normal cellular functions (reviewed by Benskey *et al*, 2016). Particularly the changes seen after seeding with PFFs are supportive of this hypothesis. As previously shown and confirmed in this study through seeding of fluorescently tagged  $\alpha$ -syn fibrils, the aggregates formed are chiefly composed of endogenous  $\alpha$ -syn, with very little of the initial PFF seed being part of the developed inclusions (Luk *et al*, 2009). The concept of sequestration is further reinforced by the complete absence of inclusions and toxicity in  $\alpha$ -syn null mice seeded with PFFs (Volpicelli-Daley *et al*, 2011; Luk *et al*, 2012a). To complicate things even further, recent evidence suggests that microglial activity can contribute to both detrimental and protective mechanisms in neurodegenerative diseases (Morris *et al*, 2013; Miyamoto *et al*, 2016; Tang & Le, 2016). In our model, the infusion of PFFs did not cause overt and chronic microglial activation at the observed time point, but additional experiments might be necessary to gain a broader picture about the glial involvement in  $\alpha$ -syn-affected synapse dynamics.

From our imaging data, we cannot pin down which of these described mechanisms exactly are involved in the loss of spines, which emphasizes the need for further studies for clarification. Furthermore, as our *in vivo* data suggest, the mechanism underlying synapse loss and the shift in morphology may not even be uniform throughout the course of disease. Spine dynamics were found to be changed remarkably depending on the age of the animal upon observation. The decrease in gained spines observed in 3-month-old animals caused a progressive spine loss and is morphologically reflected in the diminished fraction of thin spines, which are known to correspond to non-synaptic transient precursors of the larger stabilized spines (Holtmaat *et al*, 2005; Arellano *et al*, 2007). Contrarily, in the two older groups (6 and 12 months), further spine loss was restrained by an elevation of the daily turnover ratios. This was in turn reflected by an increase in the fraction of thin spines.

Thus, we propose that the observed spine remodeling in these animals represents a compensatory mechanism for the loss of absolute spine number, thereby strengthening the remaining synaptic contacts.

In both our seeding and transgenic model, proteinaceous aggregates are present in the neocortex, albeit in two histopathological variances: while the PDGF promoter in the transgenic model drives a more or less uniform accumulation of non-fibrillary (Masliah, 2000)  $\alpha$ -syn in cortical neurons and synapses, seeding of PFFs leads to the formation and maturation of fibrillary Lewy-like structures in neurons connected to the dorsal striatum. Our results from our *in vivo* study in young transgenic mice are in line with the dendritic spine phenotype which can be induced through inoculation with PFFs. Dendritic spine loss in layer V pyramidal neurons as well as a redistribution of spine morphologies toward less thin spines can be observed 5 months after inoculation with PFFs. The observed spine loss was independent of whether the respective dendrite was spatially close to the cortical layer V, in which neuronal  $\alpha$ -syn

inclusions were most pronounced. Interestingly, dystrophic deformation of apical tuft dendrites was present in PFF-seeded brains. Dendritic varicosities have been described in other progressive neurodegenerative diseases and have been linked to dendritic spine loss in scrapie-injected rodents (Fuhrmann *et al*, 2007) and an Alzheimer's disease model (Bittner *et al*, 2010). The presence of axonal varicosities caused by  $\alpha$ -synuclein seeding has been reported (Rockenstein *et al*, 2005); furthermore, it has been shown that inclusions mature and condense over time and that aggregate bearing neurons selectively degenerate (Osterberg *et al*, 2015). Therefore, it seems likely that the degeneration of the respective cell body and the accompanying transport deficits are the cause for dystrophies and contribute to spine loss in our PFF-seeded brains.

For answering scientific questions, animal models in principle comprise advantages as well as drawbacks (Bezard *et al*, 2013). For example, all available genetic mouse models of synucleinopathies are able to model only a subset of symptoms known in the human disease cases. Promoter-driven protein expression is

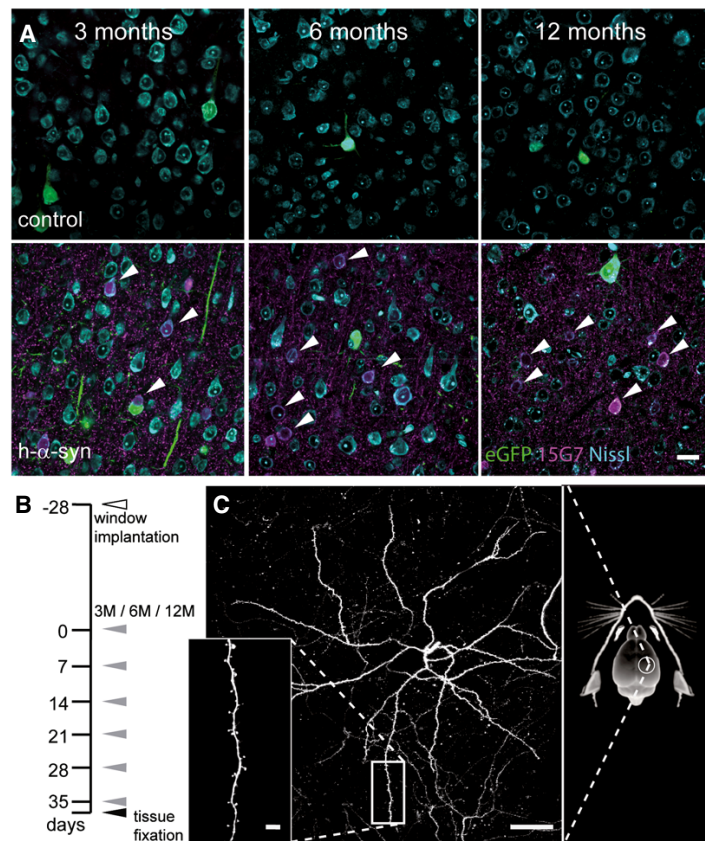


**Figure 5. Cortical  $\alpha$ -synuclein accumulation and long-term *in vivo* imaging of PDGF-h- $\alpha$ -syn  $\times$  GFP-M mice.**

A Immunostaining with 15G7 antibody shows cortical layer V overexpression of  $\alpha$ -synuclein (magenta) including accumulation in cell bodies (arrows).  
 B Experimental timeline: 4 weeks after window implantation (white arrowhead), imaging was performed over 6 weeks, once every 7 days (gray arrowheads) and finally followed by perfusion and tissue fixation directly after the last imaging session (black arrowhead).  
 C Overview and detailed projections of eGFP-labeled layer V apical dendrites in the somatosensory cortex, imaged through a chronic cranial window.

Data information: Scale bars: 20  $\mu$ m (A), 50  $\mu$ m (C), 5  $\mu$ m (C, inset).

limited to a cell population in which the promoter is active and is even complicated through the fact that background strain might affect the expression pattern (Chesselet *et al.*, 2008). Apart from that,  $\alpha$ -synuclein pathology induced by seeding of PFFs can be induced in wild-type animals (Luk *et al.*, 2012a) in a dose- and region-specific manner. Here, however, the unphysiologically large protein amount used for “planting the seed” should be considered. One strong point of our combined approach was to apply and compare both models, in order to best break down the actual structural impact of  $\alpha$ -syn accumulation on cortical neurons. Collectively, our results support the idea that  $\alpha$ -syn homeostasis is constantly balanced on a knife-edge and that perturbations that change its expression produces neurotoxicity with a common mechanism in which the critical events are protein misfolding, aggregate deposition, aggregate propagation, and synaptic dysfunction (Jucker & Walker, 2011; Guo & Lee, 2014; Luna & Luk, 2015). Our data provide evidence for the harmful structural consequences of excessive wild-type  $\alpha$ -synuclein on cortical dendrites throughout different pathological stages and may pave the way toward new therapeutic strategies for PD and DLB that focus on the maintenance of synaptic function.

## Materials and Methods

### Animals

PDGF-h- $\alpha$ -syn animals were obtained from QPS Austria Neuropharmacology (Grambach, Austria) and bred on a C57Bl/6 background. These transgenic mice overexpress human  $\alpha$ -synuclein (h- $\alpha$ -syn) under the regulatory control of the human platelet-derived growth factor- $\beta$  (PDGF- $\beta$ ) promoter (Masliah, 2000). Expression is strongest in the neocortex, hippocampus, olfactory bulb, and limbic system, leading to intraneuronal and synaptic  $\alpha$ -syn accumulation as early as 3 months of age (Fig 5A and Appendix Fig S6A–D) as well as progressive motor deficits (Masliah, 2000; Amschl *et al.*, 2013). Furthermore, C57Bl/6 wild type, Thy1-eGFP transgenic mice (GFP-M) (Jackson Laboratory, Bar Harbor, ME, USA), and  $\alpha$ -syn knock-out (SNCA KO) mice (Abeliovich *et al.*, 2000) were used. For *in vivo* imaging, the heterozygous PDGF-h- $\alpha$ -syn  $\times$  GFP-M (termed h- $\alpha$ -syn in this paper) line was created by interbreeding and the experiment involved three age cohorts of both male and female mice, in which mice were 3, 6 or 12 months old at the first imaging time point. All animals were housed in groups under pathogen-free conditions and bred in the animal housing facility at the Center for Neuropathology and Prion Research of the Ludwig Maximilians University of Munich, with food and water provided *ad libitum* (21  $\pm$  2°C, at 12/12-h light/dark cycle). After cranial window implantation, mice were housed separately. All experiments were approved by the Bavarian government (Az. 55.2-1-54-2532-163-13) and performed according to the animal protection law.

### Injection material and stereotactic injection

Recombinant wild-type mouse  $\alpha$ -synuclein was expressed in BL21 (DE3) *E. coli* using a pRK172 plasmid (kind gift from Kelvin Luk and Virginia Lee, University of Pennsylvania, USA) as previously described (Nuscher *et al.*, 2004; Kostka *et al.*, 2008). Briefly,

*Escherichia coli* BL21(DE3) (Invitrogen, MA, USA) were transformed with the plasmid, and expression was induced with isopropyl  $\beta$ -D-1-thiogalactopyranoside (IPTG, Peqlab, Erlangen, Germany). Cells were lysed by boiling after heat-inactivation of proteases. After centrifugation, the supernatant was filtered through Filtropur S 0.2 filters (Sarstedt, Nümbrecht, Germany), loaded on a HiTrap Q HP anion-exchange column (5 ml, GE Healthcare, Munich, Germany) and eluted with a linear 25 mM to 500 mM NaCl gradient. Synuclein containing fractions were concentrated using VivaSpin 2 columns (Sartorius, Göttingen, Germany). Protein concentration was assessed to 5 mg/ml in 50 mM Tris-HCl, pH = 7.0. After freezing in liquid nitrogen, the protein was stored at  $-80^{\circ}\text{C}$ . Appendix Fig S2A shows blots from the monomer preparation. Preformed fibrils (PFFs) were assembled from purified  $\alpha$ -synuclein monomer (5 mg/ml) by incubation at  $37^{\circ}\text{C}$  with constant agitation (1,400 rpm) in an orbital mixer (Eppendorf, Hamburg, Germany) for 96 h and stored at  $-80^{\circ}\text{C}$  (Conway *et al.*, 2000; Deeg *et al.*, 2015). For fluorescent labeling, purified  $\alpha$ -synuclein monomer (3.75 mg/ml, containing 100 mM NaHCO<sub>3</sub>) was incubated with 0.34 mg/ml Alexa Fluor<sup>®</sup> 488 NHS Ester (Life Technologies, Darmstadt, Germany) for 18 h at  $4^{\circ}\text{C}$ . The remaining free fluorophore was removed from the solution using PD-10 columns (GE Healthcare, PA, USA) according to the manufacturer's recommendations prior to fibril assembly as described above. Directly before injection, an aliquot of PFFs was sonicated four times with a handheld probe (SonoPuls Mini 20, MS1.5, Bandelin, Berlin, Germany) according to the following protocol: amplitude 30%; time 15 s (pulse on 3 s, pulse off 6 s). Two-month-old mice (male or female) were anesthetized with ketamine/xylazine (0.13/0.01 mg/g body weight; WDT/Bayer Health Care, Garbsen/Leverkusen, Germany) and stereotactically injected with 5  $\mu\text{l}$  (25  $\mu\text{g}$ ) of PFFs into the dorsal striatum (coordinates relative to the bregma: +0.2 mm anterior, +2.0 mm from midline, +2.6 mm beneath the dura) of the right hemisphere using a 5- $\mu\text{l}$  Hamilton syringe. Injections were performed at 400 nl/min with the needle in place after injection for at least 5 min. Control animals received sterile PBS or 5  $\mu\text{l}$  of 5 mg/ml monomeric  $\alpha$ -synuclein. Animals were monitored regularly after the surgery and sacrificed at different predetermined time points (30 days, 60 days, 90 days, 5 months, and 9 months after injections) for perfusion and tissue fixation with 4% paraformaldehyde.

### Thioflavin T binding and sucrose gradient

For *in vitro* measurement of thioflavin T (ThT) binding, 10  $\mu\text{M}$  ThT was added to 100  $\mu\text{g}/\text{ml}$  monomeric  $\alpha$ -synuclein or PFFs and incubated at  $30^{\circ}\text{C}$  for 10 min. Fluorescence signal was excited at 420–460 nm and emission detected at 460–500 nm with a spectrofluorometer (FluoStar Optima, BMG Lab Tech, Jena, Germany). Continuous sucrose-gradient assay was performed as described previously (Friedlander *et al.*, 2002; Wagner *et al.*, 2013). Briefly, six layers of solutions with decreasing sucrose concentration (50 mM Tris pH 7.5, 0.1% NP-40, 10–60% D(+)-sucrose, respectively) were filled into a 4 ml 11  $\times$  60 mm polyallomer tube (Beckman Coulter, CA, USA). Finally, 200  $\mu\text{l}$  of 5  $\mu\text{M}$  protein in 1 $\times$  TBS (pH 7.5) containing 0.1% NP-40 was loaded on the top of the gradient. Ultracentrifugation with 100,000 g at  $4^{\circ}\text{C}$  for 1 h was performed using a Sw60Ti rotor (Beckman Coulter, USA). Resulting continuous gradients were

fractionated in volumes of 200  $\mu$ l. 20  $\mu$ l per fraction was analyzed by denaturing Western blot using a monoclonal antibody against mouse- $\alpha$ -synuclein (New England Biolabs, Frankfurt, Germany).

### Electron microscopy

$\alpha$ -Synuclein fibrils diluted to 5  $\mu$ M in H<sub>2</sub>O were adsorbed onto a Formvar-coated, carbon-stabilized copper grid. The grid was then rinsed briefly with H<sub>2</sub>O and stained with uranyl acetate and lead citrate. Digital images were captured at different magnifications on a Jeol JEM-1011 TEM (JEOL Inc., MA, USA) equipped with an 11 megapixel Orius CCD digital camera (Gatan Inc. CA, USA).

### Cranial window

A cranial window was implanted over the right cortical hemisphere as previously reported (Fuhrmann *et al*, 2007). In short, the mice were given an intraperitoneal injection of ketamine/xylazine to reach surgical anesthesia. Additionally, dexamethasone (0.01 mg/g body weight; CP Pharma, Burgdorf, Germany) was intraperitoneally administered immediately before surgery (Holtmaat *et al*, 2009). A circular piece of the skull (4 mm in diameter) over the right hemisphere (centered over the parietal bone, approx. 5.5 mm caudal from the bregma and 5.5 mm lateral from midline) was removed using a dental drill (Schick-Technikmaster C1; Pluradent; Offenbach, Germany). The craniotomy was closed immediately with a round coverslip (4 mm in diameter), held with dental acrylic. A small z-shaped titan bar was glued next to the coverslip to allow repositioning of the mouse during subsequent imaging sessions. After surgery, mice received subcutaneous analgesic treatment with carprofen (5 mg/kg body weight; Rimadyl; Pfizer, NY, USA) and antibiotic treatment with cefotaxime (0.06 mg/kg body weight; Sanofi-Aventis, Frankfurt, Germany).

### Long-term *in vivo* imaging

Imaging started 4 weeks after the cranial window preparation to allow the animals to recover from surgery. After 6 weekly 2-photon *in vivo* imaging sessions, mice were sacrificed and their brains were fixed for further analyses (Fig 5B). Two-photon imaging was performed on a LSM 7 MP (Zeiss, Jena, Germany) equipped with GaAsP detectors and a 20 $\times$  water-immersion objective (W Plan-Apochromat 20 $\times$ /1.0 DIC, 1.0 NA, Zeiss, Jena, Germany). eGFP was excited at 880 nm by a Ti:Sa laser (MaiTai DeepSee, Spectra-Physics, Darmstadt, Germany), and emission was collected from 440 to 500 nm. Image stacks of 425  $\times$  425  $\times$  249  $\mu$ m<sup>3</sup> were acquired using the “z-stack” mode of the microscope control software (ZEN 2012/ZEN 2010 64-bit) with a lateral resolution of 0.83 and 3  $\mu$ m separation distance between consecutive images. Mice were anesthetized with isoflurane (CP Pharma, Burgdorf, Germany) for imaging and fixed to a custom-made head holder using the attached metal bar. In subsequent imaging sessions, previously imaged volumes were identified by eye using the unique blood vessel pattern and fine adjusted by the position of previously imaged dendrites. This method enabled precise alignment of the same imaging volume over a period of 6 weeks (Fig 5C; Helmchen & Denk, 2005). In order to maintain stable fluorescence emission levels, the laser power was adjusted relative to imaging depth.

### Image processing and analysis of *in vivo* and *ex vivo* data

For image analysis, only microscope image data with sufficient eGFP expression and good signal-to-noise ratio over time were included and the experimenter was blinded to the genotype of the mice by assigning a random number to each animal. From each mouse (male or female,  $n = 4-5$  *in vivo*,  $n = 6-7$  seeding experiment, without randomization), 9–10 dendrites from at least three different positions underneath the cranial window or in slices were analyzed. The length of individual dendrites was measured in ZEN 2012 (Zeiss). Spines identified along the dendrite were marked as gained, lost, or stable. The mean density of dendritic spines was estimated for each time point and expressed over 1  $\mu$ m of dendrite length. The stability of spines was calculated based on the amount of spines that remained unaltered for at least two subsequent imaging sessions. The spine turnover rate (TOR) was assessed based on gain and loss of spines over each day of imaging, calculated as follows:  $TOR = (N_{gained} + N_{lost}) / (2 \times N_{present}) / I_t$ , where  $N_{gained}$ ,  $N_{lost}$ , and  $N_{present}$  represent the number of gained, lost, or total spines at time points of interest, respectively, while  $I_t$  is the number of days between consecutive imaging sessions. *Ex vivo* image analysis measurements were performed manually from maximal projection images of deconvoluted (AutoQuantX3, Media Cybernetics) confocal stacks. All spines along the dendrite were marked and categorized into three morphologically different classes, according to established criteria (Jung *et al*, 2011). For analysis of the dendritic diameter, length measurements were taken every 40 pixels along the dendritic shaft (control: 756 measurements,  $n = 6$ , PFF-seeded: 840 measurements,  $n = 7$ ) using ImageJ. To quantify the density of glutamatergic presynaptic boutons VGLUT1-positive Imaris 7.7.2 software was applied to detect VGLUT1-positive puncta. In detail, the spots detection algorithm was applied using an estimated diameter of 0.5  $\mu$ m in  $xy$  and an 1.5  $\mu$ m in  $z$ . Background subtraction was enabled, and region-growing type was set to local contrast with a manual threshold of 30 defined for all datasets. Only spots with a  $xy$  diameter greater than 0.4  $\mu$ m were counted as boutons. The data were compiled in MATLAB using ImarisXT interface.

### Statistical analysis

The sample size of animals and imaged dendrites per animal were chosen according to our previous experience in long-term imaging (Neuner *et al*, 2014; Filser *et al*, 2015). Graphs were created, and statistics were calculated in Prism v 5.04 (GraphPad Software, San Diego, CA, USA). For *in vivo* time series data, two-way ANOVA followed by the Bonferroni's *post hoc* test was used to compare the variance of spine parameters assessed over time in control and h- $\alpha$ -syn animals. For assessment of inter-group differences at single time points, Student's *t*-test (unpaired, two-sided) was applied. Normal distribution was assumed according to the central limit theorem, as spine densities were calculated as the means of means for every mouse. For *t*-tests, the variance between groups was tested (*F*-test) and not found to be significantly different. Data are expressed as mean  $\pm$  SEM unless otherwise indicated, with  $P < 0.05$  defining differences as statistically significant (\* $P < 0.05$ ; \*\* $P < 0.01$ ; \*\*\* $P < 0.001$ ; for *post hoc* test: # $P < 0.05$ ; ## $P < 0.01$ ).

**The paper explained****Problem**

Parkinson's disease (PD) and is the second most common neurodegenerative disease with a prominent loss of nigrostriatal dopaminergic neurons. The resultant dopamine deficiency underlies the onset of typical motor symptoms. Apart from this, PD and other neurodegenerative conditions featuring misfolded and aggregated forms of the synaptic protein  $\alpha$ -synuclein ( $\alpha$ -syn) are frequently accompanied by cognitive decline and dementia, arising from the structural and functional changes in the brain cortical synapses. The role of  $\alpha$ -syn in the impairment of cortical circuitries and synaptic plasticity remains incompletely understood. We therefore investigated how  $\alpha$ -synuclein accumulation affects the plasticity of dendritic spines as the loss of these small protrusions from the neuronal dendritic shaft is widely considered a structural correlate for cognitive decline.

**Results**

Our study of the cortex involved two distinct *in vivo* mouse models: Long-term *in vivo* two-photon imaging of apical dendrites was performed in mice overexpressing wild-type human  $\alpha$ -syn. Additionally, intracranial injection of preformed  $\alpha$ -syn fibrils was performed to seed cortical  $\alpha$ -syn pathology in mice without an additional disease-related transgene. We find that  $\alpha$ -synuclein overexpressing mice show decreased spine density and abnormalities in spine dynamics in an age-dependent manner. We also provide evidence for the detrimental effects of seeded  $\alpha$ -syn aggregates on dendritic architecture, as we observed spine loss as well as dystrophic deformation of dendritic shafts in layer V pyramidal neurons of the cortex.

**Impact**

Our results demonstrate the impact of cortical  $\alpha$ -syn in a time-resolved manner and provide a link to the pathophysiology underlying dementia associated with  $\alpha$ -synucleinopathies. They may also enable the evaluation of potential drug candidates on dendritic spine pathology *in vivo*.

**Immunohistochemistry and confocal microscopy**

Animals in deep ketamine/xylazine anesthesia were killed by transcardiac perfusion with 1× phosphate-buffered saline (PBS) followed by 4% paraformaldehyde (w/v). The brains were postfixed in PBS containing 4% paraformaldehyde overnight before cutting 60- $\mu$ m-thick coronal sections on a vibratome (VT 1000S from Leica, Wetzlar, Germany). Immunofluorescence staining was performed on free-floating sections. Primary antibody incubation (overnight or 48 h (anti-VGLUT1), 4°C) was followed by 2 h of secondary antibody incubation at room temperature. Appendix Table S1 lists the antibodies used in this study. For unambiguous analysis of GFP-labeled neurons in eGFP-M mice, slices for spine analysis were re-stained with anti-GFP Alexa Fluor<sup>®</sup> 488 antibody (Invitrogen, Life Technologies GmbH). Sections for the study of neuronal  $\alpha$ -syn accumulation were incubated with a fluorescent Nissl stain (NeuroTrace™ 435/455, Thermo Fisher Scientific, USA). For mounting on glass coverslips, VECTASHIELD<sup>®</sup> Mounting Medium (Vector Laboratories) was used. Laser wavelengths used for excitation and collection range of emitted signals were as follows: Alexa Fluor<sup>®</sup> 488/eGFP—488 nm/500–550 nm; Alexa Fluor<sup>®</sup> 594—561 nm/585–743; Alexa Fluor<sup>®</sup> 647—633 nm/long-pass 650 nm; Nissl—750 nm/435–485 nm. Analysis of dendritic spines was limited to cortical apical dendrites from layer V neurons, cropped, and imaged at high

resolution. For imaging of presynaptic boutons, three-dimensional 16-bit data stacks of 1,024 × 1,024 × 26 pixels were acquired from four different positions in the somatosensory cortex at a lateral resolution of 0.1  $\mu$ m/pixel and an axial resolution of 0.4  $\mu$ m/pixel. Appendix Fig S6E–H illustrates the automatic bouton detection applying the algorithm.

**Expanded View** for this article is available online.

**Acknowledgements**

We thank Katharina Bayer, Sarah Hanselka, and Eric Griebinger for their excellent technical support and animal care. We like to give special thanks to Prof. Virginia Lee and Dr. Kelvin Luk for providing us with the plasmid for  $\alpha$ -syn expression and to S. Tahirovic for advice and kindly providing the CD68 antibody. We also thank MM. Dorostkar, S. Crux, S. Filser, and C. Sgobio for scientific support and advice on the manuscript. This work was funded the Munich Cluster for Systems Neurology SyNergy (EXC 1010).

**Author contributions**

SB performed design, data collection, analysis and interpretation of experiments and wrote the manuscript. EFR contributed to the data collection in *in vivo* experiments. FP analyzed presynaptic terminals. LB-L provided electron micrographs from  $\alpha$ -synuclein PFFs. AG and FS provided experimental material and expertise in  $\alpha$ -synuclein purification in PFF assembly. EFR and FS helped with manuscript preparation. JH supervised the study; contributed to conception, design, and manuscript writing; and provided financial support and final approval of the manuscript.

**Conflict of interest**

The authors declare that they have no conflict of interest.

**References**

- Aarsland D, Beyer MK, Kurz MW (2008) Dementia in Parkinson's disease. *Curr Opin Neurol* 21: 676–682
- Abeliovich A, Schmitz Y, Fariñas I, Choi-Lundberg D, Ho W-H, Castillo PE, Shinsky N, Verdugo JMG, Armanini M, Ryan A *et al* (2000) Mice lacking  $\alpha$ -Synuclein display functional deficits in the nigrostriatal dopamine system. *Neuron* 25: 239–252
- Amschl D, Neddens J, Havas D, Flunkert S, Rabl R, Römer H, Rockenstein E, Masliah E, Windisch M, Hutter-Paier B (2013) Time course and progression of wild type  $\alpha$ -Synuclein accumulation in a transgenic mouse model. *BMC Neurosci* 14: 6
- Arellano JI, Espinosa A, Fairén A, Yuste R, DeFelipe J (2007) Non-synaptic dendritic spines in neocortex. *Neuroscience* 145: 464–469
- Bellucci A, Zaltieri M, Navarra L, Grigoletto J, Missale C, Spano P (2012) From  $\alpha$ -synuclein to synaptic dysfunctions: new insights into the pathophysiology of Parkinson's disease. *Brain Res* 1476: 183–202
- Benskey MJ, Perez RG, Manfredsson FP (2016) The contribution of alpha synuclein to neuronal survival and function – Implications for Parkinson's disease. *J Neurochem* 137: 331–359
- Bezard E, Yue Z, Kirik D, Spillantini MG (2013) Animal models of Parkinson's disease: limits and relevance to neuroprotection studies. *Mov Disord* 28: 61–70
- Bittner T, Fuhrmann M, Burgold S, Ochs SM, Hoffmann N, Mitteregger G, Kretschmar H, LaFerla FM, Herms J (2010) Multiple events lead to dendritic spine loss in triple transgenic Alzheimer's disease mice. *PLoS One* 5: e15477



- Burn DJ (2004) Cortical Lewy body disease. *J Neurol Neurosurg Psychiatry* 75: 175–178
- Burre J, Sharma M, Sudhof TC (2015) Definition of a molecular pathway mediating  $\alpha$ -synuclein neurotoxicity. *J Neurosci* 35: 5221–5232
- Byth LA (2014)  $Ca^{2+}$ - and CaMKII-mediated processes in early LTP. *Ann Neurosci* 21: 151–153
- Chesselet M-F, Fleming S, Mortazavi F, Meurers B (2008) Strengths and limitations of genetic mouse models of Parkinson's disease. *Parkinsonism Relat Disord* 14: S84–S87
- Clayton DF, George JM (1999) Synucleins in synaptic plasticity and neurodegenerative disorders. *J Neurosci Res* 58: 120–129
- Conway KA, Harper JD, Lansbury PT (2000) Fibrils formed *in vitro* from  $\alpha$ -Synuclein and two mutant forms linked to Parkinson's disease are typical amyloid. *Biochemistry* 39: 2552–2563
- Cookson MR, van der Brug M (2008) Cell systems and the toxic mechanism(s) of  $\alpha$ -synuclein. *Exp Neurol* 209: 5–11
- Day M, Wang Z, Ding J, An X, Ingham CA, Shering AF, Wokosin D, Ilijic E, Sun Z, Sampson AR et al (2006) Selective elimination of glutamatergic synapses on striatopallidal neurons in Parkinson disease models. *Nat Neurosci* 9: 251–259
- Deeg AA, Reiner AM, Schmidt F, Schueder F, Ryazanov S, Ruf VC, Giller K, Becker S, Leonov A, Griesinger C et al (2015) Anle138b and related compounds are aggregation specific fluorescence markers and reveal high affinity binding to  $\alpha$ -synuclein aggregates. *Biochim Biophys Acta* 1850: 1884–1890
- Dickson DW, Crystal HA, Bevona C, Honer W, Vincent I, Davies P (1995) Correlations of synaptic and pathological markers with cognition of the elderly. *Neurobiol Aging* 16: 285–298
- Diogenes MJ, Dias RB, Rombo DM, Vicente Miranda H, Maiolino F, Guerreiro P, Nasstrom T, Franquelim HG, Oliveira LMA, Castanho MARB et al (2012) Extracellular alpha-synuclein oligomers modulate synaptic transmission and impair LTP via NMDA-receptor activation. *J Neurosci* 32: 11750–11762
- Fiala JC, Spacek J, Harris KM (2002) Dendritic spine pathology: cause or consequence of neurological disorders? *Brain Res Rev* 39: 29–54
- Filser S, Ovsepian SV, Masana M, Blazquez-Llorca L, Brandt Elvang A, Volbracht C, Müller MB, Jung CKE, Herms J (2015) Pharmacological inhibition of BACE1 impairs synaptic plasticity and cognitive functions. *Biol Psychiatry* 77: 729–739
- Finkelstein DI, Hare DJ, Billings JL, Sedjahtera A, Nurjono M, Arthofer E, George S, Culvenor JG, Bush AI, Adlard PA (2016) Clioquinol improves cognitive, motor function, and microanatomy of the alpha-synuclein hA53T transgenic mice. *ACS Chem Neurosci* 7: 119–129
- Friedlander G, Schonberger O, Horonchik L, Yedidia Y, Shaked G, Gabizon R, Taraboulos A (2002) Protease-sensitive scrapie prion protein in aggregates of heterogeneous sizes. *Biochemistry* 41: 12868–12875
- Fuhrmann M, Mitteregger G, Kretzschmar H, Herms J (2007) Dendritic pathology in prion disease starts at the synaptic spine. *J Neurosci* 27: 6224–6233
- Furukawa K, Matsuzaki-Kobayashi M, Hasegawa T, Kikuchi A, Sugeno N, Itoyama Y, Wang Y, Yao PJ, Bushlin I, Takeda A (2006) Plasma membrane ion permeability induced by mutant alpha-synuclein contributes to the degeneration of neural cells. *J Neurochem* 97: 1071–1077
- Garcia-Reitböck P, Anichtchik O, Bellucci A, Iovino M, Ballini C, Fineberg E, Ghetti B, Della Corte L, Spano P, Tofaris GK et al (2010) SNARE protein redistribution and synaptic failure in a transgenic mouse model of Parkinson's disease. *Brain* 133: 2032–2044
- Grutzendler J, Narayanan K, Gan W-B (2002) Long-term dendritic spine stability in the adult cortex. *Nature* 420: 810–812
- Guo JL, Lee VMY (2014) Cell-to-cell transmission of pathogenic proteins in neurodegenerative diseases. *Nat Med* 20: 130–138
- Helmchen F, Denk W (2005) Deep tissue two-photon microscopy. *Nat Methods* 2: 932–940
- Hettiarachchi NT, Parker A, Dallas ML, Pennington K, Hung C-C, Pearson HA, Boyle JP, Robinson P, Peers C (2009)  $\alpha$ -Synuclein modulation of  $Ca^{2+}$  signaling in human neuroblastoma (SH-SY5Y) cells. *J Neurochem* 111: 1192–1201
- Holtmaat AJGD, Trachtenberg JT, Wilbrecht L, Shepherd GM, Zhang X, Knott GW, Svoboda K (2005) Transient and persistent dendritic spines in the neocortex *in vivo*. *Neuron* 45: 279–291
- Holtmaat A, Bonhoeffer T, Chow DK, Chuckowree J, De Paola V, Hofer SB, Hübener M, Keck T, Knott G, Lee W-CA et al (2009) Long-term, high-resolution imaging in the mouse neocortex through a chronic cranial window. *Nat Protoc* 4: 1128–1144
- Hughes AJ, Daniel SE, Kilford L, Lees AJ (1992) Accuracy of clinical diagnosis of idiopathic Parkinson's disease: a clinico-pathological study of 100 cases. *J Neurol Neurosurg Psychiatry* 55: 181–184
- Hüls S, Högen T, Vassallo N, Danzer KM, Hengerer B, Giese A, Herms J (2011) AMPA-receptor-mediated excitatory synaptic transmission is enhanced by iron-induced  $\alpha$ -synuclein oligomers:  $\alpha$ -synuclein oligomers alter synaptic transmission. *J Neurochem* 117: 868–878
- Jucker M, Walker LC (2011) Pathogenic protein seeding in Alzheimer disease and other neurodegenerative disorders. *Ann Neurol* 70: 532–540
- Jung CKE, Fuhrmann M, Honarnejad K, Van Leuven F, Herms J (2011) Role of presenilin1 in structural plasticity of cortical dendritic spines *in vivo*: effect of PS1 on structural plasticity. *J Neurochem* 119: 1064–1073
- Kostka M, Högen T, Danzer KM, Levin J, Habeck M, Wirth A, Wagner R, Glabe CG, Finger S, Heinzelmann U et al (2008) Single particle characterization of iron-induced pore-forming  $\alpha$ -synuclein oligomers. *J Biol Chem* 283: 10992–11003
- Kramer ML, Schulz-Schaeffer WJ (2007) Presynaptic alpha-synuclein aggregates, not lewy bodies, cause neurodegeneration in dementia with Lewy bodies. *J Neurosci* 27: 1405–1410
- Krüger R, Kuhn W, Müller T, Woitalla D, Graeber M, Kösel S, Przuntek H, Epplen JT, Schöls L, Riess O (1998) Ala30Pro mutation in the gene encoding alpha-synuclein in Parkinson's disease. *Nat Genet* 18: 106–108
- Lücking CB, Brice A (2000) Alpha-synuclein and Parkinson's disease. *Cell Mol Life Sci* 57: 1894–1908
- Luk KC, Song C, O'Brien P, Stieber A, Branch JR, Brunden KR, Trojanowski JQ, Lee VM-Y (2009) Exogenous  $\alpha$ -synuclein fibrils seed the formation of Lewy body-like intracellular inclusions in cultured cells. *Proc Natl Acad Sci USA* 106: 20051–20056
- Luk KC, Kehm V, Carroll J, Zhang B, O'Brien P, Trojanowski JQ, Lee VM-Y (2012a) Pathological  $\alpha$ -synuclein transmission initiates Parkinson-like neurodegeneration in nontransgenic mice. *Science* 338: 949–953
- Luk KC, Kehm VM, Zhang B, O'Brien P, Trojanowski JQ, Lee VMY (2012b) Intracerebral inoculation of pathological  $\alpha$ -synuclein initiates a rapidly progressive neurodegenerative  $\alpha$ -synucleinopathy in mice. *J Exp Med* 209: 975–986
- Luna E, Luk KC (2015) Bent out of shape:  $\alpha$ -synuclein misfolding and the convergence of pathogenic pathways in Parkinson's disease. *FEBS Lett* 589: 3749–3759
- Masliah E (2000) Dopaminergic loss and inclusion body formation in alpha-synuclein mice: implications for neurodegenerative disorders. *Science* 287: 1265–1269

- Masuda-Suzukake M, Nonaka T, Hosokawa M, Oikawa T, Arai T, Akiyama H, Mann DMA, Hasegawa M (2013) Prion-like spreading of pathological  $\alpha$ -synuclein in brain. *Brain* 136: 1128–1138
- McNeill TH, Brown SA, Rafols JA, Shoulson I (1988) Atrophy of medium spiny I striatal dendrites in advanced Parkinson's disease. *Brain Res* 455: 148–152
- Miyamoto A, Wake H, Ishikawa AW, Eto K, Shibata K, Murakoshi H, Koizumi S, Moorhouse AJ, Yoshimura Y, Nabekura J (2016) Microglia contact induces synapse formation in developing somatosensory cortex. *Nat Commun* 7: 12540
- Morris GP, Clark IA, Zinn R, Vissel B (2013) Microglia: a new frontier for synaptic plasticity, learning and memory, and neurodegenerative disease research. *Neurobiol Learn Mem* 105: 40–53
- Murmu RP, Li W, Holtmaat A, Li J-Y (2013) Dendritic spine instability leads to progressive neocortical spine loss in a mouse model of Huntington's disease. *J Neurosci* 33: 12997–13009
- Nemani VM, Lu W, Berge V, Nakamura K, Onoa B, Lee MK, Chaudhry FA, Nicoll RA, Edwards RH (2010) Increased expression of  $\alpha$ -synuclein reduces neurotransmitter release by inhibiting synaptic vesicle recluster after endocytosis. *Neuron* 65: 66–79
- Neuner J, Ovsepian SV, Dorostkar M, Filser S, Gupta A, Michalak S, Biel M, Herms J (2014) Pathological  $\alpha$ -synuclein impairs adult-born granule cell development and functional integration in the olfactory bulb. *Nat Commun* 5: 3915
- Nikolaus S, Antke C, Müller H-W (2009) *In vivo* imaging of synaptic function in the central nervous system. *Behav Brain Res* 204: 1–31
- Nuscher B, Kamp F, Mehnert T, Odoy S, Haass C, Kahle PJ, Beyer K (2004)  $\alpha$ -synuclein has a high affinity for packing defects in a bilayer membrane: a thermodynamics study. *J Biol Chem* 279: 21966–21975
- Oaks AW, Frankfurt M, Finkelstein DI, Sidhu A (2013) Age-dependent effects of A53T alpha-synuclein on behavior and dopaminergic function. *PLoS One* 8: e60378
- Osterberg VR, Spinelli KJ, Weston LJ, Luk KC, Woltjer RL, Unni VK (2015) Progressive aggregation of alpha-synuclein and selective degeneration of lewy inclusion-bearing neurons in a mouse model of parkinsonism. *Cell Rep* 10: 1252–1260
- Oueslati A (2016) Implication of alpha-synuclein phosphorylation at S129 in synucleinopathies: what have we learned in the last decade? *J Parkinsons Dis* 6: 39–51
- Parkkinen L, Kauppinen T, Pirttilä T, Autere JM, Alafuzoff I (2005)  $\alpha$ -Synuclein pathology does not predict extrapyramidal symptoms or dementia. *Ann Neurol* 57: 82–91
- Patt S, Gertz HJ, Gerhard L, Cervós-Navarro J (1991) Pathological changes in dendrites of substantia nigra neurons in Parkinson's disease: a Golgi study. *Histol Histopathol* 6: 373–380
- Penzes P, Cahill ME, Jones KA, VanLeeuwen J-E, Woolfrey KM (2011) Dendritic spine pathology in neuropsychiatric disorders. *Nat Neurosci* 14: 285–293
- Perry VH, Nicoll JAR, Holmes C (2010) Microglia in neurodegenerative disease. *Nat Rev Neurol* 6: 193–201
- Picconi B, Piccoli G, Calabresi P (2012) Synaptic dysfunction in Parkinson's disease. In *Synaptic plasticity: dynamics, development and disease*, Kreutz RM, Sala C (eds), pp 553–572. Vienna: Springer
- Polymeropoulos MH, Lavedan C, Leroy E, Ide SE, Dehejia A, Dutra A, Pike B, Root H, Rubenstein J, Boyer R et al (1997) Mutation in the alpha-synuclein gene identified in families with Parkinson's disease. *Science* 276: 2045–2047
- Rocheffort NL, Konnerth A (2012) Dendritic spines: from structure to *in vivo* function. *EMBO Rep* 13: 699–708
- Rockenstein E, Mallory M, Hashimoto M, Song D, Shults CW, Lang I, Masliah E (2002) Differential neuropathological alterations in transgenic mice expressing alpha-synuclein from the platelet-derived growth factor and Thy-1 promoters. *J Neurosci Res* 68: 568–578
- Rockenstein E, Schwach G, Ingolic E, Adame A, Crews L, Mante M, Pfragner R, Schreiner E, Windisch M, Masliah E (2005) Lysosomal pathology associated with alpha-synuclein accumulation in transgenic models using an eGFP fusion protein. *J Neurosci Res* 80: 247–259
- Sacino AN, Brooks M, McKinney AB, Thomas MA, Shaw G, Golde TE, Giasson BI (2014a) Brain injection of  $\alpha$ -synuclein induces multiple proteinopathies, gliosis, and a neuronal injury marker. *J Neurosci* 34: 12368–12378
- Sacino AN, Brooks M, Thomas MA, McKinney AB, McGarvey NH, Rutherford NJ, Ceballos-Diaz C, Robertson J, Golde TE, Giasson BI (2014b) Amyloidogenic  $\alpha$ -synuclein seeds do not invariably induce rapid, widespread pathology in mice. *Acta Neuropathol* 127: 645–665
- Schmidt F, Levin J, Kamp F, Kretzschmar H, Giese A, Bötzel K (2012) Single-channel electrophysiology reveals a distinct and uniform pore complex formed by  $\alpha$ -synuclein oligomers in lipid membranes. *PLoS One* 7: e42545
- Shepherd GMG (2013) Corticostriatal connectivity and its role in disease. *Nat Rev Neurosci* 14: 278–291
- Shrivastava AN, Redeker V, Fritz N, Pieri L, Almeida LG, Spolidoro M, Liebmann T, Bousset L, Renner M, Lena C et al (2015)  $\alpha$ -Synuclein assemblies sequester neuronal 3-Na<sup>+</sup>/K<sup>+</sup>-ATPase and impair Na<sup>+</sup> gradient. *EMBO J* 34: 2408–2423
- Simón-Sánchez J, Schulte C, Bras JM, Sharma M, Gibbs JR, Berg D, Paisan-Ruiz C, Lichtner P, Scholz SW, Hernandez DG et al (2009) Genome-wide association study reveals genetic risk underlying Parkinson's disease. *Nat Genet* 41: 1308–1312
- Sousa VL, Bellani S, Giannandrea M, Yousuf M, Valtorta F, Meldolesi J, Chieregatti E (2009)  $\alpha$ -Synuclein and its A30P mutant affect actin cytoskeletal structure and dynamics. *Mol Biol Cell* 20: 3725–3739
- Spillantini MG, Schmidt ML, Lee VM, Trojanowski JQ, Jakes R, Goedert M (1997) Alpha-synuclein in Lewy bodies. *Nature* 388: 839–840
- Spillantini MG, Crowther RA, Jakes R, Hasegawa M, Goedert M (1998)  $\alpha$ -Synuclein in filamentous inclusions of Lewy bodies from Parkinson's disease and dementia with Lewy bodies. *Proc Natl Acad Sci USA* 95: 6469–6473
- Suárez LM, Solís O, Caramés JM, Taravini IR, Solís JM, Murer MG, Moratalla R (2014) L-DOPA treatment selectively restores spine density in dopamine receptor D2-expressing projection neurons in dyskinetic mice. *Biol Psychiatry* 75: 711–722
- Tang Y, Le W (2016) Differential roles of M1 and M2 microglia in neurodegenerative diseases. *Mol Neurobiol* 53: 1181–1194
- Tenreiro S, Reimão-Pinto MM, Antas P, Rino J, Wawrzycka D, Macedo D, Rosado-Ramos R, Amen T, Waiss M, Magalhães F et al (2014) Phosphorylation modulates clearance of alpha-synuclein inclusions in a yeast model of parkinson's disease. *PLoS Genet* 10: e1004302
- Terry RD, Masliah E, Salmon DP, Butters N, DeTeresa R, Hill R, Hansen LA, Katzman R (1991) Physical basis of cognitive alterations in alzheimer's disease: synapse loss is the major correlate of cognitive impairment. *Ann Neurol* 30: 572–580
- Trachtenberg JT, Chen BE, Knott GW, Feng G, Sanes JR, Welker E, Svoboda K (2002) Long-term *in vivo* imaging of experience-dependent synaptic plasticity in adult cortex. *Nature* 420: 788–794
- Tsaneva-Atanasova K, Burgo A, Galli T, Holcman D (2009) Quantifying neurite growth mediated by interactions among secretory vesicles, microtubules, and actin networks. *Biophys J* 96: 840–857

- Volles MJ, Lee S-J, Rochet J-C, Shtilerman MD, Ding TT, Kessler JC, Lansbury PT (2001) Vesicle permeabilization by protofibrillar  $\alpha$ -synuclein: implications for the pathogenesis and treatment of Parkinson's disease. *Biochemistry* 40: 7812–7819
- Volpicelli-Daley LA, Luk KC, Patel TP, Tanik SA, Riddle DM, Stieber A, Meaney DF, Trojanowski JQ, Lee VM-Y (2011) Exogenous  $\alpha$ -synuclein fibrils induce Lewy body pathology leading to synaptic dysfunction and neuron death. *Neuron* 72: 57–71
- Wagner J, Ryazanov S, Leonov A, Levin J, Shi S, Schmidt F, Prix C, Pan-Montojo F, Bertsch U, Mitteregger-Kretschmar G et al (2013) Anle138b: a novel oligomer modulator for disease-modifying therapy of neurodegenerative diseases such as prion and Parkinson's disease. *Acta Neuropathol* 125: 795–813
- Winner B, Regensburger M, Schreglmann S, Boyer L, Prots I, Rockenstein E, Mante M, Zhao C, Winkler J, Masliah E et al (2012) Role of  $\alpha$ -synuclein in adult neurogenesis and neuronal maturation in the dentate gyrus. *J Neurosci* 32: 16906–16916
- Yuste R, Bonhoeffer T (2001) Morphological changes in dendritic spines associated with long-term synaptic plasticity. *Annu Rev Neurosci* 24: 1071–1089
- Zaja-Milatovic S, Keene CD, Montine KS, Leverenz JB, Tsuang D, Montine TJ (2006) Selective dendritic degeneration of medium spiny neurons in dementia with Lewy bodies. *Neurology* 66: 1591–1593
- Zarranz JJ, Alegre J, Gómez-Esteban JC, Lezcano E, Ros R, Ampuero I, Vidal L, Hoenicka J, Rodriguez O, Atarés B et al (2004) The new mutation, E46K, of  $\alpha$ -synuclein causes parkinson and Lewy body dementia. *Ann Neurol* 55: 164–173



**License:** This is an open access article under the terms of the Creative Commons Attribution 4.0 License, which permits use, distribution and reproduction in any medium, provided the original work is properly cited.

## **Appendix for**

### **Seeding and transgenic overexpression of $\alpha$ -synuclein triggers dendritic spine pathology in the neocortex**

Sonja Blumenstock, Eva F. Rodrigues, Finn Peters, Lidia Blazquez-Llorca, Felix Schmidt,  
Armin Giese and Jochen Herms\*

**\*To whom correspondence should be addressed:** [jochen.herms@med.uni-muenchen.de](mailto:jochen.herms@med.uni-muenchen.de)

## Table of contents

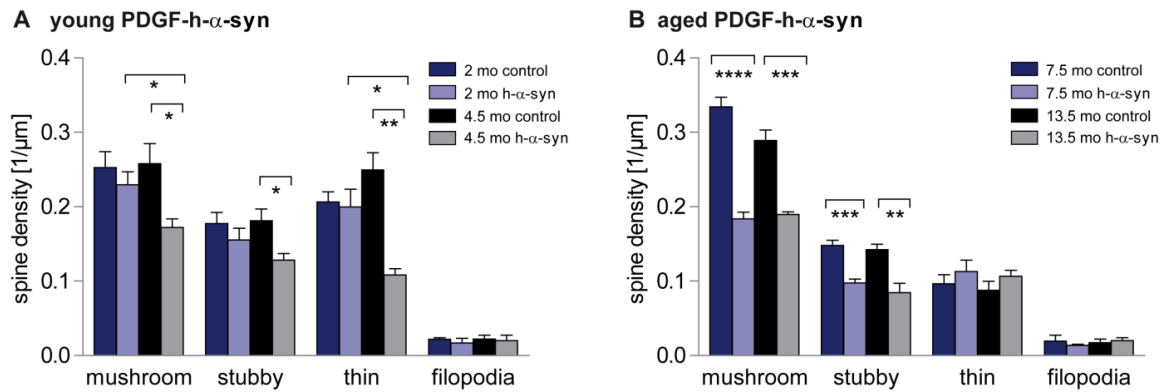
Appendix Table S1: Antibodies used in this study .....	2
Appendix Figure S1. Spine morphology changes in $\alpha$ -syn transgenic mice.....	3
Appendix Figure S2. Distribution of phosphorylated $\alpha$ -syn aggregates in the mouse brain.....	4
Appendix Figure S3: Templated misfolding of $\alpha$ -synuclein.....	5
Appendix Figure S4. Presence of microglia in the neocortex.....	6
Appendix Figure S5. Spine morphology changes in PFF-seeded mice (5 mo post-injection). 7	
Appendix Figure S6. Presynaptic glutamatergic bouton density does not differ in seeded or transgenic mice.....	8

**Appendix Table S1. Antibodies used in this study**

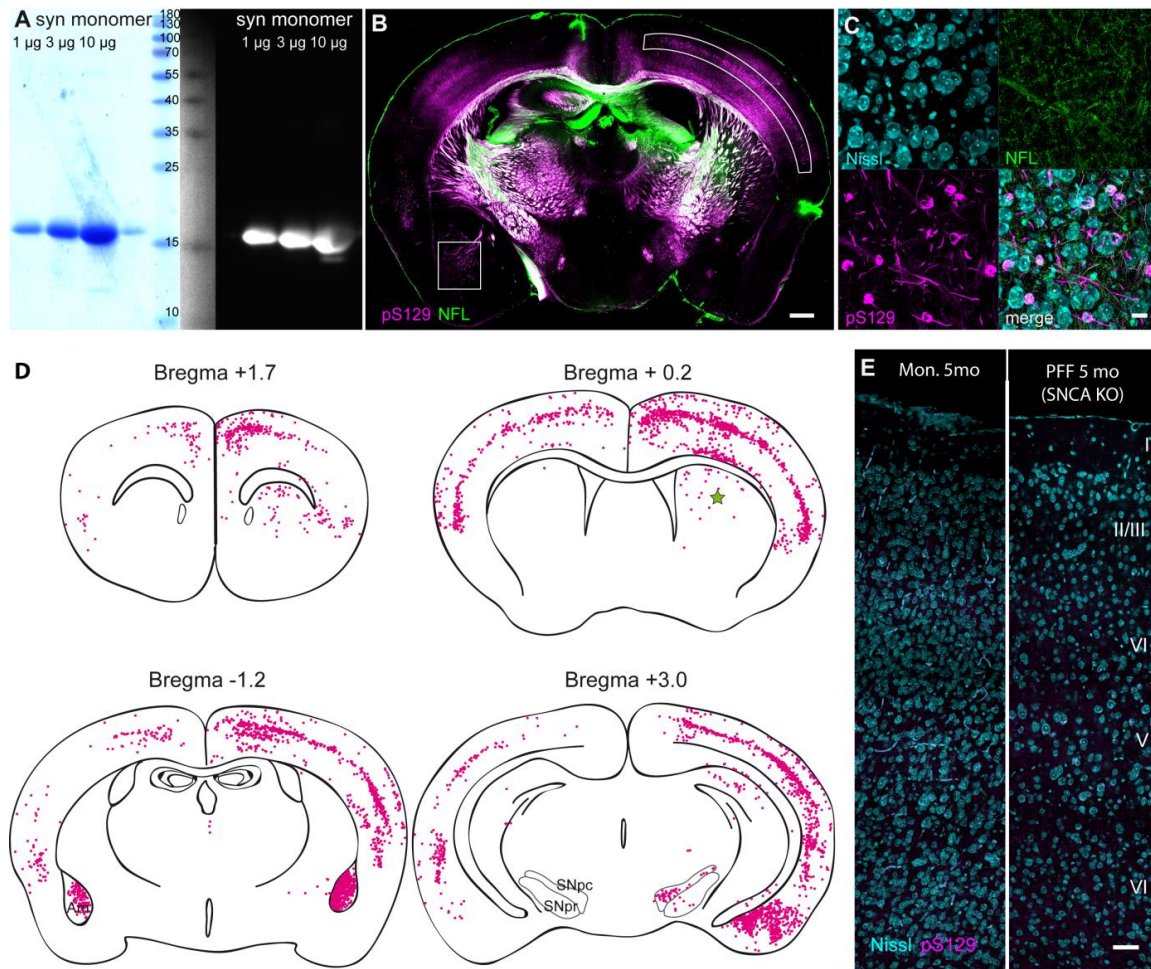
<b>Antibody</b>	<b>Source</b>	<b>Host</b>	<b>Dilution</b>
<b>Mouse <math>\alpha</math>-syn</b>	New England Biolabs (4179 S)	rabbit monoclonal	1:1000 (WB)
<b>15G7 human <math>\alpha</math>-syn</b>	(Neumann <i>et al.</i> , 2002)	rat monoclonal	1:500 (IF)
<b>pS129 <math>\alpha</math>-syn</b>	Abcam (ab59264)	rabbit polyclonal	1:200 (IF)
<b>Ubiquitin</b>	Abcam (ab7780)	rabbit polyclonal	1:500 (IF)
<b>Neurofilament-L (DA2)</b>	Cell Signaling (2835 S)	mouse monoclonal	1:200 (IF)
<b>Iba-1</b>	Wako (019-19741)	rabbit polyclonal	1:500 (IF)
<b>CD68</b>	BioRad (MCA 1957)	rat monoclonal	1:1000 (IF)
<b>VGLUT1</b>	Millipore (AB5905)	guinea pig polyclonal	1:200 (IF)
<b>anti-GFP Alexa488</b>	Invitrogen (A21311)	rabbit polyclonal	1:500 (IF)
<b>anti-rabbit Alexa 647</b>	Invitrogen (A21245)	goat polyclonal	1:200 (IF)
<b>anti-rat Alexa 647</b>	Invitrogen (A21247)	goat polyclonal	1:200 (IF)

**Reference:**

1. Neumann, M. *et al.* Misfolded proteinase K-resistant hyperphosphorylated  $\alpha$ -synuclein in aged transgenic mice with locomotor deterioration and in human  $\alpha$ -synucleinopathies. *J. Clin. Invest.* **110**, 1429–1439 (2002).

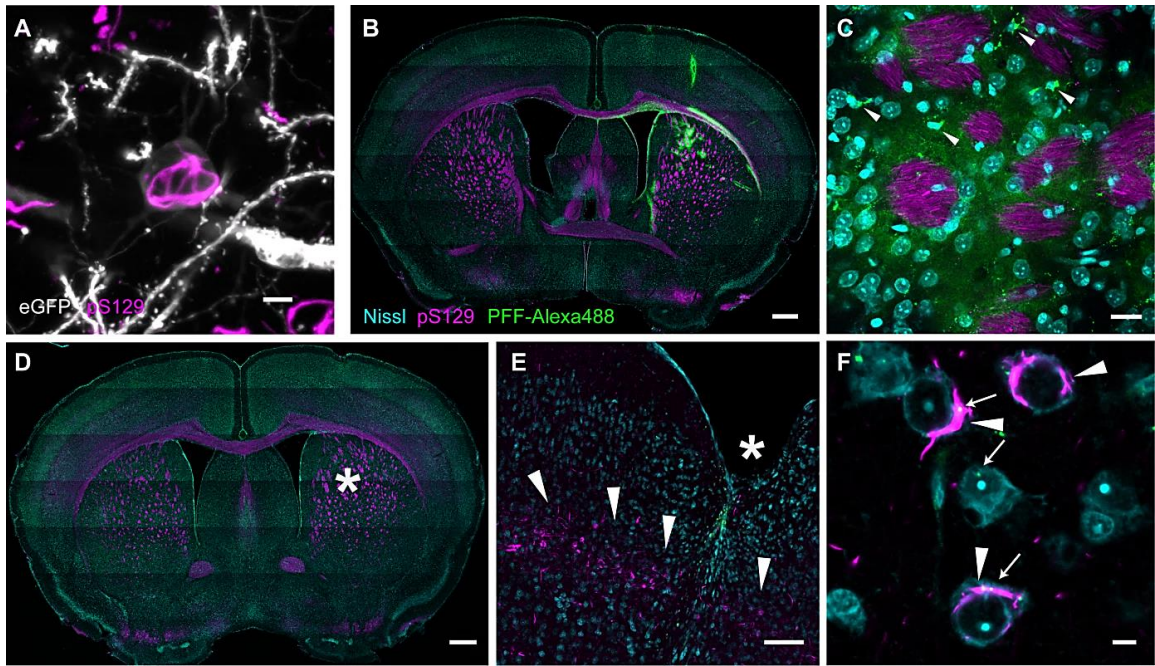


**Appendix Figure S1. Spine morphology changes in  $\alpha$ -syn transgenic mice.** Absolute densities of mushroom, stubby and thin spines in apical tuft dendrites of PDGF-h-a-syn mice compared to controls. (A) In young adult (2 and 4.5 months old) mice, the densities of mushroom ( $p_{\text{syn } 2/4.5\text{mo}} = 0.0326$ ;  $p_{\text{ctrl/syn } 4.5\text{mo}} = 0.0255$ ), stubby ( $p_{\text{syn } 2/4.5\text{mo}} = 0.025$ ) and thin spines ( $p_{\text{syn } 2/4.5\text{mo}} = 0.0107$ ;  $p_{\text{ctrl/syn } 4.5\text{mo}} = 0.0012$ ) are decreased. (B) In aged (7.5 and 13.5 months old) mice, the densities of mushroom ( $p_{7.5\text{mo}} < 0.0001$ ;  $p_{13.5\text{mo}} = 0.0005$ ) and stubby spines ( $p_{7.5\text{mo}} = 0.0009$ ;  $p_{13.5\text{mo}} = 0.008$ ) are decreased in h-a-syn mice compared to controls. A:  $n = 3$  (control 2 mo),  $n = 4$  animals per group. B:  $n = 4$  animals per group, mean with s.e.m; \* $p < 0.05$ , \*\* $p < 0.01$ . Student's t-test.

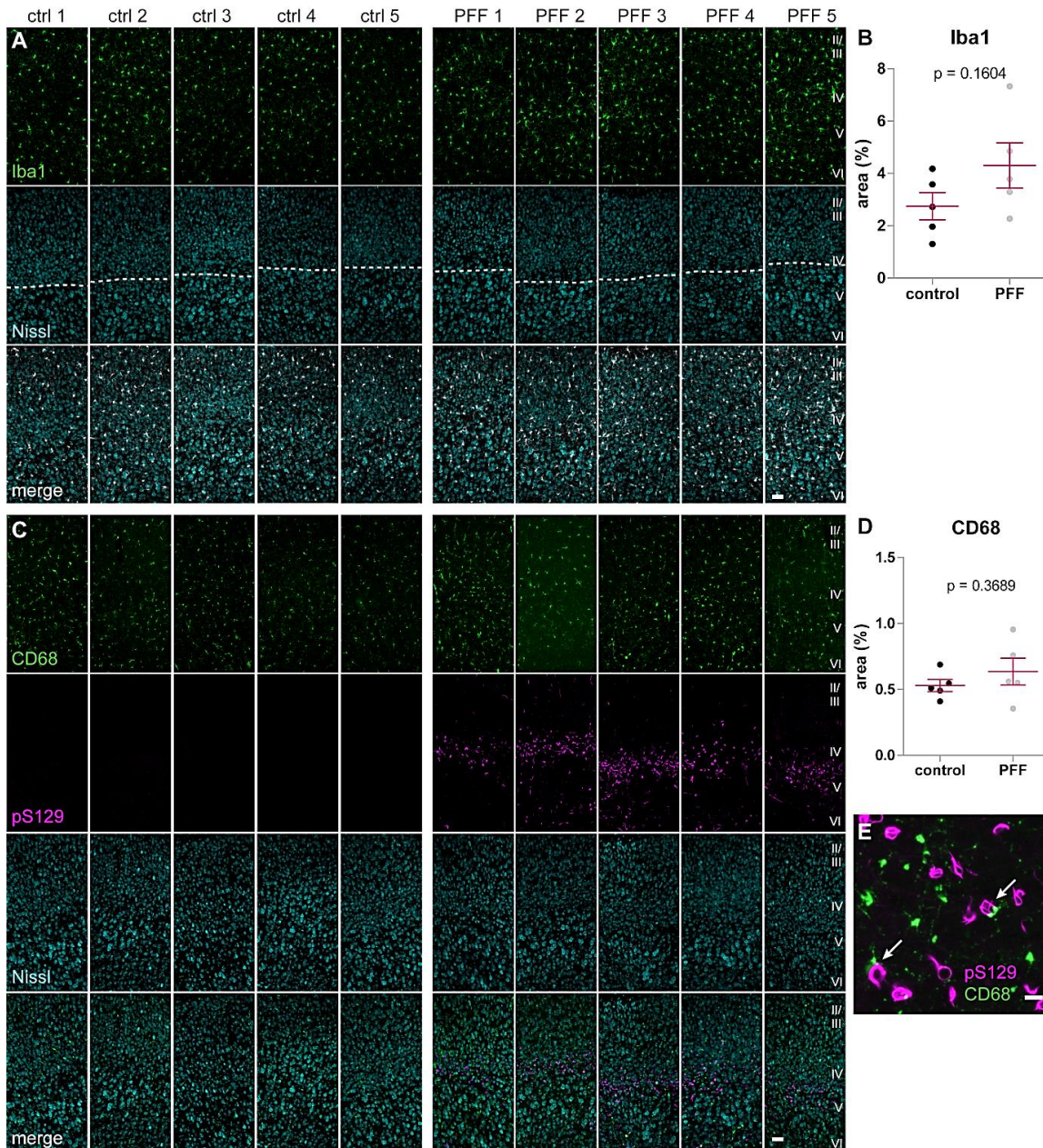


**Appendix Figure S2. Distribution of phosphorylated  $\alpha$ -syn aggregates in the mouse brain.** (A) Full coomassie blot and western blot against mouse  $\alpha$ -syn (14 kDa) from the initial monomer preparation of mouse  $\alpha$ -syn, demonstrating the purity of the sample before PFF production. (B) 5 months after striatal injection, dense neuronal pS129-immunopositive inclusions are present most prominent in the ipsilateral cortex (layer IV and V) of the injection site and in the amygdala. Due to known cross-reactivity of the pS129  $\alpha$ -synuclein antibody with phosphorylated neurofilament subunit L (NFL), white matter tracts are stained as well (C) Double staining (in the amygdala) distinguishes between false positive staining of white matter and pathological  $\alpha$ -synuclein aggregates in cell bodies and neurites. (D) Spread of  $\alpha$ -syn aggregates 5 months after seeding. Magenta dots mark the position of intracellular aggregates. Am: amygdala, SNpc: substantia nigra pars compacta, SNpr: substantia nigra pars reticulata. (E) Injection with monomeric  $\alpha$ -synuclein into mice expressing endogenous  $\alpha$ -syn or PFFs into SNCA KO mice does not lead to the spreading of  $\alpha$ -syn aggregates. Image stacks (B,C,E) are depicted as maximum intensity projections. Scale bars: B = 500  $\mu$ m; C = 20  $\mu$ m; E = 50  $\mu$ m.

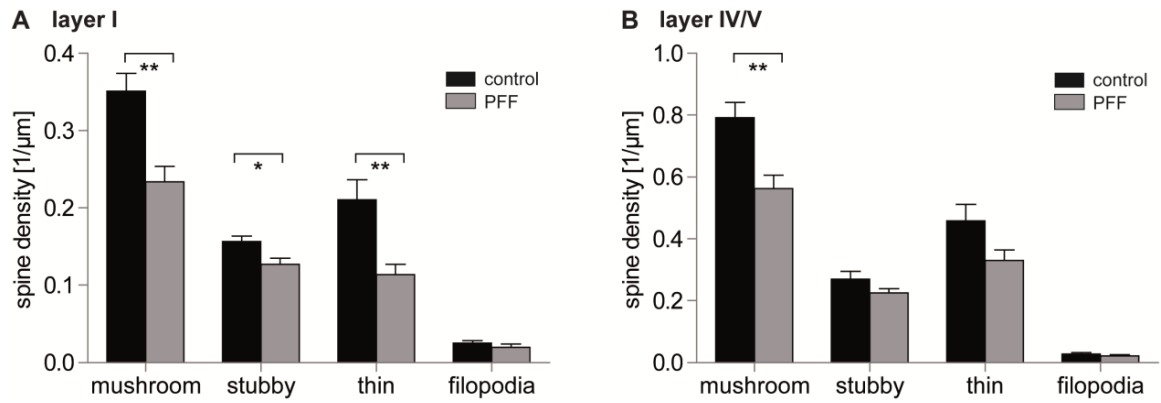




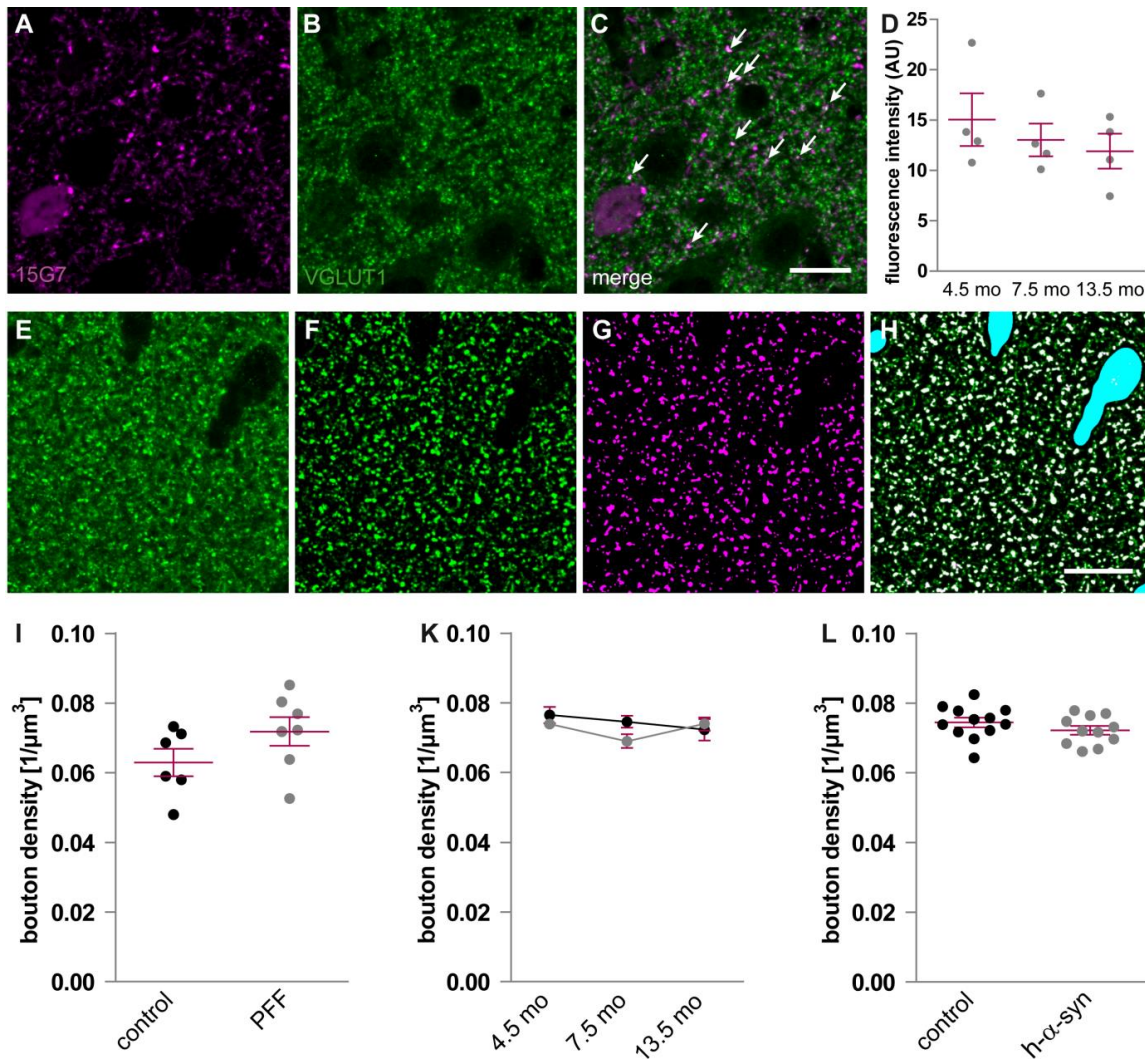
**Appendix Figure S3: Templated misfolding of  $\alpha$ -synuclein.** (A) Neocortical layer V pyramidal neuron containing a phosphorylated  $\alpha$ -synuclein inclusion. (B) Brain overview at 1 day post-injection (dpi) with fluorescently labeled PFFs. (C) Injection site in the striatum at 1 dpi. White arrowheads mark cells that have internalized fluorescent PFFs. (D) Brain overview at 6 dpi shows that fluorescently labeled PFFs have been removed from the injection site (asterisk). (E, F) At 30 dpi, small puncta of fluorescent PFFs locate to the injection canal (asterisk) and to some cortical cell bodies (arrows). The developing phospho- $\alpha$ -syn inclusions (arrowheads) however, consist largely of non-fluorescent  $\alpha$ -synuclein (F). Scale bars: B,D = 500  $\mu$ m; E = 100  $\mu$ m; C = 50  $\mu$ m; A,F = 5  $\mu$ m.



**Appendix Figure S4. Presence of microglia in the neocortex.** 5 months post-injection with PFFs or PBS (ctrl), staining across cortical layers II-VI were performed against (A) Iba1, marking the total number of microglia (layer IV is indicated as a dashed line, as no double staining with pS129 could be performed) and (C) CD68, marking actively phagocytic microglia. (B,D) area coverage of microglia in % in maximum intensity projections of 10 $\mu$ m of cortical thickness (scaling Z = 2  $\mu$ m). (E) occasional colocalization of CD68 positive microglia and pS129 positive aggregates (white arrows) is present in layer IV. *n* = 5 animals per group, mean with s.e.m; Student's t-test. Scale bars: A,C = 50  $\mu$ m; E = 10  $\mu$ m.



**Appendix Figure S5. Spine morphology changes in PFF-seeded mice (5 mo post-injection).** Absolute densities of mushroom, stubby and thin spines in (A) apical tuft dendrites of layer I ( $p_{\text{mushroom}} = 0.0029$ ,  $p_{\text{stubby}} = 0.0179$ ,  $p_{\text{thin}} = 0.0058$ ) and (B) layer IV/V apical dendrites ( $p_{\text{mushroom}} = 0.0046$ ) in PFF seeded mice compared to controls.  $n = 6$  (control),  $n = 7$  (PFF) animals, mean with s.e.m; \* $p < 0.05$ , \*\* $p < 0.01$ . Student's t-test.



**Appendix Figure S6. Presynaptic glutamatergic bouton density does not differ in seeded or transgenic mice.** (A) Transgenic  $\alpha$ -syn expression and (B) glutamatergic presynapses (C) show overlapping confocal signal. White arrows exemplarily mark double-stained boutons. (D) The expression level of  $\alpha$ -syn does not differ significantly across age groups. (E) VGLUT1 immunosignal in green exhibiting a spot-like pattern. (F) The same image is shown after local background subtraction to diminish intensity variations among different stacks and Gaussian filtering to reduce image noise. (G) VGLUT1-positive puncta representing single boutons are shown in magenta as detected by automatic spot detection using Imaris software. (H) Overlay of VGLUT1 immunosignal (green) and the detected boutons (magenta). Cyan color highlights regions that were automatically detected as blood vessels and were excluded from the analyzed volume. (I) The bouton density between control and PFF mice does not differ.  $n=6-7$  animals per group, Mann-Whitney-U-Test,  $P>0.05$ . (K) The bouton density does not show a change with age nor between the groups. Two-way analysis of variance “age”  $F_{(2)}=1.32$ ,  $p>0.05$  and “interaction”  $F_{(2)}=1.5$ ,  $p>0.05$ ;  $n = 4$  animals per group. (L) Since age had no effect on bouton density mice of all three age cohorts were pooled and the groups were compared using the unpaired t-test;  $p > 0.05$ ,  $n = 12$  animals per group, mean with s.e.m. Scale bars:  $15 \mu\text{m}$ .

2.2 Impaired plasticity of cortical dendritic spines in P301S tau transgenic mice [2]

## **2.2 Impaired plasticity of cortical dendritic spines in P301S tau transgenic mice [2]**

RESEARCH

Open Access

# Impaired plasticity of cortical dendritic spines in P301S tau transgenic mice

Nadine A Hoffmann<sup>1,2</sup>, Mario M Dorostkar<sup>1,2</sup>, Sonja Blumenstock<sup>2</sup>, Michel Goedert<sup>3</sup> and Jochen Herms<sup>2,4\*</sup>

## Abstract

**Background:** Illuminating the role of the microtubule-associated protein tau in neurodegenerative diseases is of increasing importance, supported by recent studies establishing novel functions of tau in synaptic signalling and cytoskeletal organization. In severe dementias like Alzheimer's disease (AD), synaptic failure and cognitive decline correlate best with the grade of tau-pathology. To address synaptic alterations in tauopathies, we analyzed the effects of mutant tau expression on excitatory postsynapses *in vivo*.

**Results:** Here we followed the fate of single dendritic spines in the neocortex of a tauopathy mouse model, expressing human P301S mutated tau, for a period of two weeks. We observed a continuous decrease in spine density during disease progression, which we could ascribe to a diminished fraction of gained spines. Remaining spines were enlarged and elongated, thus providing evidence for morphological reorganization in compensation for synaptic dysfunction. Remarkably, loss of dendritic spines in cortical pyramidal neurons occurred in the absence of neurofibrillary tangles (NFTs). Therefore, we consider prefibrillar tau species as causative for the observed impairment in spine plasticity.

**Conclusions:** Dendritic spine plasticity and morphology are altered in layer V cortical neurons of P301S tau transgenic mice *in vivo*. This does not coincide with the detection of hyperphosphorylated tau in dendritic spines.

**Keywords:** Tau, P301S mutation, Dendritic spines, Synaptic plasticity, Two photon *in vivo* imaging

## Background

Intracellular aggregates of the microtubule-associated protein tau are found in a large number of neurodegenerative diseases, including AD and frontotemporal dementia and parkinsonism linked to chromosome 17 (FTDP-17) [1,2]. In these so-called tauopathies, hyperphosphorylation of tau promotes its detachment from microtubules, resulting in tau mislocalization to the somatodendritic compartment, where it forms oligomers, neuropil threads and NFTs. The pathological mechanisms triggered by abnormal tau remain largely unknown, especially with regard to synaptic failure. In sporadic AD, tau-pathology precedes deposition of extracellular amyloid- $\beta$  and correlates best with the grade of dementia [3]. Moreover, synaptic dysfunction is believed to be the primary cause of cognitive decline in AD and other dementias [4]. Thus, for understanding the

pathological mechanisms causing tauopathies, as well as for the development of therapies, illuminating the effects of tau on synapses is indispensable.

Recently, Hoover et al. showed that dendritic spines are the locus of early synaptic malfunction caused by tau. Thereby, mistargeting of hyperphosphorylated tau to intact spines mediates synaptic dysfunction independently of neurodegeneration [5]. This detrimental role of hyperphosphorylated and misdistributed tau is further supported by the finding that dendritic tau mediates amyloid- $\beta$  toxicity [6] and tau knockout prevents early lethality and behavioural deficits in an AD mouse model [7]. Dendritic spines and synaptic pathology in tauopathy mouse models have also been analyzed by other groups, obtaining divergent results: rTg4510 mice, transgenic for human tau with the FTDP-17 mutation P301L, show reduced spine density and impaired dendritic complexity of pyramidal neurons in the cortex, both in the absence and presence of NFTs [8,9]. Synapse loss in the hippocampus before the emergence of fibrillary tangles was described for a mouse line expressing P301S mutated

\* Correspondence: jochen.herms@dzne.de

<sup>2</sup>Department of Translational Brain Research, German Center for Neurodegenerative Diseases (DZNE), Munich, Germany

<sup>4</sup>Munich Cluster of Systems Neurology (SyNergy), Munich, Germany  
Full list of author information is available at the end of the article

human tau under the murine prion promoter [10]. A reduced hippocampal spine density was also found in Tau<sub>RD</sub>/ΔK280 mice, expressing proaggregation mutant tau [11]. Conversely, an age-dependent increased spine density in cortical layer III, but no alterations in the hippocampus were reported for transgenic mice expressing human P301L or wildtype tau [12]. In cortical layer III pyramidal neurons of mice expressing all six human tau isoforms instead of murine tau, the spine volume decreases with advancing age, while spine density stays unaffected [13]. Since these studies were based on fixed brain tissue, so far, dendritic spine plasticity has not been analyzed in a tauopathy mouse model *in vivo*. Therefore, alterations in the total number of spines could not be attributed to changes in spine kinetics.

In this study, we investigated the effects of mutant tau expression on the structural plasticity of dendritic spines in P301S Tau mice [14]. They express human tau protein bearing an FTDP-17 mutation [15] under the control of the murine *thy1*-promoter. FTDP-17 patients carrying this mutation suffer from an early onset, rapidly progressive frontotemporal dementia and parkinsonism in combination with epileptic seizures [16]. Homozygous P301S Tau mice similarly exhibit severe tau-pathology already at 5–6 months of age: Abundant intracellular filaments composed of hyperphosphorylated tau deposit in several regions of the central nervous system (CNS), especially the brain stem and spinal cord [14,17–20]. Progressive neuron loss, accompanied by neuroinflammation, can be found in cortical layers I/II [21], but early behavioral abnormalities have been reported well before the onset of neurodegeneration [22].

By means of long-term two-photon *in vivo* imaging, we found a progressive spine loss on apical tuft dendrites of cortical layer V neurons in 4-month-old P301S Tau mice. The remaining spines were enlarged in head volume and increased in length. Immunohistochemical characterization of the analyzed pyramidal neurons revealed them to be bare of NFTs or hyperphosphorylated tau. In contrast to other brain regions like hippocampal CA3 pyramidal neurons, where abundant deposits of hyperphosphorylated tau can be found in dendritic spines, these were absent in the cerebral cortex. This observation is in line with what is seen in the brain tissue of AD patients [23,24].

## Methods

### Transgenic mice

For two-photon *in vivo* imaging, homozygous mice transgenic for the 383 amino acid isoform of human tau protein with the familial FTDP-17 mutation P301S [14] were crossbred with mice of the YFP-H line [25] (obtained from The Jackson Laboratory, Bar Harbor, ME, USA). Mice homozygous for tau (P301S Tau x YFP-H mice) were

used in experiments, while mice lacking mutant tau served as wildtype controls. The mice were exclusively male and the offspring of the same founder animals. Tau homozygosity was determined by real time PCR. Mice were group housed under pathogen-free conditions until surgery from which on they were singly housed. All procedures were performed in accordance with an animal protocol approved by the Ludwig Maximilian University of Munich and the Government of Upper Bavaria (ref. num. 55.2-1.54-2531-110-06).

### Cranial window surgery

A chronic cranial glass window was implanted over the right hemisphere of the cerebral cortex (Figure 1a), applying the open skull preparation as previously described [26,27]: The mice were anesthetized by an intraperitoneal injection of ketamine/xylazine (130 and 10 μg/g body weight, respectively). Additionally, anti-inflammatory dexamethasone (6 μg/g body weight) was administered intraperitoneally and body temperature was maintained by a heating pad. A circular piece of the skull, 4 mm in diameter, was removed above the somatosensory cortex (centered at the right parietal bone, approximately 2 mm caudal of the bregma and 2.5 mm lateral of the midline), using a dental drill (Schick-Technikmaster C1; Pluradent; Offenbach, Germany). To close the craniotomy, a round coverslip (5 mm in diameter) was glued to the skull using dental acrylic (Cyano-Veneer fast; Heinrich Schein Dental Depot, Munich, Germany). A small metal bar, containing a screw thread, was mounted next to the coverslip to allow fixation and precise repositioning of the mouse head during subsequent imaging sessions. After surgery, mice received a subcutaneous analgesic dose of carprofen (7.5 μg/g body weight Rimadyl; Pfizer, New York, USA).

### Long-term two-photon *in vivo* imaging

To avoid neuroinflammatory responses, *in vivo* imaging was performed after a 3 week recovery period. Each imaging session lasted for no longer than 60 min during which mice were anesthetized by an intraperitoneal injection of ketamine/xylazine (130/10 μg/g body weight) and body temperature was maintained by a heating pad. YFP was excited by a titanium-sapphire laser (MaiTai, Spectra-Physics, Darmstadt, Germany) at 880 nm and the emission was collected using a 500–550 nm band-pass filter (LSM 5MP, Carl Zeiss MicroImaging GmbH, Jena, Germany). Less than 50 mW laser power was delivered to the tissue to prevent laser-induced phototoxicity. A 20x water-immersion objective (1.0 NA; Carl Zeiss MicroImaging GmbH) was used to acquire overview stacks of 425 × 425 × 350 μm<sup>3</sup>, starting at the brain surface, with 0.41 × 0.41 × 3.00 μm<sup>3</sup> xyz-scaling. Subsequently, single spiny dendritic elements at a depth of 50–120 μm of this volume were imaged at high resolution

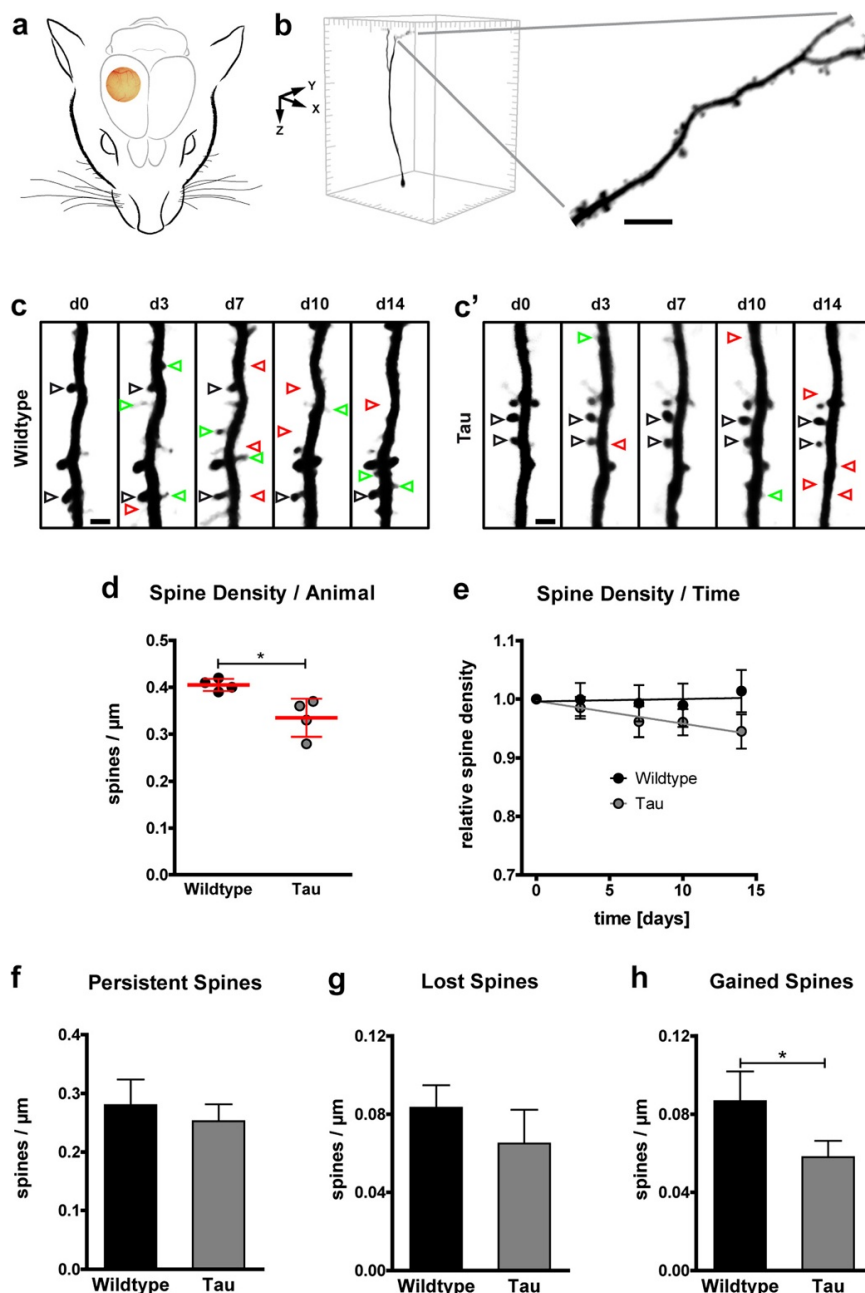


**Figure 1** Decreased dendritic spine density and impaired spine kinetics in P301S Tau mice. **a** Location of the chronic cranial glass window, as implanted for long-term *in vivo* imaging of YFP-expressing neurons. **b** Example of an isolated, volume rendered layer V neuron in a  $425 \times 425 \times 550 \mu\text{m}^3$  xyz-stack of the somatosensory cortex. A section of an apical tufted dendrite, stretching in parallel to the brain surface, is shown in higher magnification (maximum intensity projection; scale bar:  $5 \mu\text{m}$ ). **c-c'** Dendritic elements in 4-month-old wildtype (**c**) and P301S Tau mice (**c'**) were analyzed by high-resolution two-photon *in vivo* imaging over a time period of two weeks (d: day). Repetitive imaging allows discrimination of stable, gained, and lost spines (black, green, and red arrowheads respectively; maximum intensity projections; scale bars:  $2 \mu\text{m}$ ). **d** Spine density was reduced in P301S Tau mice at the first *in vivo* imaging session. Presented are means per animal of 8 mice; 61–82 dendrites per group; 14–22 dendrites per mouse; means  $\pm$  SD per group in red. **e** During the following 14 days, the spine density stayed stable in wildtype mice but further declined in P301S Tau mice. Presented are means  $\pm$  SEM of 28–41 dendrites in 3–4 mice per group, 8–12 dendrites per mouse; normalized to the first imaging day. Line, linear fit.  $p < 0.01$  (F test of means). **f-h** In P301S Tau mice, the densities of persistent (**f**) and lost spines (**g**) was not significantly impaired, while the density of gained spines was decreased (**h**). Presented are means  $\pm$  SD of 3–4 mice per group; 28–41 dendrites; 8–12 dendrites per mouse. **b, c, e, f & g**: Unpaired *t* test; \*  $p < 0.05$ .



( $0.16 \times 0.16 \times 1.00 \mu\text{m}^3$  xyz-scaling). To ensure that these apical tuft dendrites arose from layer V neurons, and exclude YFP-expressing layer II/III neurons, only dendrites protruding a depth of  $350 \mu\text{m}$  were chosen (Figure 1b). In subsequent imaging sessions, previously imaged regions were relocalized and precisely aligned based on the unique pattern of blood vessels, neuronal cell bodies, and their processes. Laser intensity was adjusted to keep the emitted YFP fluorescence stable.

### Immunohistochemistry

Brains of 4- and 6-month-old P301S Tau x YFP-H mice of mixed sex were processed for immunohistochemistry. Following transcardial perfusion of the mice with phosphate buffered saline (PBS) and 4% paraformaldehyde (PFA) in PBS at  $4^\circ\text{C}$ , brains were removed and fixed in 4% PFA in PBS over night at  $4^\circ\text{C}$ . In an attempt to improve tissue preservation for tau detection in dendritic spines, as described by Kremer et al. (2011), some mice were alternatively perfused with PBS at  $4^\circ\text{C}$ , brains were removed and hemispheres were fixed over night at  $4^\circ\text{C}$  in either 4% PFA in PBS or in Bouin solution (71.4% saturated picric acid, 23.8% formaldehyde, 4.8% glacial acetic acid).  $100 \mu\text{m}$  free-floating frontal sections of the somatosensory cortex were cut on a vibratome (VT1000S, Leica Microsystems GmbH, Wetzlar, Germany). During all following steps, the sections were kept on a shaker at room temperature. To permeabilize the tissue, the sections were incubated over night in 2% Triton X-100 in PBS.

For AT8-, AT180-, and HT7-stainings, background signal was reduced using Endogenous Biotin-Blocking Kit E-21390 (Molecular Probes, Eugene, OR, USA). Sections were incubated in 10% normal goat serum (NGS), 1% bovine serum albumin (BSA), and 0.1% Triton X-100 in PBS before primary antibody incubation in 5% BSA and 0.1% Triton X-100 in PBS over night. The following monoclonal antibodies, conjugated to biotin, were used in 1:200 dilutions: HT7 recognizing human tau, AT8 recognizing human and murine tau phosphorylated at S202 and T205, and AT180 recognizing human and murine tau phosphorylated at T231 and S235 (all from Thermo Scientific Pierce Protein Research Products, Rockford, IL, USA). Enzyme-mediated antibody-detection was performed using TSA™ kit #26 (Invitrogen, Carlsbad, CA, USA) with HRP-streptavidin (1:200) in 1% BSA in PBS and Alexa Fluor 647 tyramide (1:200), according to the manufacturers' instructions.

For AT100-stainings, non-specific epitopes were blocked with Casein I-Block (Invitrogen) for 1 hour. AT100 (Thermo Scientific Pierce Protein Research Products), recognizing human and murine tau phosphorylated at Alzheimer-specific epitopes S212 and T214, was applied for 4 hours, diluted 1:200 in PBS. Detection was performed by incubating the sections with secondary

anti-mouse antibody conjugated to Alexa Fluor 647 (1:200 in PBS; Invitrogen) for 4 hours.

For all stainings, sections were finally washed 5x10 min with PBS before mounting on glass coverslips using fluorescence mounting medium (Dako, Glostrup, Denmark).

### Confocal microscopy

Fluorescence images were acquired with a confocal laser scanning microscope, mounted on an inverted microscope support (LSM 510 and AxioVert 200, Carl Zeiss MicroImaging GmbH). Alexa Fluor 488 was excited by an argon laser at 488 nm and emission was collected using a 500–550 nm bandpass filter. Alexa Fluor 647 was excited by a helium-neon laser at 633 nm and emission was collected using a 650 nm longpass filter.

For the AT8-YFP-correlation, a 40x oil-immersion objective (Plan-Apochromat, NA 1.3; Carl Zeiss MicroImaging GmbH) was used to obtain  $360 \times 360 \times 50 \mu\text{m}^3$  stacks with  $0.35 \times 0.35 \times 2.00 \mu\text{m}^3$  xyz-scaling. Per animal 10 stacks of layer V neurons were analyzed.

### Image processing and data analysis

Dendritic spine density was determined using ZEN 2011 Light Edition software (version 7.0, Carl Zeiss MicroImaging GmbH). Images were corrected with a gamma of 0.45 and spines were counted manually by scrolling through the z-stacks. In time-series, a dendritic spine was defined as the same if its location did not change within a range of  $1 \mu\text{m}$  along the dendrite. Since z-scaling was limited to  $1 \mu\text{m}$ , only protrusions emanating laterally from the dendritic shaft were analyzed.

For morphological spine analysis, the three-dimensional *in vivo* images were deconvolved (AutoQuant, version X2.0.1, Media Cybernetics, Bethesda, USA) and semi-automatically remodelled (Imaris 6.1.5, Bitplane, Zurich, Switzerland). Spine subtypes were identified using the Imaris XT spine classification module, based on the following hierarchical algorithms (adapted from [28]): mushroom spine: “max\_width(head)/min\_width(neck) > 1.4 and max\_width(head) >  $0.4 \mu\text{m}$  and min\_width(neck) >  $0 \mu\text{m}$ ”; stubby spine: “length(spine)/mean\_width(neck)  $\leq 3$  or min\_width(neck) =  $0 \mu\text{m}$  or >  $0.5 \mu\text{m}$ ”; thin spine: length(spine)/mean\_width(neck) > 3.

Analysis was performed blinded in respect to mouse genotype.

YFP- and / or AT8-positive layer V pyramidal neurons were counted manually using ZEN 2011 Light Edition software (version 7.0; Carl Zeiss MicroImaging GmbH).

All data are presented as mean  $\pm$  SD or  $\pm$  SEM, as stated in the figure legends. Statistical differences between two groups were determined using unpaired *t* test. Since spine head volumes had a log-normal distribution, in this exceptional case the *t* test was done on log-transformed data. All other measurements represent

means of means, which according to the central limit theorem approximate a normal distribution. Therefore, we used a parametric test. The slope from a linear regression was tested for statistical difference from zero by *F* test. Statistical analysis and graphs were done using Prism software (version 5.04, GraphPad Software Inc., La Jolla, CA, USA). Figures were arranged using Adobe Illustrator CS4 Extended software (version 11.0.2, Adobe Systems, San Jose, CA, USA).

## Results

In order to analyze the effects of cortical tau-pathology on dendritic spines, we performed long-term two-photon *in vivo* imaging of P301S Tau mice (Figure 1a). The line was crossbred with mice of the YFP-H line, expressing yellow fluorescent protein in a subset of cortical neurons, i.e. layer II/III and V pyramidal neurons (Figure 1b). Thus, we were able to follow the fate of individual dendritic spines in 4-month-old homozygous P301S Tau mice and age-matched wildtype mice through a chronic cranial window (Figure 1c-c').

### Decreased cortical spine density in P301S tau mice

The spine densities of apical tuft dendrites of layer V neurons showed high variance, ranging from 0.24 to 0.60 spines/ $\mu\text{m}$  in wildtype mice and 0.20 to 0.60 spines/ $\mu\text{m}$  in P301S Tau mice. Overall, we found a reduction in the mean spine density of P301S Tau mice by 17% ( $0.34 \pm 0.04$  compared to  $0.41 \pm 0.01$  spines/ $\mu\text{m}$  in wildtype mice, Figure 1d). By relocalizing and repeatedly imaging the same dendritic elements every 3–4 days for a period of two weeks (Figure 1c-c'), we observed further aggravation of total spine loss in P301S Tau mice during disease progression: The relative spine density declined to  $0.94 \pm 0.15$  of the initial value, while remaining unchanged in wildtype mice ( $1.01 \pm 0.13$ ; Figure 1e).

### Tau transgene expression affects spine kinetics

High-resolution, long-term *in vivo* imaging enables very detailed analysis of spine kinetics (Figure 1c-c'). By carefully following the fate of single spines, the densities of stable, gained, and lost spines can be determined for each consecutive imaging session, providing a measurement of synaptic plasticity. We detected no significant change in the densities of persistent spines (i. e. stable for at least one week; Figure 1f) and lost spines (i. e. disappearing from one to the consecutive imaging session; Figure 1g) in P301S Tau mice. However, while in wildtype mice the permanent loss and gain of spines was well-balanced ( $0.083 \pm 0.012$  vs.  $0.087 \pm 0.015$  spines/ $\mu\text{m}$ , respectively; Figure 1g-h), the spine turnover in P301S Tau mice was shifted: The density of gained spines (i. e. newly emerging from one to the consecutive imaging session) was reduced ( $0.058 \pm 0.008$  spines/ $\mu\text{m}$ ), compared

to wildtype mice (Figure 1h). Therefore, we could attribute the constant loss of total spines to a diminished formation of new spines caused by tau transgene expression.

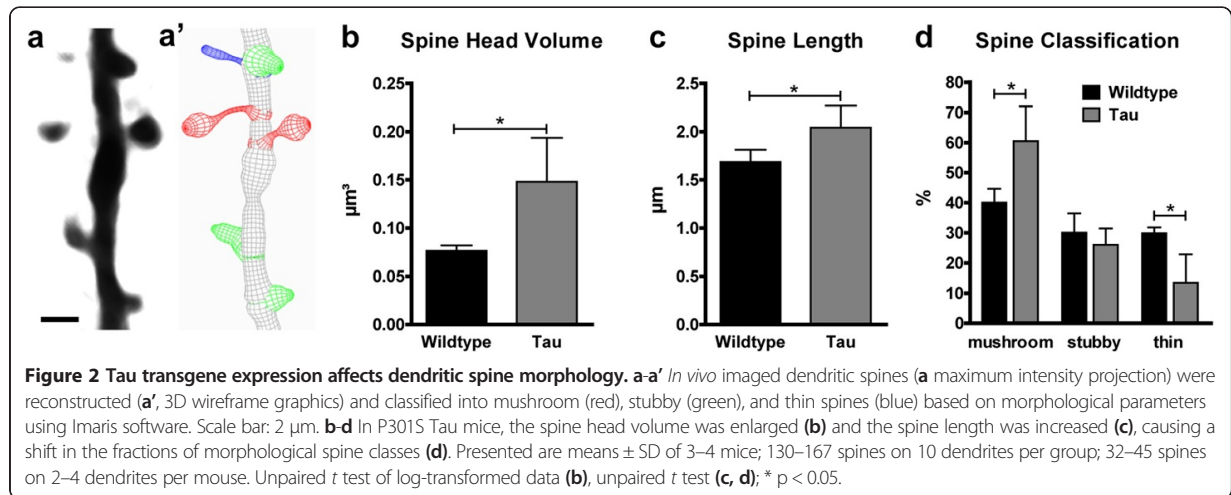
Homozygous P301S Tau mice show age-dependent neurodegeneration – especially in the brainstem [14], but also in superficial cortical layers, where mainly GABAergic interneurons are affected [21]. In order to determine whether YFP-expressing cortical neurons get lost, we followed the fate of layer V neurons' apical dendritic trees as well as layer II/III neuronal somata in 4-month-old P301S Tau mice. However, in a time period of up to 6 weeks we did not detect the disappearance of any dendritic branches or the loss of a single neuron (analysis of 199 cells in 5 mice; data not shown).

### Morphological spine alterations in P301S tau mice

Since dendritic spine function and morphology are strongly correlated, we performed three-dimensional reconstructions of the *in vivo* imaged dendritic spines to compare morphological parameters (Figure 2a-a'). Thereby, we found the spines of P301S Tau mice to be strongly enlarged in spine head volume ( $0.15 \pm 0.05 \mu\text{m}^3$  compared to  $0.08 \pm 0.01 \mu\text{m}^3$  in wildtype; Figure 2b), accompanied by a smaller increase in spine length ( $2.04 \pm 0.14 \mu\text{m}$  compared to  $1.69 \pm 0.13 \mu\text{m}$  in wildtype; Figure 2c). Moreover, we classified the spines according to their length, maximum head width, mean and minimum neck width into thin, stubby, and mushroom spines. In P301S Tau mice, the fraction of thin spines was strongly reduced ( $15.39 \pm 10.43$  compared to  $28.23 \pm 7.42$  spines/ $\mu\text{m}$  in wildtype), while we measured a gain in mushroom spines ( $58.63 \pm 16.96$  compared to  $39.58 \pm 7.92$  spines/ $\mu\text{m}$  in wildtype). The stubby spine fraction, however, was not significantly changed (Figure 2d).

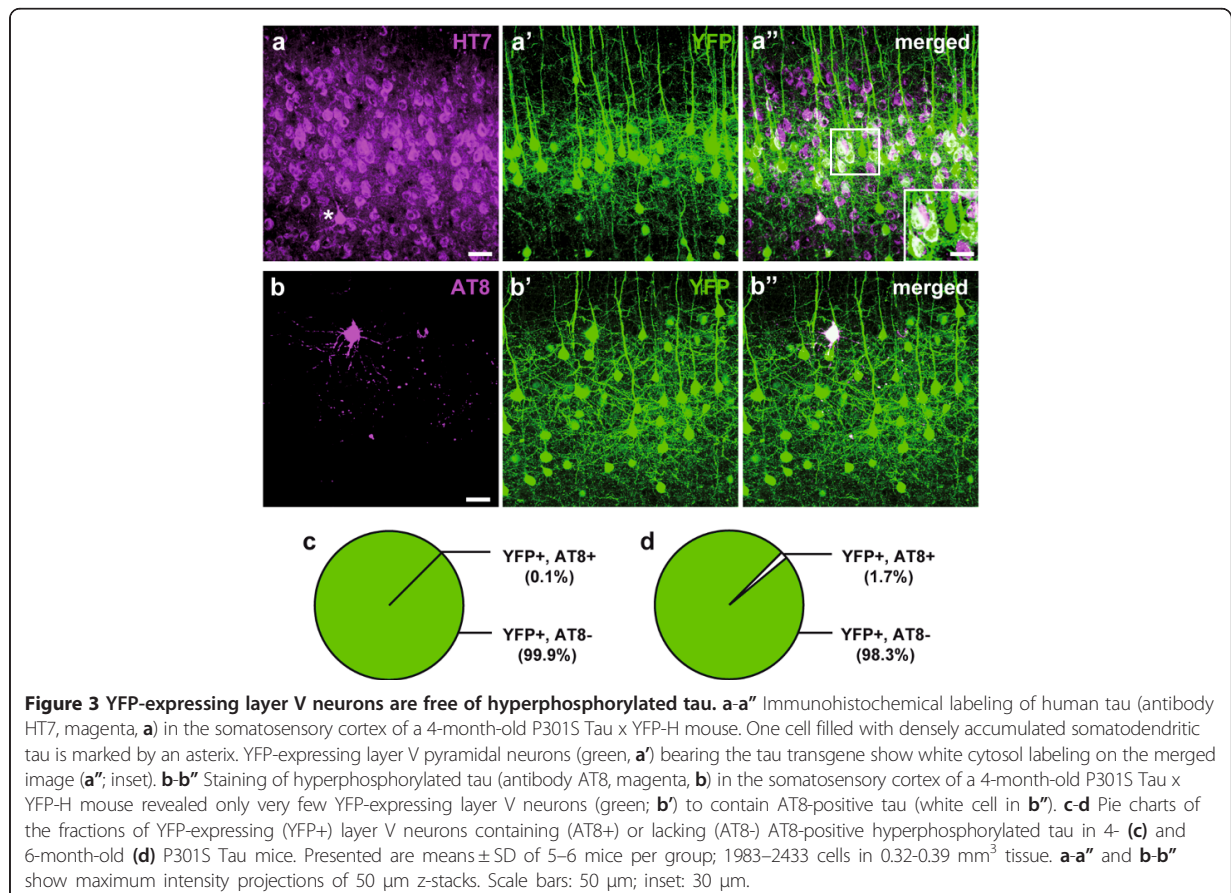
### Cortical spine impairments in the absence of NFTs

In search for the causative pathological process underlying the described spine alterations in P301S Tau mice, we focused on tau-pathology in YFP-expressing cortical layer V neurons, the apical tufted dendrites of which we imaged. In the transgenic mice both YFP and the mutant human tau are expressed in neuronal subsets under the control of the murine *thy1*-promoter. Expression patterns of the transgenes can vary nevertheless, depending on stochastic factors upon transgene insertion. To verify if the dendrites imaged *in vivo* belonged to neurons expressing the human tau transgene, we performed immunohistochemical labelling for human tau on brain slices (antibody HT7; Figure 3a). Correlating the HT7-staining with the YFP-expression (Figure 3a'), we found most of the YFP-positive layer V neurons to show at least weak somatic HT7 immunoreactivity (Figure 3a''). Despite the broad expression of both proteins in the neocortex, it is not possible to verify that all of the analyzed neurons did express the tau transgene.



Homozygous P301S Tau mice develop severe tau-pathology with abundant filaments of hyperphosphorylated tau in the cerebral cortex already at young ages [14,21]. Hence, we expected many of the YFP-expressing layer V neurons to contain pre-tangle or tangle-like tau-

aggregates. In search for a fluorescent, brain-permeable dye for *in vivo* labelling of these tau-deposits, we tested the amyloid-binding Congo red derivative FSB ((trans,trans)-1-fluoro-2,5-bis(3-hydroxycarbonyl-4-hydroxy)styrylbenzene) [29,30], which stains filamentous tau in the spinal cord and



retina of P301S Tau mice, as shown earlier by other groups and us [19,31,32]. Applying the same method we did, however, not succeed in labelling any intracellular tau filaments in the cerebral cortex with FSB, detectable by *in vivo* imaging. Analysis of brain sections from FSB-injected mice revealed many labelled cells in the brain stem though, serving as a positive control. To further exclude the presence of NFTs in superficial cortical layers, we also tested thioflavin S. This well-established amyloid-binding fluorophore marks NFTs, such as in the brain of the rTg4510 tauopathy mouse model [9,33]. Since fluorescence spectra of YFP and thioflavin S largely overlap, we used P301S Tau mice lacking the YFP-transgene to apply thioflavin S according to the published protocol [33]. Again, no specific signal of the dye could be detected. Even 6-month-old mice, at the stage when the animals die as a consequence of the tau-pathology in the brain stem, were bare of FSB- or thioflavin S-labelled cells in the accessible cortical regions.

In default of an *in vivo* dye, we stained brain sections for hyperphosphorylated tau using the antibody AT8 (Figure 3b-b"). To our surprise, we found AT8-positive tau only in a marginal fraction of YFP-expressing layer V neurons in 4-month-old P301S Tau mice ( $0.12 \pm 0.13\%$ , i.e. 3 of 2433 YFP + cells were AT8+; furthermore, 19 AT8+ cells did not express YFP (data not shown); Figure 3c), and even in 6-month-old mice ( $1.69 \pm 2.87\%$ , i.e. 34 of 1983 YFP + cells were AT8+; furthermore, 146 AT8+ cells did not express YFP (data not shown); Figure 3d). Hence, we conclude that the neurons imaged *in vivo* most likely did not contain detectable amounts of somatodendritic hyperphosphorylated tau nor NFTs which could account for the observed spine abnormalities.

#### Immunohistochemical stainings do not reveal tau in cortical spines

Since there is recent evidence that mislocalization of hyperphosphorylated tau to dendritic spines leads to synaptic impairments [5], we next aimed to look for tau in spines of cortical layer V neurons. Quantitative biochemical methods such as protein-detection in synaptosome- and PSD-fractions cannot detect alterations in specific populations of neurons and are therefore unable to distinguish broad systemic effects from more subtle changes in neuronal subpopulations. Therefore, we decided to perform immunohistochemical stainings for tau on fixed brain slices of the cortical region analyzed *in vivo* using the phosphorylation-dependent antibodies AT8, AT100, and AT180 (Figure 4a-f).

We found AT8-positive hyperphosphorylated tau in the somatodendritic and axonal compartments of several neurons, as well as in neuritic dystrophies and neuropil threads, but never in dendritic spines (Figure 4a-c"). The

sparse labeling with AT100 and AT180 was usually restricted to the soma and the main shaft of the arising apical dendrite (Figure 4d-e), in a few cases also staining higher-order distal dendritic branches in a punctate pattern (Figure 4f). Unlike the phospho-tau stains, a large number of neurons were labelled with the human tau specific antibody HT7, congruent to the pan-neuronal expression of the transgene (Figure 3a). Only a few cells, however, showed neuritic staining and in none of those dendritic spines were stained.

Also after application of an alternative brain tissue fixation technique using Bouin solution, which is supposed to improve tau detection [12], (phospho-)tau could not be observed in cortical dendritic spines. These results were furthermore affirmed by DAB-stainings of conventional paraffin sections, thus avoiding impairments of antibody penetration due to section thickness. The usage of enzyme-mediated antibody detection provides strong signal enhancement, enabling tau localization even in very fine structures like axons or thin dendritic branches (Figure 4c', c"). By analyzing YFP-negative cells (Figure 4c-j), we also excluded detractions of antibody-binding by the presence of YFP in the post-synaptic compartment. Yet, when analyzing different brain regions like hippocampal CA3 (Figure 4g-j), AT8-positive tau was clearly localized in neuronal spiny protrusions (inset Figure 4g). AT100- and AT180-labeling was again less pronounced (Figure 4h-j), resembling the cortical staining pattern. These findings hint at distinctive pathological mechanisms, leading to brain region and neuronal subtype specific tau mislocalization in tauopathies.

#### Discussion and conclusions

##### Dendritic spine abnormalities in tauopathy mouse models

The generation of dozens of tau transgenic mouse models during the past years (reviewed in [34,35]) has facilitated studying the potential role of tau in neurodegenerative diseases (reviewed in [2,15]). However, with regard to synaptic density and dendritic spine morphology, inconsistent effects of tau on synapses have been described, strongly depending on the tauopathy model, the stage of the disease and the brain region analyzed [9,10,12,13]. All these approaches were performed *ex vivo*, therefore missing kinetic spine data which can only be obtained by *in vivo* imaging as presented in our study.

Dendritic spines are not rigid structures but rather bear a strong potential for morphological plasticity, thus enabling neurons to modify their synaptic interconnections, the correlates of learning and memory [36]. While the majority of spines is stable, a small fraction is permanently retracted or newly formed, even in the adult brain [20]. Underlying changes in dendritic actin filaments, modifying spine morphology, can occur on time scales from seconds to hours [37]. Changes in the total

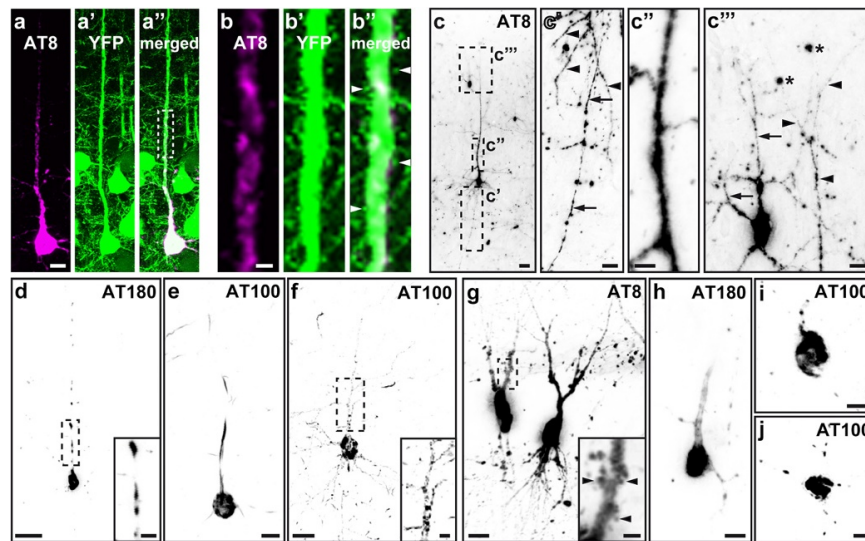


**Figure 4 Failure to detect tau in cortical dendritic spines by means of immunohistochemistry.** Immunohistochemical labeling of hyperphosphorylated tau (antibodies AT8, AT100, and AT180) in cortical layer V pyramidal neurons (a-f) and hippocampal CA3 neurons (g-j). a-a'' YFP-expressing neuron, filled with somatodendritic AT8-positive tau. The marked section of the apical dendrite (dashed rectangle in a'') is shown in higher magnification in b-b'', demonstrating that the protruding YFP-positive dendritic spines (exemplarily marked by arrowheads) are bare of hyperphosphorylated tau. c Example of a YFP-negative layer V neuron (c'-c''), magnifications of the regions marked by dashed rectangles, containing AT8-positive tau in its soma, axon (arrows in c'), basal dendrites (arrowheads in c'), apical dendritic shaft (c''), and higher-order distal dendritic branches (arrowheads in c''). An adjacent AT8-positive layer II/III neuron shows a similar punctate pattern of hyperphosphorylated tau in its dendritic filaments (arrows in c''), not to be mistaken for emanating spines. AT8-labeling is also found irregularly in the neuropil, for example in neuritic dystrophies (asterisks in c''). Different from the cortex, in hippocampal CA3 neurons, AT8-positive hyperphosphorylated tau was frequently found in spiny protrusions (inset in g, arrows). Images show maximum intensity projections. In c-j, images were inverted for contrast enhancement. Scale bars: 2  $\mu$ m (b), 5  $\mu$ m (c'' & insets d, f & g), 10  $\mu$ m (a, c', c'', e, h-j), 20  $\mu$ m (c, d, f & g).

number of spines such as a reduced spine density can therefore result from either a loss of persistent spines, a diminished fraction of new spines or an enhanced fraction of retracted spines.

We measured a reduced spine density on apical tuft dendrites of cortical layer V pyramidal neurons in 4-month-old homozygous P301S Tau mice which further decreased during the two weeks imaging period. Obtaining kinetic data on single spine level, this was attributed to a diminished density of gained spines, while the stable (respectively persistent) and lost spine densities were largely unaffected compared to wildtype mice. The remaining spines underwent morphological reorganization: They were longer and the head volume was strongly enlarged, thus increasing the mushroom spine fraction at the cost of the thin spines.

Numerous studies have shown that spine volume is proportional to the size of the postsynaptic density and the AMPA ( $\alpha$ -amino-3-hydroxy-5-methyl-4-isoxazole propionic acid) receptor content (reviewed in [38]). Thus, we propose that the observed spine remodelling displays a compensatory mechanism for the loss of total spine number, thereby strengthening the remaining synaptic contacts. Moreover, the decrease in gained spines is morphologically

reflected in the diminished fraction of thin spines, which commonly correspond to non-synaptic transient precursors of the larger established spines [39,40].

Previous studies on tauopathy mouse models have obtained divergent results with regard to dendritic spines: While in most models, the spine density was found to be reduced [8-10], in others an increased [12] or unchanged spine density [13] was observed. Direct comparison of the results is hindered by both genetic differences of the mouse models used as well as specific properties of the diverse neuronal populations analyzed. However, detrimental effects of abnormal tau were found in most studies, thereby causing a loss of dendritic spines. Our study adds the important finding that expression of P301S mutant human tau impairs spine turnover and morphology, leading to a net loss of spines, accompanied by structural reorganization.

#### Mislocalization of hyperphosphorylated tau to spines

It was reported recently that tau localization to dendritic spines mediates synaptic dysfunction in FTDP-17 and AD mouse models [5,6]. This was shown mainly by analyzing cultured hippocampal neurons of mice expressing P301L mutated, truncated, or wildtype human tau (lines

rTg4510, pR5,  $\Delta$ tau74, and rTg21221). Pre- and postsynaptic accumulations of hyperphosphorylated tau in the hippocampus have also been shown for other tau transgenic mice (lines Tet-hTauP301L, 3xTg-AD, and PS19) by means of electron microscopy [10,41,42]. Moreover, tau was found to be associated to PSD95 in forebrain extracts of rTg4510 and rTg21221 mice [40] and present in a few dendritic spines of cortical neurons in rTg4510 mice [8].

When we investigated brain slices of P301S Tau mice utilizing immunohistochemistry, hyperphosphorylated tau could also clearly be located in dendritic spiny protrusions of CA3 hippocampal neurons. However, we never detected tau in dendritic spines of pyramidal neurons in the cortical regions accessible for *in vivo* imaging. The protein was even absent from spines of neurons in which the somatodendritic compartment was almost completely filled with filamentous hyperphosphorylated tau.

The brain region specific mislocalization of hyperphosphorylated tau to dendritic spines in the tauopathy mouse model analyzed here is supported by very similar findings in AD patients. There, only the thorny excrescences of CA3 hippocampal neurons contain hyperphosphorylated tau, but not dendritic spines in other fields of the hippocampal formation or the adjacent cortex [23,24]. Unlike dendritic spines of cortical pyramidal neurons, which have an actin-based cytoskeleton, the CA3 thorny excrescences occasionally contain microtubules [43,44]. This explains the presence of microtubule-associated proteins like tau inside the spiny protrusions. In conclusion, we suggest different mechanisms underlying synaptic impairment in tauopathies, depending on specific characteristics of the affected neuronal populations. Moreover, these accumulations of hyperphosphorylated tau in hippocampal postsynapses could also cause dysfunctions of the local or further interconnected neuronal networks. Thus, impaired hippocampal signaling might contribute indirectly to cortical spine pathology.

#### **Axonal pathology and local network dysfunction causing spine impairments**

Methodical restrictions make it nearly impossible to synchronously follow the fate of single dendritic spines and their presynaptic counterparts (i. e. axonal boutons) *in vivo*. Hence, with our kinetic data we cannot clarify if the loss of spines is a primary or secondary event, caused by axonal pathology which is known to be very prominent in tauopathies [45-47]. Given the lack of tau transgene expression in a fraction of YFP-positive layer V neurons makes it even more likely that presynaptic failure partially accounts for the dendritic spine impairments.

Moreover, a severe neuron loss in superficial cortical layers, mainly affecting GABAergic interneurons, was reported for homozygous P301S Tau mice already at the

age of 3 months [21]. Since those inhibitory interneurons also form connections with pyramidal cells [48], a decline in inhibition might lead to a compensatory reduction of excitatory synapses. Neurodegeneration in P301S Tau mice, which could only partially be correlated to intracellular tau-deposits, is also accompanied by inflammatory responses [17]. Microglia and astrocytes are known to be critically involved in healthy brain homeostasis and synaptic maintenance [49-51]. Therefore, the induction of inflammatory processes can have significant implications on dendritic spine plasticity, thus preventing the emergence of new spines or causing morphological alterations. Summarized, the observed changes in dendritic spines might be an indirect effect, caused by axonal pathology or local network dysfunction.

#### **In search for the toxic tau species**

We demonstrated in this study, that dendritic spine loss and remodelling in cortical neurons of P301S Tau mice occur in the absence of hyperphosphorylated tau accumulation. This is in line with other studies showing that tau-aggregates and even NFTs are not sufficient to cause cognitive decline or neurodegeneration: In a reversible tauopathy mouse model, memory function recovered after tau transgene suppression despite continuing NFT build-up [52]. Furthermore, structural and functional neuronal changes in different tauopathy mice are independent of the presence of NFTs [9,10], and accumulation of insoluble tau does not necessarily affect spine density and morphology [53]. On the other hand, there is strong evidence for the existence of neurotoxic prefibrillar tau dimers and higher order oligomeric aggregates in tauopathies such as AD [54-56]. Also, a dendritic function of tau monomers was suggested to mediate excitotoxicity in AD mouse models [6]. Therefore, we argue for prefibrillar tau as the toxic species in tau-dependent neurodegenerative diseases. Further studies will be needed to clarify the specific pathogenic mechanism and to finally find ways of disease prevention, arrest, or even cure.

#### **Competing interests**

The authors declare that they have no conflict of interests.

#### **Authors' contributions**

NAH conceived experiments and performed experiments, statistical analysis, manuscript drafting and manuscript assembly. MMD participated in statistical analysis and manuscript drafting. SB provided technical support. MG contributed materials and provided technical support. JH conceived experiments and participated in manuscript drafting. All authors read and approved the final manuscript.

#### **Acknowledgements**

This work was supported by grants from the Deutsche Forschungsgemeinschaft (DFG, SFB 596, A13) and the EU (NeuroGSK3; FP7-223276). We would like to thank Sonja Steinbach and Eric Griessinger for their excellent technical assistance and Julia Geyer, Pitt Liebmann, and Patrizia Bonert for their invaluable aid in taking care of the animals.

#### Author details

<sup>1</sup>Center for Neuropathology and Prion Research, Ludwig-Maximilians University, Munich, Germany. <sup>2</sup>Department of Translational Brain Research, German Center for Neurodegenerative Diseases (DZNE), Munich, Germany. <sup>3</sup>Medical Research Council Laboratory of Molecular Biology, Cambridge, UK. <sup>4</sup>Munich Cluster of Systems Neurology (SyNergy), Munich, Germany.

Received: 29 October 2013 Accepted: 1 November 2013

Published: 17 December 2013

#### References

1. Lee VM, Goedert M, Trojanowski JQ: Neurodegenerative tauopathies. *Annu Rev Neurosci* 2001, **24**:1121–1159.
2. Morris M, Maeda S, Vossel K, Mucke L: The many faces of tau. *Neuron* 2011, **70**(3):410–426.
3. Braak H, Thal DR, Ghebremedhin E, Del Tredici K: Stages of the pathologic process in Alzheimer disease: age categories from 1 to 100 years. *J Neuropathol Exp Neurol* 2011, **70**(11):960–969.
4. Selkoe DJ: Alzheimer's disease is a synaptic failure. *Science* 2002, **298**(5594):789–791.
5. Hoover BR, Reed MN, Su J, et al: Tau mislocalization to dendritic spines mediates synaptic dysfunction independently of neurodegeneration. *Neuron* 2010, **68**(6):1067–1081.
6. Ittner LM, Ke YD, Delerue F, Bi M, Gladbach A, van Eersel J, Wolfing H, Chieng BC, Christie MJ, Napier IA: Dendritic function of tau mediates amyloid- $\beta$  toxicity in Alzheimer's disease mouse models. *Cell* 2010, **142**:387–397.
7. Roberson ED, Scearce-Levie K, Palop JJ, Yan F, Cheng IH, Wu T, Gerstein H, Yu G-Q, Mucke L: Reducing endogenous tau ameliorates amyloid  $\beta$ -induced deficits in an Alzheimer's disease mouse model. *Science* 2007, **316**:750–754.
8. Kopeikina KJ, Polydoro M, Tai HC, Yaeger E, Carlson GA, Pitstick R, Hyman BT, Spire-Jones TL: Synaptic alterations in the rTg4510 mouse model of tauopathy. *J Comp Neurol* 2013, **521**(6):1334–1353.
9. Rocher AB, Crimins JL, Amatruedo JM, Kinson MS, Todd-Brown MA, Lewis J, Luebke JL: Structural and functional changes in tau mutant mice neurons are not linked to the presence of NFTs. *Exp Neurol* 2010, **223**(2):385–393.
10. Yoshiyama Y, Higuchi M, Zhang B, Huang S-M, Iwata N, Saido TC, Maeda J, Suhara T, Trojanowski JQ, Lee VM-Y: Synapse loss and microglial activation precede tangles in a P301S tauopathy mouse model. *Neuron* 2007, **53**(3):337–351.
11. Mocanu M-M, Nissen A, Eckermann K, et al: The potential for  $\beta$ -structure in the repeat domain of tau protein determines aggregation, synaptic decay, neuronal loss, and coassembly with endogenous tau in inducible mouse models of tauopathy. *J Neurosci* 2008, **28**(3):737–748.
12. Kremer A, Maurin H, Demedts D, Devijver H, Borghgraef P, Van Leuven F: Early improved and late defective cognition is reflected by dendritic spines in tau.P301L mice. *J Neurosci* 2011, **31**(49):18036–18047.
13. Dickstein DL, Brautigam H, Stockton SD, Schmeidler J, Hof PR: Changes in dendritic complexity and spine morphology in transgenic mice expressing human wild-type tau. *Brain Struct Funct* 2010, **214**(2–3):161–179.
14. Allen B, Ingram E, Takao M, et al: Abundant tau filaments and nonapoptotic neurodegeneration in transgenic mice expressing human P301S tau protein. *J Neurosci* 2002, **22**(21):9340–9351.
15. Spire-Jones TL, Stoothoff WH, de Calignon A, Jones PB, Hyman BT: Tau pathophysiology in neurodegeneration: a tangled issue. *Trends Neurosci* 2009, **32**(3):150–159.
16. Sperfeld A, Collatz M, Baier H, et al: FTDP-17: an early onset phenotype with parkinsonism and epileptic seizures caused by a novel mutation. *Ann Neurol* 1999, **46**(5):708–715.
17. Bellucci A, Westwood AJ, Ingram E, Casamenti F, Goedert M, Spillantini MG: Induction of inflammatory mediators and microglial activation in mice transgenic for mutant human P301S tau protein. *Am J Pathol* 2004, **165**(5):1643–1652.
18. Delobel P, Lavenir I, Fraser G, Ingram E, Holzer M, Ghetti B, Spillantini MG, Crowther RA, Goedert M: Analysis of tau phosphorylation and truncation in a mouse model of human tauopathy. *Am J Pathol* 2008, **172**(1):123–131.
19. Gasparini L, Crowther RA, Martin KR, Berg N, Coleman M, Goedert M, Spillantini MG: Tau inclusions in retinal ganglion cells of human P301S tau transgenic mice: effects on axonal viability. *Neurobiol Aging* 2011, **32**(3):419–433.
20. Trachtenberg JT, Chen BE, Knott GW, Feng G, Sanes JR, Welker E, Svoboda K: Long-term in vivo imaging of experience-dependent synaptic plasticity in adult cortex. *Nature* 2002, **420**(6917):788–794.
21. Hampton DW, Webber DJ, Bilican B, Goedert M, Spillantini MG, Chandran S: Cell-mediated neuroprotection in a mouse model of human tauopathy. *J Neurosci* 2010, **30**(30):9973–9983.
22. Scattoni ML, Gasparini L, Alleva E, Goedert M, Calamandrei G, Spillantini MG: Early behavioural markers of disease in P301S tau transgenic mice. *Behav Brain Res* 2010, **208**(1):250–257.
23. Blazquez-Llorca L, Garcia-Marin V, Merino-Serrais P, Ávila J, DeFelipe J: Abnormal tau phosphorylation in the thorny excrescences of CA3 hippocampal neurons in patients with Alzheimer's disease. *J Alzheimers Dis* 2011, **26**(4):683–698.
24. Merino-Serrais P, Benavides-Piccione R, Blazquez-Llorca L, Kastanauskaitė A, Rábano A, Avila J, DeFelipe J: The influence of phospho-tau on dendritic spines of cortical pyramidal neurons in patients with Alzheimer's disease. *Brain* 2013, **136**:1913–1928.
25. Feng G, Mellor RH, Bernstein M, Keller-Peck C, Nguyen QT, Wallace M, Nerbonne JM, Lichtman JW, Sanes JR: Imaging neuronal subsets in transgenic mice expressing multiple spectral variants of GFP. *Neuron* 2000, **28**(1):41–51.
26. Fuhrmann M, Bittner T, Jung CKE, Burgold S, Page RM, Mitteregger G, Haass C, LaFerla FM, Kretschmar H, Herms J: Microglial Cx3cr1 knockout prevents neuron loss in a mouse model of Alzheimer's disease. *Nat Neurosci* 2010, **13**(4):411–413.
27. Holtmaat A, Bonhoeffer T, Chow DK, et al: Long-term, high-resolution imaging in the mouse neocortex through a chronic cranial window. *Nat Protoc* 2009, **4**(8):1128–1144.
28. Harris KM, Jensen FE, Tsao B: Three-dimensional structure of dendritic spines and synapses in rat hippocampus (CA1) at postnatal day 15 and adult ages: implications for the maturation of synaptic physiology and long-term potentiation. *J Neurosci* 1992, **12**(7):2685–2705.
29. Higuchi M, Iwata N, Matsuba Y, Sato K, Sasamoto K, Saido TC: 19 F and 1 H MRI detection of amyloid  $\beta$  plaques in vivo. *Nat Neurosci* 2005, **8**(4):527–533.
30. Sato K, Higuchi M, Iwata N, Saido TC, Sasamoto K: Fluoro-substituted and 13C-labeled styrylbenzene derivatives for detecting brain amyloid plaques. *Eur J Med Chem* 2004, **39**(7):573–578.
31. Schön C, Hoffmann NA, Ochs SM, et al: Long-term in vivo imaging of fibrillar tau in the retina of P301S transgenic mice. *PLoS One* 2012, **7**(12):e53547.
32. Velasco A, Fraser G, Delobel P, Ghetti B, Lavenir I, Goedert M: Detection of filamentous tau inclusions by the fluorescent congo red derivative FSB [(trans, trans)-1-fluoro-2,5-bis(3-hydroxycarbonyl-4-hydroxy) styrylbenzene]. *FEBS Lett* 2008, **582**(6):901–906.
33. De Calignon A, Spire-Jones TL, Pitstick R, Carlson GA, Hyman BT: Tangle-bearing neurons survive despite disruption of membrane integrity in a mouse model of tauopathy. *J Neuropathol Exp Neurol* 2009, **68**(7):757–761.
34. Brandt R, Hundelt M, Shahani N: Tau alteration and neuronal degeneration in tauopathies: mechanisms and models. *Biochim Biophys Acta* 2005, **1739**(2–3):331–354.
35. Götz J, Ittner LM: Animal models of Alzheimer's disease and frontotemporal dementia. *Nat Rev Neurosci* 2008, **9**(7):532–544.
36. Fu M, Zuo Y: Experience-dependent structural plasticity in the cortex. *Trends Neurosci* 2011, **34**(4):177–187.
37. Testa I, Urban NT, Jakobs S, Eggeling C, Willig KI, Hell SW: Nanoscopy of living brain slices with low light levels. *Neuron* 2012, **75**(6):992–1000.
38. Holtmaat A, Svoboda K: Experience-dependent structural synaptic plasticity in the mammalian brain. *Nat Rev Neurosci* 2009, **10**(9):647–658.
39. Arellano JL, Espinosa A, Fairén A, Yuste R, DeFelipe J: Non-synaptic dendritic spines in neocortex. *Neuroscience* 2007, **145**(2):464–469.
40. Holtmaat AJGD, Trachtenberg JT, Wilbrecht L, Shepherd GM, Zhang X, Knott GW, Svoboda K: Transient and persistent dendritic spines in the neocortex in vivo. *Neuron* 2005, **45**(2):279–291.
41. Harris JA, Koyama A, Maeda S, Ho K, Devidze N, Dubal DB, Yu G-Q, Masliah E, Mucke L: Human P301L-mutant tau expression in mouse entorhinal-hippocampal network causes tau aggregation and presynaptic pathology but no cognitive deficits. *PLoS ONE* 2012, **7**(9):e45881.
42. Takahashi RH, Capetillo-Zarate E, Lin MT, Milner TA, Gouras GK: Co-occurrence of Alzheimer's disease  $\beta$ -amyloid and tau pathologies at synapses. *Neurobiol Aging* 2010, **31**(7):1145–1152.

43. Chicurel M, Harris K: **Three-dimensional analysis of the structure and composition of CA3 branched dendritic spines and their synaptic relationships with mossy fiber boutons in the rat hippocampus.** *J Comp Neurol* 1992, **325**(2):169–182.
44. Sorra K, Harris K: **Overview on the structure, composition, function, development, and plasticity of hippocampal dendritic spines.** *Hippocampus* 2000, **10**(5):501–511.
45. Higuchi M, Lee VMY, Trojanowski JQ: **Tau and axonopathy in neurodegenerative disorders.** *Neuromolecular Med* 2002, **2**(2):131–150.
46. Leroy K, Bretteville A, Schindowski K, Gilissen E, Authélet M, De Decker R, Yilmaz Z, Buée L, Brion J-P: **Early axonopathy preceding neurofibrillary tangles in mutant tau transgenic mice.** *Am J Pathol* 2007, **171**(3):976–992.
47. Spittaels K, Van den Haute C, Van Dorpe J, *et al*: **Prominent axonopathy in the brain and spinal cord of transgenic mice overexpressing four-repeat human tau protein.** *Am J Pathol* 1999, **155**(6):2153–2165.
48. Druga R: **Neocortical inhibitory system.** *Folia Biol* 2009, **217**:201–217.
49. Kettenmann H, Kirchhoff F, Verkhratsky A: **Microglia: new roles for the synaptic stripper.** *Neuron* 2013, **77**(1):10–18.
50. Wake H, Moorhouse A, Jinno S, Kohsaka S, Nabekura J: **Resting microglia directly monitor the functional state of synapses in vivo and determine the fate of ischemic terminals.** *J Neurosci* 2009, **29**(13):3974–3980.
51. Wake H, Moorhouse AJ, Miyamoto A, Nabekura J: **Microglia: actively surveying and shaping neuronal circuit structure and function.** *Trends Neurosci* 2013, **36**(4):209–217.
52. SantaCruz K, Lewis J, Spires T, *et al*: **Tau suppression in a neurodegenerative mouse model improves memory function.** *Science* 2005, **309**(5733):476–481.
53. Shahani N, Subramaniam S, Wolf T, Tackenberg C, Brandt R: **Tau aggregation and progressive neuronal degeneration in the absence of changes in spine density and morphology after targeted expression of Alzheimer's disease-relevant tau constructs in organotypic hippocampal slices.** *J Neurosci* 2006, **26**(22):6103–6114.
54. Lasagna-Reeves CA, Castillo-Carranza DL, Sengupta U, Guerrero-Munoz MJ, Kiritoshi T, Neugebauer V, Jackson GR, Kaye R: **Alzheimer brain-derived tau oligomers propagate pathology from endogenous tau.** *Sci Rep* 2012, **2**:700.
55. Patterson KR, Remmers C, Fu Y, *et al*: **Characterization of prefibrillar tau oligomers in vitro and in Alzheimer disease.** *J Biol Chem* 2011, **286**(26):23063–23076.
56. Ward SM, Himmelstein DS, Lancia JK, Binder LI: **Tau oligomers and tau toxicity in neurodegenerative disease.** *Biochem Soc Trans* 2012, **40**(4):667–671.

doi:10.1186/2051-5960-1-82

**Cite this article as:** Hoffmann *et al*: Impaired plasticity of cortical dendritic spines in P301S tau transgenic mice. *Acta Neuropathologica Communications* 2013 **1**:82.

**Submit your next manuscript to BioMed Central and take full advantage of:**

- Convenient online submission
- Thorough peer review
- No space constraints or color figure charges
- Immediate publication on acceptance
- Inclusion in PubMed, CAS, Scopus and Google Scholar
- Research which is freely available for redistribution

Submit your manuscript at  
www.biomedcentral.com/submit





## **2.3 *In vivo* imaging reveals reduced activity of neuronal circuits in the mouse tauopathy model.**

Marinković P<sup>1</sup>, Blumenstock S<sup>1,2</sup>, Goldstein P<sup>3</sup>, Korzhova V<sup>1</sup>, Knebl A<sup>1</sup>, Peters F<sup>1</sup>, Stancu IC<sup>4</sup>, Dewachter I<sup>4</sup> and Herms J<sup>1,2,5</sup>.

<sup>1</sup>German Center for Neurodegenerative Diseases (DZNE), Munich, Germany.

<sup>2</sup>Munich Cluster of Systems Neurology (SyNergy), Munich, Germany.

<sup>3</sup>Max Planck Institute of Neurobiology, Dept. Synapses - Circuits Plasticity.

<sup>4</sup>Alzheimer Dementia Group, Department of Cell Physiology, Institute of Neuroscience, Catholic University of Louvain.

<sup>5</sup>Center for Neuropathology and Prion Research, Ludwig-Maximilians University, Munich, Germany.

### **Abstract**

Pathological alternations of tau protein play a significant role in the emergence and progression of neurodegenerative disorders. Tauopathies are characterized by the detachment of tau protein from microtubules and by subsequent aberrant hyperphosphorylation, localization and aggregation. The exact nature of tau species causing neuronal malfunction and degeneration is still unknown. Here, we took advantage of the possibility to experimentally induce the formation of neurofibrillary tangles in a portion of frontal cortex neurons of P301S mice that normally don't show prominent fibrillary tau aggregation. By using *in vivo* two photon microscopy we compared the activity of tangle-bearing neurons with the activity of their tangle-free neighbors. Our results reveal a clear reduction of activity in P301S cortical neurons independent of NFT presence. These results clearly point to the toxic role of soluble and hyperphosphorylated tau present in the majority of these neurons.

### **Introduction**

The microtubule-associated protein tau modulates the extent and the rate of microtubule assembly. Pathological tau protein modifications are critically involved in the pathogenesis of numerous nervous system disorders, collectively known as tauopathies [84]. Tauopathies, including Alzheimers disease (AD) and frontotemporal dementia with Parkinsonism linked to chromosome 17 (FTDP-17), are characterized by tau hyperphosphorylation, detachment of tau from axonal microtubules and subsequent misfolding and aggregation. Pathological aggregates can be observed as neurofibrillary tangles (NFTs) located in neuronal cell bodies and as neuropil threads in neuronal processes. The exact nature of neurotoxic tau species inducing malfunction of neurons is still not well understood [92]. The classical view implies that NFTs are deleterious for neurons. This is corroborated by numerous studies which showed that the number and extent of NFT spread throughout the brain is positively correlated with the progression of neurodegeneration, neuronal death and cognitive decline in AD patients (reviewed by [85]). On the other hand, studies in transgenic mouse models performed with single cell resolution challenged this view. For example, no link

### 2.3 *In vivo* imaging reveals reduced activity of neuronal circuits in the mouse tauopathy model.

---

could be established between the presence of NFTs and structural and functional degeneration observed in pyramidal neurons of the frontal cortex [230]. In addition, studies coming from the Hyman lab suggested that NFT-bearing neurons can survive prolonged periods of time and that they are functionally integrated in neuronal circuits even in the late stages of the disease [231, 190, 232].

Recent studies showed that the injection of brain extracts containing fibrillary tau or the injection of synthetic tau fibrils into brains of tau transgenic mice can induce the formation and spread of NFTs [224, 227]. It was suggested that tau fibrils serve as seeds to induce templated tau aggregation. Furthermore, tau fibrils are most likely the species of tau that spread throughout the brain. These findings opened new avenues to study the impact of tau aggregates on neuronal structure and function. In this study, we wanted to take advantage of this new possibility and induced NFT formation in the neurons and circuits which normally are not affected by this type of tau aggregates.

To investigate effects of various pathological tau species on the neuronal network functioning, we combined tau seeding with *in vivo* two-photon calcium imaging in awake P301S head-fixed mice [214, 233, 227, 228]. This approach enabled us to study the functional consequences of NFT formation in intact neuronal circuits and to directly compare performance of NFT-bearing neurons with NFT-free neurons. Our results suggest that soluble, hyperphosphorylated tau species are responsible for the observed reduction in neuronal activity of cortical layer 2/3 neurons in P301S mice. Tangle formation induced by templated misfolding and aggregation of tau protein didn't induce additional deleterious effects in our assay.

### Material and Methods

#### Animals

We used homozygous transgenic mice expressing human mutant P301S tau (383 aa four-repeat isoform of human tau) under the control of the Thy1.2 promoter [214]. Tau homozygosity was determined by real time PCR. For control animals we used mice of C57BL/6J strain (WT). All procedures were performed in accordance with an animal protocol approved by Government of Upper Bavaria (ref number GZ: 55.2-1-54-2532-163-13).

#### Stereotaxic Tau-PFF and virus injection

Two months old WT or P301S mice were anesthetized with an intraperitoneal injection of ketaminexylazine (ketamine 140 mg kg<sup>-1</sup>, xylazine 10 mg kg<sup>-1</sup>). In addition, dexamethasone (6 mg kg<sup>-1</sup>) was injected intraperitoneally to prevent the development of cerebral oedema. Mice were then placed on a heating blanket and stabilized in a stereotaxic frame. Pre-aggregated Tau formed fibrils (Tau-PFFs) were prepared as previously described [228]. Tau-PFFs were briefly sonicated and mixed with AAV1.hSyn1.mRuby2.GSG.P2A.GCaMP6s.WPRE.SV4 virus (Penn Vector Core, USA) before injection. Unilateral stereotaxic injection (right hemisphere) was performed in frontal cortex (A/P, + 2.0 mm; L, +1.4 mm, D/V, -0.7 mm). Total injected volume was 5 µL (final Tau PFFs concentration 333 µM, final virus titer 0.33 x 10<sup>13</sup> GC ml<sup>-1</sup>). Vehicle without Tau-PFFs (5 µL) was injected in the control group.

#### Cranial window implantation

Cranial window implantation was performed as previously described [201]. After stereotaxic Tau-PFFs and virus injection, a round craniotomy was made using a dental drill (Schick-Technikmaster C1; Pluraden), and immediately covered with a round coverslip (3 mm). The coverslip was sealed to the skull using dental acrylic (Cyano-Veneer fast; Schein). A custom made small metal bar was cemented next to the coverslip to allow head-fixation during training and imaging sessions. After surgery, mice received subcutaneous doses of the analgesic

### 2.3 *In vivo* imaging reveals reduced activity of neuronal circuits in the mouse tauopathy model.

---

carprofen (7.5 mg kg<sup>-1</sup>) and the antibiotic cefotaxime (5 mg kg<sup>-1</sup>). Mice with a cranial window implanted were housed individually in cages.

#### **Imaging in awake, head-fixed mice**

Imaging was performed in awake, head-fixed mice as described previously [233]. Mice were trained to head-fixation at least for seven days prior to imaging. On the first day of training, mice were handled to habituate to the researcher and to the experimental setup. An individual holding tube was assigned to each mouse, which they were allowed to explore. On the next day, in addition to habituation, mice would be occasionally head-fixed after passing through the holding tube for a brief period of time (10 s – 30 s). In following days, periods of head-fixation were gradually increased up to 1 hour at the end of training. Care was taken for the mice to feel comfortable in the holding tube and individual adjustments were made for each mouse if necessary. During head-fixation, mice typically showed long episodes of quiet wakefulness (quiet) interrupted by brief episodes of intensive whisking and movement (active). Therefore, we used whisking movement as an indicator of behavioral state (quiet vs. active).

Imaging started at least 21 days after surgery to allow mice to recover and cranial windows to clear. Before each imaging session, mice were head-fixed and placed under the microscope for 5 min to habituate. Imaging was performed in the dark without any stimuli. *In vivo* time-lapse image series of spontaneous activity of layer 2/3 frontal cortex neurons were acquired using the La Vision Trim Scope (La Vision BioTec GmbH, Germany) equipped with tunable Ti:sapphire two-photon lasers (Coherent Chameleon, Coherent USA and Mai Tai, Spectra Physics USA). The setup was controlled using La Vision Inspector software (La Vision BioTec GmbH, Germany). For recording calcium transients from layer 2/3 neurons, the laser was tuned to 940 nm which enabled simultaneous excitation of mRuby2 and GCaMP6s.

In order to visualize NFTs *in vivo*, we injected FSB i.p. 24 h – 48 h prior to imaging [234, 191]. Excited at 700 – 750 nm by the two-photon laser, FSB provided robust and bright NFT labeling. Laser power was kept under 80 mW at all times, measured at the back-focal plane of the objective. All time-lapse movies

## 2. Results

---

were taken at the frame rate of  $> 10$  Hz. For simultaneous imaging of NFTs and cortical layer 2/3 neurons labeled with GCaMP6s/mRuby2, Mai Tai tuned to 700-750 nm and Chameleon tuned to 940 nm were used in an alternate laser scan protocol. Emitted fluorescence light was split at 495 nm and 560 nm and detected by photomultiplier tubes. A web camera was installed and controlled by La Vison Inspector software which allowed synchronous recordings of mouse behavior and calcium transients at the same frame rate.

### Data processing and image analysis

Collected images were processed and analyzed using custom written codes in MATLAB and ImageJ software. Typical recordings consisted of three image-series. The first image series, recorded by two photon microscopy on the red channel ( $> 560$  nm), represented cell bodies labeled with mRuby2 (calcium insensitive). The second series recorded calcium changes reported by fluorescence changes of GCaMP6s in the neuronal cytoplasm (green channel 495 – 560 nm). The third – behavioral – time series was recorded by the camera. The behavior was classified as active and quiet behavioral states, using a MATLAB custom written code based on time-series recordings of whisker and body movements. Two-photon calcium imaging data was analyzed using a custom written MATLAB code. In brief, individual images from a single time series were aligned to each other in the x-y plane. Image registration parameters (x/y shift) were estimated using a Fourier transform based approach [235] on image data from the mRuby2 (structural) channel [236]. Regions of interest (ROIs) were manually identified using custom written software in MATLAB. For each ROI, a raw GCaMP6s fluorescence time series was constructed by averaging the pixel values within the region of interest for each individual imaging frame. Time series were corrected for contamination by local neuropil fluorescence and for changes in fluorescence caused by movement along the z-axis (in/out of plane movement) using the following method: local neuropil fluorescence was calculated by averaging all pixel values in an approximately 30  $\mu\text{m}$  ring around the ROI, excluding other ROIs. The effect of z-movement on the fluorescence intensity of an ROI was determined from the mRuby2 fluorescence within the ROI. The contribution

### 2.3 *In vivo* imaging reveals reduced activity of neuronal circuits in the mouse tauopathy model.

---

of the local neuropil signal ( $F_{neuropil}$ ) and z-motion ( $F_{motion}$ ) to the fluorescence within the ROI ( $F_{ROI_{raw}}$ ) was estimated using linear regression (equation 1). Finally, the median of the corrected time series ( $F_{ROI_{corrected}}$ ) was re-adjusted to the median of the original time series ( $F_{ROI_{raw}}$ ).

Equation 1:

$$F_{ROI_{raw}} = ROI_{corrected} + a \cdot F_{neuropil} + b \cdot F_{motion}$$

The relative fluorescence change over baseline,  $\Delta F/F$ , was calculated according to equation 2, where  $F_t$  is the absolute fluorescence at imaging frame  $t$ . Baseline fluorescence  $F_{0t}$  was calculated using a sliding window approach by – for each frame – averaging the lowest 50% fluorescence values in a 30 second sliding window before imaging frame  $t$  [237].

Equation 2:

$$\Delta F_t = \frac{F_t - F_{0t}}{F_{0t}}$$

Transient detection was performed using following criteria:  $> 3.5$  SD, rising time 0.2 s, decay time 0.5 s, inter-peak interval  $> 0.7$  s. Correlations in time series of  $\Delta F/F$  calcium activity were calculated using the Pearson correlation coefficient on z-scored segments.

#### Statistics

Two-way analysis of variance (ANOVA), followed by Bonferroni's multiple comparison test, and Student's t-tests were used. Statistical analysis were performed with GraphPad Prism software Version 5.04 (GraphPad Software Inc., La Jolla, CA, USA). P-values are reported and outlined as follows: \*P  $< 0.05$ , \*\*P  $< 0.01$  and \*\*\*P  $< 0.001$ . Mean with S.E.M. are indicated.

## Results

### Injection of Tau-PFFs induces rapid formation of neurofibrillary tangles in P301S mice

Using immunohistochemistry, we didn't observe NFT formation in the frontal cortex of WT mice which had been stereotactically inoculated with vehicle or Tau-PFFs (Figure 2.16 A and B). Similarly, histological analysis revealed no formation of NFTs in P301S mice injected with vehicle (Figure 2.16 C).

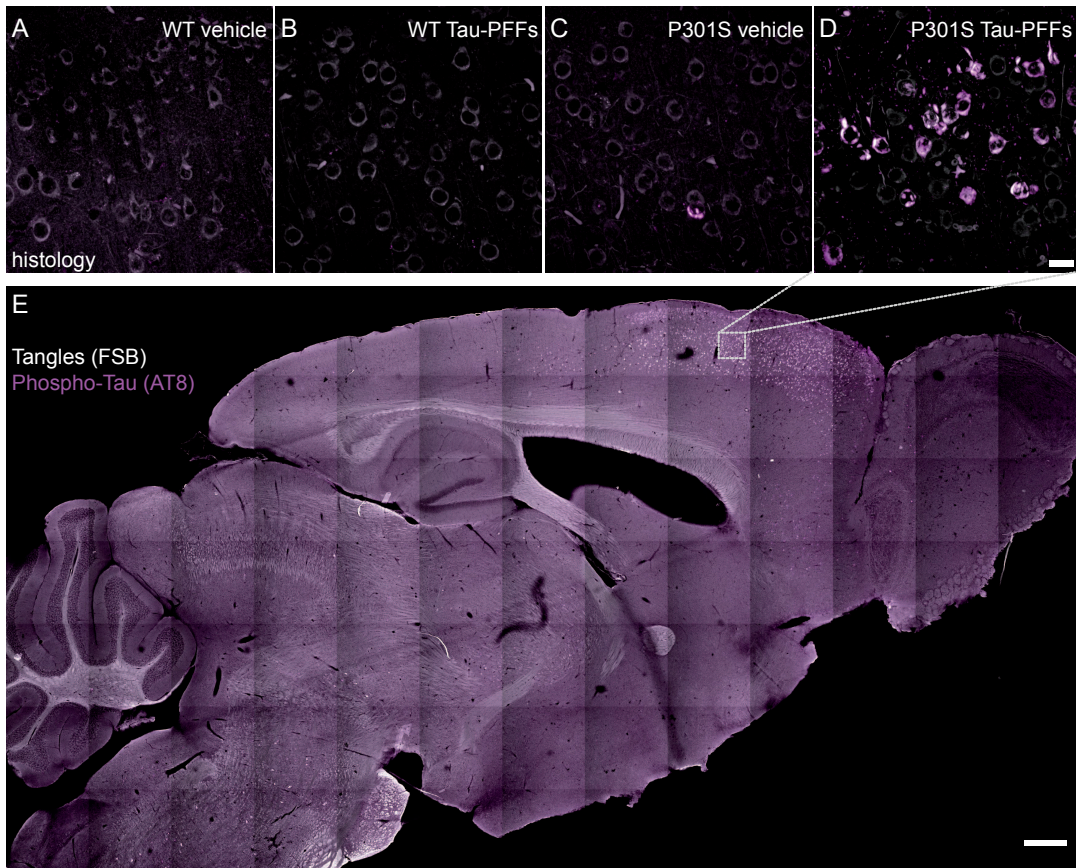


**Figure 2.16. Seeding of Tau PFFs causes local formation of NFTs.**(A-D) Frontal cortex of mice two weeks after injection at two months of age. (A) WT injected with vehicle; (B) WT injected with Tau-PFFs; (C) P301S injected with vehicle; (D) P301S injected with Tau-PFFs. Staining: FSB (white) and AT8 (magenta). Scale bar = 20  $\mu$ m. (E) Sagittal brain section of the homozygous P301S mouse injected with Tau-PFFs, also shown in detail in D. Scale bar = 500  $\mu$ m.

However, an injection of Tau-PFFs in P301S mice caused rapid and robust formation of NFTs in the frontal cortex (Figure 2.16 D and E), which were



### 2.3 *In vivo* imaging reveals reduced activity of neuronal circuits in the mouse tauopathy model.

hyperphosphorylated (AT8 positive) and expressed a  $\beta$ -sheet-rich amyloid structure (FSB positive). Morphologically, these intracellular aggregates displayed a "flame-like" shape, which is characteristic for NFTs.

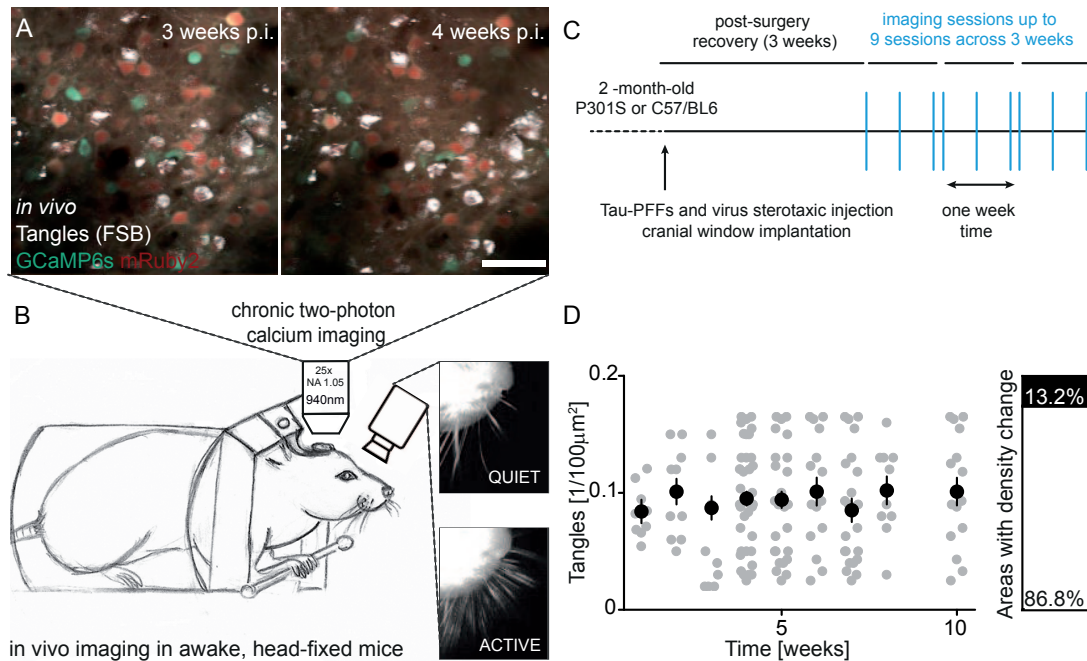


**Figure 2.17. Chronic two-photon calcium imaging in the tauopathy model.** (A) AAV1 transduced neurons are labeled with mRuby2 (red) and GCaMP6s (green). NFTs are labeled with FSB (white). The same neuronal population can be relocated over time (3 weeks post-injection (left) vs 4 weeks post-injection (right)) Images were made by averaging > 50 images acquired at > 10 Hz. (B) Schematic of a head-fixed mouse in the experimental setup with the camera for recording of behavior. Scale bar = 50  $\mu$ m. (C) Schematic of the experimental protocol. (D) Left: density of tangles over time. Black circles represent mean values  $\pm$  S.E.M. Gray circles represent individual fields of view. Right: percentage of fields of view in which changes of NFT density was observed.

We next wanted to detect NFTs *in vivo* using a cranial window preparation. In our experiments, it typically takes about three weeks after surgery for the cranial window to become clear and suitable for *in vivo* imaging. At this time-point and using i.p. injections of FSB dye, NFTs are easily detectable in the frontal cortex of P301S mice injected with Tau-PFFs (Figure 2.17 A). This provided an excellent opportunity to investigate the functional consequences of NFT formation on the single neuron level using two-photon *in vivo* calcium imaging (Figure 2.17 B). We were able to record over time from identical neuronal populations

## 2. Results

---

in order to follow individual neurons (Figure 2.17 A and B). Furthermore, using FSB staining we could easily differentiate between tangle-bearing neurons and their tanglefree neighbors. Our experimental design (Figure 2.17 C) allowed us to record from 4580 neurons over 3 or more time points in a total of 23 mice.

In order to investigate how fast NFTs form in our model and if there is formation of novel NFTs over time, we used i.p. injections of FSB to label all NFTs formed upon a given time-point. We performed this experiment in a separate cohort of mice which we followed up to 10 weeks after Tau-PFFs injection, in order to compare the density and presence of NFTs in same area over time (Figure 2.17 D). To our surprise, *in vivo* two-photon imaging revealed that NFTs form already within one week after injection. Our results show that NFT density does not change significantly over time after that (Figure 2.17 D, left panel). In rare cases, we could observe formation of novel NFTs (7 out of 53 areas (13.2% of total area); imaged in 9 mice, total 8 new NFTs; Figure 2.17 D, right panel). All events of newly formed NFTs occurred in the first three weeks after injection, i.e. when functional imaging is still not possible due to limited clarity of the cranial window. Furthermore, no NFT detected using *in vivo* two-photon imaging disappeared over the imaging period.

### **Neuronal activity is reduced in P301S mice independently of the presence of NFTs**

To investigate the functional consequences of NFT formation, we used two-photon calcium imaging in awake, head-fixed mice. We were able to simultaneously record calcium transients from 50 – 150 neurons in one field of view (Figure 2.18 A and B, left panel) at the single-neuron level. Three fluorescent channels were recorded simultaneously: mRuby2 (red), GCaMP6s (green) and FSB (blue). Transients were furthermore assigned to occur either during active or quiet behavioral states, by correlation with the whisking behavior of mice during the experiment (Figure 2.18 A and B, right panel).

2.3 *In vivo* imaging reveals reduced activity of neuronal circuits in the mouse tauopathy model.

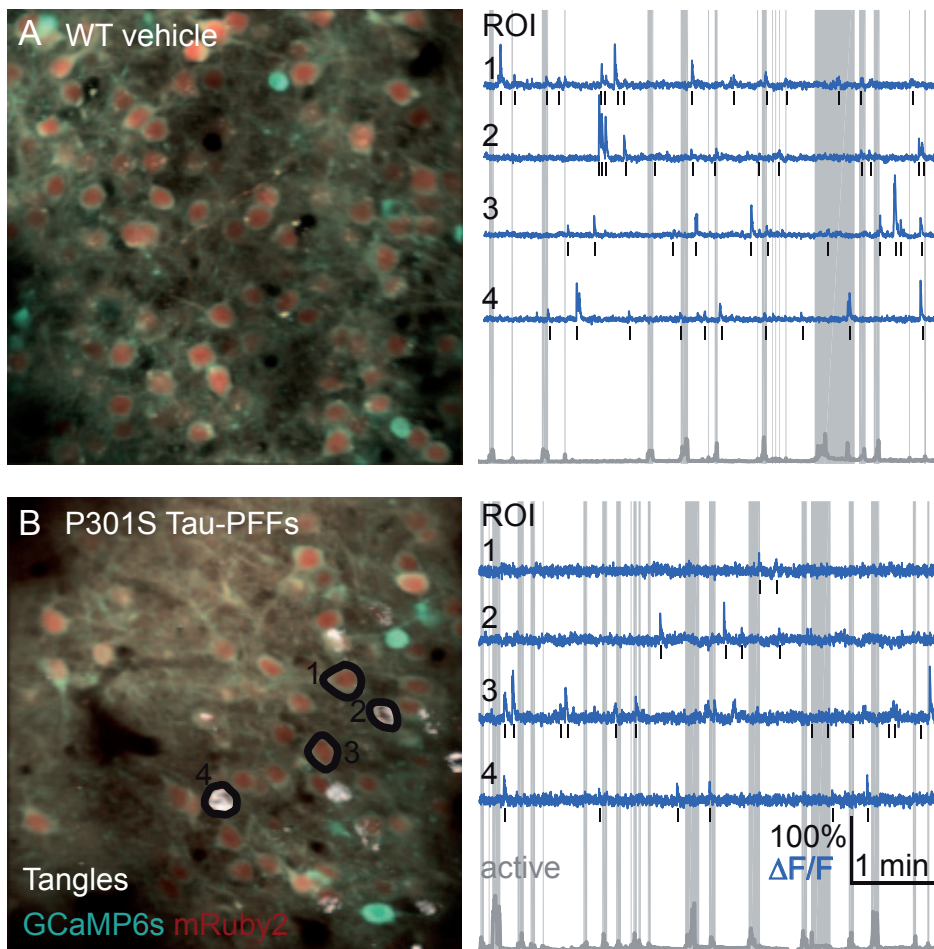


**Figure 2.18. Recording of neuronal activity in awake mice.** (A): Representative *in vivo* recordings from WT mice injected with vehicle. (B) representative recordings from P301S mice injected with Tau PFFs. Left panel: AAV1 transduced neurons are labelled with mRuby2 (red) and GCaMP6s (green). NFTs are labeled with FSB (white). Images were taken by averaging > 50 images acquired at > 10 Hz using a two-photon microscope. Scale bar = 50  $\mu\text{m}$ . Right panel: traces (blue) extracted from annotated ROIs (black) during quiet and active (grey shade) behavioral states classified based on changes in whisking movement (gray trace in the bottom).

The results showed that during both quiet and active behavioral states, neurons in P301S transgenic mice injected with Tau-PFFs show a clear reduction of activity, as measured by the number of calcium transients per minute (Figure 2.19 A). Two-way ANOVA analysis showed a significant effect between phenotypes (WT vs. P301S;  $F_{(1,19)} = 15,61$ ,  $p < 0,001$ ). The effects between the treatment groups (vehicle vs. Tau-PFFs) and the interaction within groups were not significant:  $F_{(1,19)} = 0,05$ ,  $P = 0,83$  and  $F_{(1,19)} = 0.16$ ,  $P = 0,69$ , respectively.

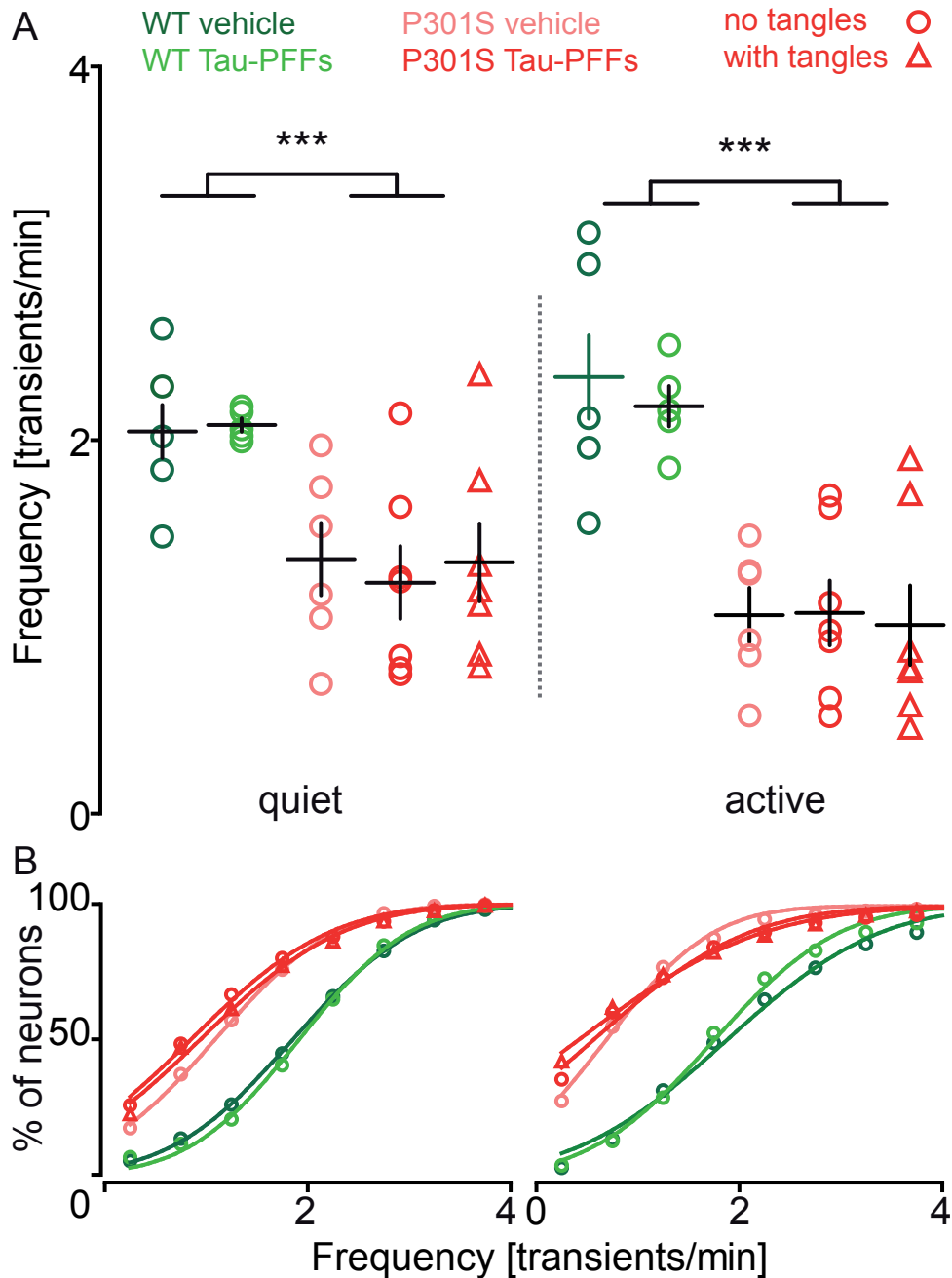


**Figure 2.19. Neuronal activity is reduced in P301S mice independently NFT presence (A)** Mean frequency of calcium transients during quiet and active states. All neurons detectable in three or more imaging time-points were included in the analysis. WT injected with vehicle (dark green), WT injected with Tau PFFs (light green) P301S injected with vehicle (light red), P301S injected with Tau-PFFs (dark red). The P301S group seeded with Tau-PFFs is further divided into tangle-free (red circles) and tangle-bearing neurons (red triangles). Symbols represent individual mice,  $n = 5-7$  mice per group, as illustrated; black lines represent mean value  $\pm$  SEM. \*\*\*,  $P < 0.001$  WT vs. P301S, two-way ANOVA. **(B)** Cumulative frequency plots of the data shown in the upper panel.

### 2.3 *In vivo* imaging reveals reduced activity of neuronal circuits in the mouse tauopathy model.

---

Closer analysis revealed no difference between tangle bearing neurons and their tangle-free neighbors during quiet wakefulness (Figure 2.19 A, red circles vs. red triangles, left panel). Very similar results were obtained when we analyzed activity during active phases. Again, only the phenotype effect was significant ( $F_{(1,19)} = 27,79$ ,  $p < 0,0001$ ). The effect of treatment (vehicle vs. Tau-PFFs) and the interaction were not significant:  $F_{(1,19)} = 0.6454$ ,  $P = 0.4317$  and  $F_{(1,19)} = 0.01604$ ,  $P = 0.9006$ . Similar to the quiet state, no difference in transient frequency between tangle bearing neurons and their tangle-free neighbors was observed during the active state (Figure 2.19 A, red circles vs. red triangles, right panel). To present the frequency distribution of individual neurons, we plotted the results as cumulative frequency graphs. In both quiet (left panel) and active (right panel) states, the curves of WT mice are clearly shifted to the left compared to the curves of P301S mice (Figure 2.19 B). The injection of vehicle or Tau-PFFs had no effect on the frequency distribution in neither phenotype cohort. Again, no difference between tangle-bearing and tanglefree neurons was observed.

### Discussion

In our study, we aimed to assess the impact of various pathological tau species on neuronal functioning. We therefore combined injection of Tau- PFFs with chronic *in vivo* two-photon calcium microscopy in a mouse model overexpressing human Tau with the P301S mutation. This approach enabled us to directly compare the effects of soluble, hyperphosphorylated tau with impact of NFT formation on the activity of individual neurons and neuronal circuits. By recording ongoing cortical activity in same neuronal population over prolonged time periods, we were furthermore able to partially mimic pathologic conditions in which changes gradually take place over the course of disease.

P301S mice are a well characterized mouse model exhibiting some essential features of a human tauopathy and were used in this study [214]. One reason for deliberately choosing this mouse model was the fact that these mice do not show formation on NFTs in the frontal cortex and only a subset of frontal cortex neurons contain substantial amounts of soluble hyperphosphorylated tau [2]. However, we demonstrate that injection of Tau-PFFs into the brains of these mice causes rapid formation of NFTs in the frontal cortex which could readily be detected using FSB dye [234, 191].

In this study, we used synthetic, pre-aggregated Tau fragments (Tau-PFFs), containing the four repeat domain of Tau with the P301L mutation [228]. Therefore, there is the possibility that observed tau-aggregates represent simply passive uptake of injected fibrils and are not the product of templated misfolding and aggregation of endogenous tau. Two lines of evidence argue against such a possibility. The aggregates are strongly stained with the anti-Tau Phospho-S202/T205 antibody (AT8). The AT8 epitope is not present on Tau-PFFs used for injection and therefore the aggregates that we observed are made, at least partially, from full-length endogenous tau. In addition, WT mice do not show any accumulation of tau upon injection of Tau-PFFs further opposing the passive uptake possibility.

In order to investigate the formation of novel NFTs in the frontal cortex, we continuously performed *in vivo* imaging of the mice up to 10 weeks after Tau-PFF injection. Interestingly, we didn't observe profound *de novo* formation

### 2.3 *In vivo* imaging reveals reduced activity of neuronal circuits in the mouse tauopathy model.

---

of NFTs, suggesting that mechanisms of local spreading are not present in our model. Basically all the NFTs were formed within first week after Tau-PFF injection. We believe that the rare cases in which we could observe appearance of NFTs in our images are rather due to accumulation of FSB upon repeated injections and/or due to improved clarity of cranial window. Up to date, no study followed formation of NFTs using chronic *in vivo* imaging. Previous *in vivo* studies mainly used histological analysis to assess the level of NFT spreading upon injection of seeding material (Tau-PFFs or brain homogenates containing the tau fibrils). In all these studies relatively slow progression (> 6 months) of NFT formation was shown and mainly in anatomically connected regions [224, 227, 229]. Therefore, it is possible that our mice too, would develop novel NFTs after a prolonged period of time. This however is not feasible in the homozygous P301S mice used in our study, as they develop severe motor deficits and have to be sacrificed due to ethical reasons already with 6 months of age. These results also raise an important question of careful titration of the injected Tau-PFF dose and appropriate choice of mouse recipient line in order to best mimic the seeding and spreading observed in human patients.

Our *in vivo* recordings indicate clear overall reduction in spontaneous activity of layer 2/3 neurons in P301S mice compared to WT mice. In P301S mice, which overexpress a mutated human tau isoform, a subset of cortical neurons contains substantial amounts of soluble hyperphosphorylated tau [2]. Interestingly, after injection of Tau-PFFs and subsequent formation of NFTs, neuronal circuits showed similar spontaneous activity rates as the circuits without NFTs. Specifically on the single neuron level, the tangle-bearing neurons had very similar transient frequencies in both quiet and active phases as the tangle-free neurons. This indicates that formation of NFTs in neurons do not induce additional effects in neuronal functioning. Of course, we cannot exclude that subtle structural and functional changes might take place which cannot be recorded in our assay.

Numerous studies have aimed to elucidate the effect of NFT formation on neuronal activity. Of particular interest for our work are those studies who investigated this matter on the single-neuron level and that differentiated between the tangle-bearing and tangle-free neurons. Studies coming from the Lübke lab investigated this in detail in cortical neurons in acute slice preparation [230]. Their

## 2. Results

---

results indicated that structural and functional changes in tau mutant mice are not linked to the presence of NFTs. However, they also reported increased activity of neurons in transgenic mice in response to stimulation. An *in vivo* study from the Hyman lab showed that tangle-bearing neurons are performing equally well as the tangle-free neurons [232]. Both groups of neurons were demonstrated to preserve their resting calcium levels and neuronal tuning and show similar values as the neurons in the WT control group. Finally, an important recent *in vivo* study investigated the ongoing activity in cortical neurons in intact circuits [238]. Although the authors do not differentiate between cortical neurons based on NFT presence, they find overall reduction in spontaneous activity, confirming a disruptive role of pathological tau.

Taken together our results point to the pathological role of tau species which are present before the formation of NFTs. The source for these protein species is mislocalized tau protein in the somatodendritic compartment which becomes misfolded and pathologically phosphorylated. This leads to formation of soluble oligomers and prefibrillar tau. In addition, it is reasonable to assume that toxic species could also involve small tau fibrils which still do not reach the critical size and concentration to form NFTs. NFT formation, on the other hand, might be the part of a disease off pathway as proposed by Bradley Hyman and coauthors [239, 232, 67]. Taken together these and our results could have an implication in the choice of the right therapeutic strategy in treating tauopathy patients. The results of this study advise caution in approaches aimed to dissolve or to prevent formation of tau aggregates and rather support the development of therapies focused on eliminating toxic soluble tau species.



# Discussion

## 3.1 *In vivo* two-photon imaging in the neocortex of the mouse

In contrast to the human neocortex, which is folded into a complex landscape of gyri and sulci, the surface of the mouse neocortex is smooth. This feature and its exposed position on the brain surface make it ideal for chronic structural investigations using *in vivo* two-photon microscopy, as two-photon lasers may penetrate tissue to a maximum of 1000  $\mu\text{m}$  [201]. The mouse cortex is furthermore organized into six layers with different cell types and laterally into a map of functionally distinct regions, which have been mapped into a 3D brain atlas [240]. Hence the study of structural alterations in physiologic and pathological conditions can be performed in a site-directed manner. The microscopy of living tissue used in this work holds two advantages over *ex vivo* studies and was essential for the questions addressed: (i) fine cellular structures like dendritic spines can be monitored in their physiological environment. For neuroscientists and for the studies presented in this thesis, this has particular value, as neurons are part of a vast and diverse neuronal and non-neuronal network, contributing to their structure and function; (ii) individual structures can be monitored over extended periods of time, which allows making statements about their development in physiological and pathological conditions. In the present work, this enabled valuable data on the dynamics of NFT development or on progressive structural changes in synucleinopathy and tauopathy mouse models.

The limitations of this technique involve its great complexity. *In vivo* experiments are time-consuming as well as technically advanced and financially expensive, which often limits the practicable sample size of mice involved in the experiment. Moreover, the maximal penetration depth of the two-photon laser determines the structures that can be accessed at all, which typically are located on the brain surface. The midbrain and the substantia nigra central to PD research cannot be accessed and the hippocampus, involved as it is in learning and memory and therefore of interest to dementia researchers, can only be imaged *in vivo* by removing the overlaying cortex [241, 242].

It is of particular importance to avoid physical and psychological stress for

the experimental animals, partly but not solely because chronic stress has been shown to have negative influence on synaptic plasticity and spine density [243]. Care should also be exercised by the choice of anesthesia like Ketamin/Xylazin or Isoflurane used in mice for *in vivo* imaging, which naturally also influence the nervous system. Ketamin/Xylazin has been shown to affect the turnover of dendritic spines in young neurons [244] and the survival of developing GABAergic interneurons as well as dendritic tree growth [245]. The alternative isofluoran-based anesthesia might increase tau phosphorylation and amyloid pathology in AD mouse models [246, 247]. Yet other studies could not show an effect of anesthesia on the development and dynamics of dendritic spines [248]. In any case of anesthetizing mice, it is important to ensure the maintenance of their body temperature. Hypothermia in mice is originally an adaptation to hibernation [249] and induces biochemical changes such as reduced phosphorylation of proteins due to inhibition of kinases. As the phosphorylation state of tau and  $\alpha$ -syn proteins affects their conformation and their pathogenicity, hypothermia should therefore be avoided [250].

Imaging of awake mice circumvents the restrictions entailed by anesthesia, but requires the mouse to be well-trained and habituated to the environment of the microscope and especially to head-fixation. The obtainment of stable microscopic images is only possible if the mouse is physically quiet during the imaging session. On the plus side stands the possibility to obtain functional images of network activity unaffected by anesthetic effects. In the summarized studies for this thesis, *in vivo* two-photon microscopy was used to obtain both structural and functional data. By interbreeding transgenic mouse lines modeling  $\alpha$ -synucleinopathy and tauopathy with the fluorescent reporter lines GFP-M or YFP-H, respectively, a subset of entire layer V cortical pyramidal neurons of the neocortex were labeled with eGFP or YFP, enabling the structural imaging of apical dendrites over time. Functional imaging of network activity was performed in a tauopathy model using virus-mediated expression of the  $\text{Ca}^{2+}$  indicator GCaMP6s. Being mindful of the points mentioned above, imaging sessions awake and under anesthesia did not persist for longer than one hour and hypothermia was avoided.

## 3.2 Seeding of pathogenic proteins

From *in vitro* biophysical studies it is known that fibril formation follows a nucleated polymerization mechanism. After a nucleation phase, in which multimerization of the protein is energetically unfavorable, cooperative oligomer growth and fibril formation occur through rapid monomer addition [28] and produces typical amyloid inclusions [251]. This process can be initiated (seeded) by the introduction of pathogenic protein fibrils (the seed) into a biological system, which may be ranging in complexity from cell-based assays to *in vivo* brain tissue, and is thought to be the underlying mechanism of spreading of  $\alpha$ -syn or tau pathology along neural axes in the brain (reviewed by [252, 109]). In the present work, the seeding of both  $\alpha$ -synuclein and tau was used to complement experiments with transgenic mouse models. The intention of this was to: (i) study the potential spread of pathogenic proteins across brain regions, (ii) induce the formation of nature LB-like and NFT-like inclusions and study their structural and functional consequences and (iii) gain information about which species of  $\alpha$ -syn or tau might be responsible for the observed changes.

### 3.2.1 alpha-synuclein

The templated misfolding and propagation of  $\alpha$ -synuclein is an intriguing part of its nature and has relevance for the pathogenesis of  $\alpha$ -synucleinopathies. It can be experimentally mimicked by the inoculation of either brain homogenates containing misfolded  $\alpha$ -syn species [217] or of *in vitro* preformed fibrils [253, 133, 223] into cell culture and animal models.

The exact way by which misfolded species spread from cell to cell is not entirely clarified yet, but several options have been described. Mediating  $\alpha$ -syn release, direct penetration of cellular membranes has been shown [254] as well as the release in clear vesicles [255] or via exosomes in a calcium-dependent manner [256].  $\alpha$ -syn oligomers present in the extracellular space were also observed to be taken up by neurons via trans-synaptic dissemination and transported via retrograde axonal transport to the soma [257]. Other uptake mechanisms include endocytosis and membrane-receptor mediated access [255]. Using mi-

crofluidic chambers to separate aggregate-developing donor cells and synaptically connected naïve acceptor neurons, it was shown that PFFs can be transported in both the anterograde and retrograde directions but that synaptic contact is not required for transmission [258, 134].

For our study on the impact of  $\alpha$ -syn on cortical synapses [1],  $\alpha$ -syn PFFs were injected into the dorsal striatum of experimental mice. The striatum is an important connection between the cortex and the midbrain, and is directly involved in the circuit-level changes that affect the direct and the indirect pathways in PD (reviewed by [259]). Seeding of  $\alpha$ -syn PFFs into the mouse striatum has been described previously [223]. In our study, progressive intraneuronal aggregation of endogenous  $\alpha$ -syn was detected in the neocortex as early as 30 days post-injection of PFFs. Until 9 months post-injection,  $\alpha$ -syn aggregates condensed and matured to fibrillary structures [260]. 5 months after seeding, the ipsilateral cortex — particularly in layer IV — and the amygdala were the most prominently affected brain regions.  $\alpha$ -syn aggregates were also detected in the contralateral cortex and the substantia nigra. From previous data tracing the projections from and to the dorsal striatum, the topographical pattern of  $\alpha$ -syn inclusions observed here can be in part ascribed to retrograde and anterograde spreading [261]. Histochemically, the  $\alpha$ -syn aggregates possessed several features characteristic for Lewy bodies in the human disease. They were hyper-phosphorylated [262] at Ser129 and could be stained with Thioflavin S, a fluorescent marker for amyloidogenic structures [39]. Finally, they were positive for ubiquitin [263], which represents a cellular tag marking them for degradation. There was no evidence for seeded  $\alpha$ -syn aggregate formation in mice lacking endogenous  $\alpha$ -syn (SNCA-KO) and experiments using fluorescently tagged  $\alpha$ -syn PFFs indicated that inclusions did not simply consist of PFFs taken up by cells, but had formed from endogenous  $\alpha$ -syn. This confirms that  $\alpha$ -syn can undergo templated conversion and aggregation, as it was previously shown by others.

### 3.2.2 Tau

Similar to  $\alpha$ -syn, tau protein can undergo templated misfolding, also by its interaction with various co-factors [67]. Likewise, experimentally seeding tau pathol-

### 3. Discussion

---

ogy has been described in various cellular and *in vivo* systems [224, 227, 228, 264].

The identification of cellular mechanisms for tau spreading revealed several variances. The trans-synaptic pathway for movement of tau between cells, as suggested by Braak et al. [71] was confirmed by Calafate et al. Their study explored tau propagation using a microfluidic chamber and demonstrated that both synaptic connectivity and synaptic activity increases tau-propagation [265]. Furthermore, tau has been described to be directly secreted into the medium via exosomes and then taken up by co-cultured cells [266, 267, 268]. Uptake mechanisms include fluid phase endocytosis, macropinocytosis and bulk endocytosis [136, 137] Once inside cells, misfolded tau can be transported anterogradely as well as retrogradely and mislocalizes from the axon to the somatodendritic compartment [264].

In our study on the impact of tau on network activity, tau PFFs were injected directly into the cortex of P301S mice, where they rapidly triggered intracellular aggregation of tau. These inclusions displayed a flame-like shape, characteristic for human NFTs present in AD brains. They were also hyper-phosphorylated [269] as demonstrated by IHC using the AT8 antibody, which recognizes the phosphorylation at Ser202/Thr205. By their positivity for FSB, a small and blood-brain-barrier permeating fluorescent molecule, *in vivo* [191] the amyloid nature of the tau inclusions was confirmed. In accordance with existing data, the seeding of PFFs into wild-type mouse brain did not lead to the formation of amyloid inclusions. A recent study demonstrated that unique pathological tau conformers from AD brains are able to transmit tau pathology in nontransgenic mice, but PFFs are not [226]. These findings highlight important differences between artificially generated tau fibrils and ones that develop within AD brains.

In contrast to other studies, the development of NFT-like inclusions was restricted to the site of injection in our experiments. Considering the time-frame of three weeks between seeding and *in vivo* imaging, it is possible that this was too short for the relatively slow progression of NFT formation in anatomically connected regions. Other studies usually assessed tau spreading after longer periods of time (> 6 months) [224, 227, 229]. The main scientific question of our study, however, was to study local network dysfunction linked to the presence of various tau species rather than tau spreading.

### 3.2.3 Mechanistic considerations and potential pitfalls of experimental seeding

The method of inoculating pathogenic proteins to model the spread of pathogenic proteins in neurodegenerative diseases has created significant excitement and interest among researchers in the field. It undoubtedly has some advantages over — or in combination with — transgenic models in the search for novel therapeutic strategies. Using seeding as a method allows the mapping of connected neuroanatomical pathways by which the induced proteinopathy spreads. Accordingly, seeding approaches can be very useful for assessing whether pathology is able to spread from the periphery into the CNS, an important notion considering that the earliest features of PD may relate to pathology outside of the brain, like the gut [270]. On the front of therapeutics research, tackling the clearance of  $\alpha$ -syn or tau during the process of cell-to-cell transfer remains a promising approach (reviewed by [211, 252]). There are however some restrictions that should be considered as well.

In order to experimentally induce proteinopathies using PFFs, usually an excessive amount of fibrillary protein is injected into the tissue, overwhelming the natural barriers that physiologically prevent the induction and spread of pathology. The use of transgenic mice for seeding studies likewise represents an artificial enhancement of susceptibility towards a bolus insult of aggregated protein. The amount of protein injected is far higher than the protein concentrations that could be locally encountered in a physiological situation and might lead to exaggerated or false-positive findings. The intracerebral injection of PFFs in a stereotactic procedure also presents an insult to cells and brain tissue, which might artificially promote cellular uptake and could lead to proteostatic perturbations. Cellular degradation machineries, like the autophagy-lysosomal system or the ubiquitin-proteasome system, might become dysbalanced by misfolded protein species and thus contribute to the spread of pathology. Furthermore, the activation of gliosis might also facilitate the spread of pathology in both  $\alpha$ -syn and tau seeding models. Astrocytes have been shown to be actively involved in the spread of  $\alpha$ -syn pathology and the induction of inflammatory cellular damage mediated by microglia might also be a considerable factor (reviewed by

[109]). Similarly, microglial involvement is also known to aid the propagation of tau [271].

Other than that, one should consider the variances of homotypic versus heterotypic seeding. Homotypic or self-seeding suggests that conformational templating requires the presence of sequence-specific substrates, able to form the typical cross  $\beta$ -sheet conformation. It is quite clear that this process occurs during the spread of  $\alpha$ -syn pathology, supported by findings in cell lines stably overexpressing  $\alpha$ -syn lacking the NAC domain, in which PFFs fail to trigger the formation of inclusions [272, 133]. It was also reported that tau follows templated misfolding, depending on the biophysical properties of the seeding material [141]. The phenomenon of one amyloidogenic protein seeding the aggregation of another is referred to as heterotypic seeding. Indeed,  $\alpha$ -syn and tau have been shown to synergistically promote the fibrillization of each other *in vitro* [273] and in cell culture [274] and might be also relevant *in vivo*.

### 3.3 Dendritic spines in mouse models of alpha-synucleinopathy and tauopathy

Spines are experience dependent dynamic structures and a certain turnover and rearrangement of morphology can be observed even in the adult brain [275]. This enables neurons to modify their synaptic interconnections, which are the correlates for learning and memory [167]. The structural changes are based on reorganization of actin filaments within spines and can occur within seconds to hours [276]. An observed loss of spines can hence be due to e.g. the loss of persistent spines, a reduced number of newly formed spines or a general increase in the number of retracted spines. Relevant for this work is the fact that synaptic spine degeneration belongs to the early structural correlates of dementia [168, 169]. For that reason, the chronic study of synaptic plasticity using *in vivo* microscopy can give important insights about the pathophysiology of diseases like AD and PD. Several previous publications have addressed spine pathology in animal models of  $\alpha$ -synucleinopathies and tauopathies and in human patients and are summarized hereafter.



### 3.3 Dendritic spines in mouse models of alpha-synucleinopathy and tauopathy

---

The first explicit proof for dendritic spine alterations in  $\alpha$ -synucleinopathies was obtained from toxin-induced models of parkinsonism. Both 6-hydroxydopamine (6-OHDA) treated rats as well as 1-methyl-4-phenyl-1,2,3,6-tetrahydropyridine (MPTP) treated monkeys showed a 20 % reduction in striatal spine density [277, 278]. Some authors report that D2 receptor striatopallidal neurons in reserpine and 6-OHDA-treated mice selectively lose spines [279], while others found spine loss on both direct and indirect pathway neurons in 6-OHDA or MPTP-treated models [280]. In a mouse model overexpressing the human A53T  $\alpha$ -syn mutation, spine loss has been observed in the striatum and in the hippocampus [281]. In contrast, another study failed to detect striatal spine loss in A53T mice, despite a decrease in the number of SNpc neurons [282].  $\alpha$ -syn was also demonstrated to have negative impact on newly generated neurons of the hippocampus [283] and the olfactory bulb [284], particularly on their dendrite outgrowth and spine development. Finally, in brains of Parkinson's patients, the degree of spine loss correlated with the level of dopaminergic denervation of the striatum and striatal spine loss was also present in DLB brains [285, 286].

On the tauopathy front, knowledge about the effect of tau on synapses is inconsistent, strongly depending on the tauopathy model, the stage of disease progression and the brain region analyzed. Mice carrying the *MAPT* mutation P301L display impaired dendritic tree development and reduced cortical spine density independent of NFT presence [287, 230]. Spine loss was also present prior to NFT development in the hippocampus of mice expressing human P301S mutant Tau under the prion promotor [288]. In another study, spine density was found unchanged in cortical layer III neurons [289] while spine volume decreased in mice expressing all six human isoforms of tau instead of the murine protein. Even an age dependent increase in spine density in layer III cortical neurons was reported for mice expressing human P301L tau or WT tau, with no effect on the hippocampus [290]. In the light of these inconsistent findings coming from studies using various models and approaches, it is difficult to draw general conclusions about how the (over-)expression of (mutant) tau or  $\alpha$ -syn impairs dendritic spine plasticity. The aim of this work was therefore to shed some more light on the pathologic process of synapse loss in the respective neurodegenerative diseases.

#### **3.3.1 Transgenic overexpression of alpha-synuclein and mutant tau causes changes in dendritic spine plasticity**

In order to study the  $\alpha$ -syn-mediated alterations in spine plasticity over extended time periods, data on spine dynamics was obtained from mice overexpressing WT human  $\alpha$ -syn under the PDGF $\beta$  promoter at three ages. Young (3-month-old) mice showed a progressive loss of spines due to a reduced spine formation, whereas older (6 months) and aged (12 months) mice compensated the reduced overall density of spines with an increased daily turnover ratio (dTOR). Concerning spine morphology, the progressive spine loss in young h- $\alpha$ -syn mice was reflected in the diminished fraction of thin spines, which are known to partially correspond to non-synaptic and transient precursors of the larger persistent spines [291, 292]. In older mice (6- and 12-month-old), further spine loss was counterbalanced by an elevation in the dTOR, which was in turn matched by an increase in the fraction of thin spines at the cost of mushroom spines.

In our study on spines in tau transgenic mice [2], we aimed to add the dimension of spine kinetics over time to the existing knowledge, as all previous studies were based on *ex vivo* data. Chronic *in vivo* imaging of apical dendrites in the cortex of 4-month-old mice overexpressing tau protein with the P301S mutation (termed P301S mice) showed reduced and progressively decreasing density of dendritic spines. Data on spine kinetics showed that the observed spine loss was caused by a reduction in the fraction of gained spines in P301S mice compared to controls. The density fractions of lost and persistent spines remained unaffected. Concerning the morphology of the remaining spines, P301S mice showed a trend towards an increased spine volume, which correlated with the increase in the fraction of mushroom spines at the cost of the thin spine fraction. As mentioned above, thin spines are considered to correspond to developing or immature spines and this is reflected in our study in the decrease of the gained spine fraction in P301S mice. It is important to note, that the neurons imaged *in vivo* did not contain NFTs, but a majority of these cells were found to overexpress soluble and unphosphorylated tau in the subsequent *ex vivo* analysis.

### 3.3.2 Abnormal spine density, morphology and dendritic shape after alpha-synuclein seeding

The seeding of pathogenic preformed fibrils (PFFs) contrasts with classical transgenic mouse models for the study of neurodegenerative diseases and represents a fairly recent advance in the field. Nevertheless, it has generated great interest in the field of neurodegenerative disease research and a wealth of studies have addressed the routes and mechanisms of pathologic protein spread (reviewed by [293, 252]). The impact of seeded  $\alpha$ -syn inclusions on the structure of dendrites and dendritic spines, however, was unknown and for this reason was one of the aims of our study [1]. Based on the knowledge that preformed fibrils (PFFs) of  $\alpha$ -syn can induce spread of LB-like  $\alpha$ -syn aggregates [223] in WT mice, PFFs were injected into the striatum of GFP-M reporter mice bearing no additional disease-related transgene.

The analysis of spine density and morphology 5 months post-injection showed dendritic spine loss in layer V pyramidal neurons of the neocortex as well as a redistribution in the morphology towards less thin spines. Importantly, the observed spine loss was independent of a spatial proximity of the respective dendrite towards a LB-like inclusion, which indicates a dysfunction of the neuronal network rather than to a local toxic effect of  $\alpha$ -syn inclusions. The morphological change towards a decreased fraction of thin spines also indicates that less immature and developing spines are present [291, 292]. How the exact dynamics of spines are changed, however, could be the subject of a chronic *in vivo* imaging study.

Another interesting observation of the study on the  $\alpha$ -syn seeding model was the presence of dystrophic dendrites. These have been described in mouse models of prion-disease [202] and AD [294]. Additionally, varicosities in axons have been reported to be induced by  $\alpha$ -syn seeding [295]. Here, the degeneration of the respective cell body and the related axonal transport deficits could contribute to the dystrophic deformation of dendrites. In fact, it has been shown that seeded aggregates in neurons mature over time and lead to the degeneration of the respective cell body [260].

#### **3.3.3 Proposed mechanisms for alpha-synuclein and tau-mediated spine alterations**

Synapses are complex structures, consisting of several compartments structurally belonging to distinct neurons or glia. Synaptic degeneration can be based on contributions of all components and the dissection of temporal and spatial mechanisms of these pathological processes remains a challenge.

With  $\alpha$ -syn being a presynaptic protein, it seems likely that a presynaptic pathology is responsible for the neurodegenerative effect and in the case of our study, spine loss. In fact, it was shown that presynaptic microaggregates of  $\alpha$ -syn are present in the cortical and subcortical gray matter of DLB patients and that they were linked to dendritic spine loss [39]. Mechanistically,  $\alpha$ -syn was demonstrated to inhibit neurotransmitter release by reducing the size of the presynaptic vesicle recycling pool [296]. Together with the functional role  $\alpha$ -syn plays in SNARE-driven vesicle fusion for neurotransmitter release [297, 298], its role in regulating the cytoskeleton [299, 300] would certainly affect synaptic plasticity.

Relevant for the loss of synapses might also be the cascade of postsynaptic events induced by chronically elevated influx of  $\text{Ca}^{2+}$  ions, which recruits and saturates the postsynaptic membrane with AMPA receptors, which causes a decline in the ability to induce LTP and leads to overall excitotoxicity [301, 302]. However, as spine dynamics were not disturbed in the same way across the cohorts, the mechanisms involved in spine alterations might not be uniform throughout the course of disease.

One part of our study in P301S transgenic mice was to assess whether dendritic spine degeneration is linked to the presence of hyper-phosphorylated tau within spines. However, no hyper-phosphorylated Tau could be detected within spines of the cortex in P301S mice, not even in those cells in which the somatodendritic compartment was strongly positive for phospho-tau. In contrast to this, we and others could observe hyper-phosphorylated tau in spines in the hippocampus of P301S mice [2], other tauopathy and AD mouse models [288, 303] and postmortem AD brains [304, 305]. The disparate subcellular localization of tau could be explained by differential composition of the spine cytoskeleton in

### 3.3 Dendritic spines in mouse models of alpha-synucleinopathy and tauopathy

---

the cortex and the hippocampus. Whereas in cortical spines it is actin-based, CA3 hippocampal postsynapses contain microtubules [306], which can associate with tau and therefore may also explain the presence of phospho-tau.

Furthermore, the observed spine impairments could be caused by presynaptic or axonal pathology and local network dysfunction. Even though a direct follow up of both connected pre- and postsynaptic structures is scarcely achievable *in vivo*, several points indicate that these factors might play a role in spine impairments in both our tau and the  $\alpha$ -syn models. The fact that a subset of eYFP-positive layer V neurons does not express the P301S tau mutant transgene is such an indicator. Furthermore, we also did not observe the presence of  $\alpha$ -syn in dendrites of eGFP-positive layer V neurons. Instead,  $\alpha$ -syn showed a prominent presynaptic localization, which is well known from previously published literature (reviewed by [307]) and was confirmed by co-staining with a VGLUT1 antibody, a marker of glutamatergic presynapses.

As another factor that might be relevant for the observed spine alterations in the P301S model, axonal pathology is known to be prominent in tauopathies [308, 309, 310]. The P301S mouse model has also previously been shown to develop axonopathy and deposits of hyper-phosphorylated tau in the optic nerve before fibrillary tau was present in retinal ganglion cells [311]. On the neuronal network level, homozygous P301S mice were shown to exhibit astrogliosis and death of layer II/III cortical neurons at 3 months of age, with a particular vulnerability of GABAergic interneurons [312]. The degeneration of cortical interneurons could disinhibit the network, thereby causing overexcitation and degeneration of dendritic spines. A similar mechanism of dendritic spine degeneration might in fact also be true for the  $\alpha$ -syn seeding model. In the cortex of  $\alpha$ -syn seeded mice, the accumulation of fibrillary phospho-syn was observed most strongly in neurons of the layer IV, which are predominantly interneurons and project intracortically to other cells like layer II/III pyramidal neurons [259]. From our current data, the exact functional consequence on these cells is not clarified and remains the subject of study. However, it seems likely that the dysfunction of interneurons might also lead to a disinhibition of the cortical network.

Finally, the involvement of microglia as the primary immune cells of the brain, is another biological factor that could promote pathological spine loss. Microglial

activation is known to be present in PD and AD brains and both protective and detrimental contributions have been attributed (reviewed by [313, 314]). Interestingly, microglia have also been described to facilitate spine formation [315] as well as to mediate spine loss in AD [168]. From our dendritic spine study including the seeding of  $\alpha$ -syn PFFs, no unequivocal statement on the involvement of microglia can be made at this point and could be the objective of future investigation.

## 3.4 Network alterations due to aberrant expression of tau

*In vivo* recordings of network activity in P301S mice, described in the manuscript by Marinković et al., aimed to elucidate the functional changes that are linked to the presence of various pathological tau species. A combination of tau seeding and tau P301S transgenic mice were used to trigger the formation of NFTs in the frontal cortex, an area in which usually no NFTs develop in this model.

P301S transgenic mice overexpress human mutant tau which is predominantly soluble and in the frontal cortex of these mice. *In vivo* network analysis showed a clear overall reduction in spontaneous neuronal activity in these mice compared to WT controls. Interestingly, this effect was independent of the presence of NFTs after seeding, which indicates that formation of NFTs in neurons does not induce additional effects in neuronal functioning. This is in line with several studies demonstrating that tangle-bearing neurons are functionally not different from tangle-free neurons [232, 230]. However, there is also support for the disruptive role of pathological tau in the activity of cortical neurons [238]

The results of this study on network activity moreover connect to the findings of Hoffmann et al. [2], where it was previously discussed that local network alterations might give rise to the structural changes which can be observed in dendritic spine density and morphology. Our new results indicate that this in fact might be the case, as an alteration in synaptic input is known to affect synaptic plasticity (reviewed by [150]).

### 3.5 In search for toxic protein species

In neurodegenerative proteinopathies, monomeric proteins traverse several intermediate stages, before they end up in their pathologic state; mature Lewy bodies, neurofibrillary tangles, amyloid plaques or other types of insoluble deposits. Up to date, there is still considerable debate about which species of protein, whether misfolded monomers, oligomers, protofibrils or fibrils pose the greatest threat to neuronal homeostasis. Some evidence for the tau and  $\alpha$ -syn proteins indicates that NFTs and LBs might actually represent a mechanism of cells to sequester smaller and more toxic oligomers into less harmful accumulates (reviewed by [316, 317]).

There is a general consensus in the field that assigns the aggregation of  $\alpha$ -syn a main pathogenic role, but uncertainty remains about the nature of neurotoxic forms. A prominent concept states that especially  $\alpha$ -syn oligomers have such a potential. For example, the proteins with the E64K mutation fibrillize less readily than the WT protein [318] and the presence of oligomers, rather than mature fibrils, proved to correlate best with neurotoxicity in cellular systems and *in vivo* [319, 320]. Protofibrillar oligomers were also shown to alter membrane permeability, increasing  $\text{Ca}^{2+}$  influx from the extracellular to the intracellular space which causes neurotoxicity [321].  $\alpha$ -syn oligomers can also prove toxic by disrupting microtubules [322], damaging mitochondria [323] or causing lysosomal leakage [324]. It is further under debate, whether it is the process of fibril formation, rather than the  $\alpha$ -syn fibrils themselves, that has the greater impact on  $\alpha$ -syn neurotoxicity [317].

Some uncertainty also remains for the exact nature for neurotoxic tau species. Although, the number and extent of NFTs spread throughout the brain is positively correlated with the progression of neurodegeneration and cognitive decline in AD patients (reviewed by [85]), other studies challenged this view. For example, the presence of NFTs was not linked to structural and functional degeneration in a mouse model for tauopathy [230] and NFT bearing neurons were shown to survive and stay functionally intact even in phenotypically late stages [190, 325]. In a reversible tauopathy mouse model, the suppression of the *MAPT*-transgene causes an improvement in cognitive performance, despite pro-

### 3. Discussion

---

gressive NFT formation [326]. Furthermore, the presence of NFTs was found not to cause structural and functional changes in neurons in different mouse models [230, 288] or changes in dendritic spine density and morphology [327]. The maldistribution of mitochondria was additionally found to depend on soluble, non-fibrillary tau protein in tauopathy mouse models [328]. On the other hand, there are some studies supporting the toxicity of higher-order tau aggregates, like prefibrillar oligomers [329, 330]. From our present data on structural and functional alterations in the P301S model and from tau seeding however, there is stronger support for the toxicity of soluble oligomers rather than NFTs.

While numerous studies have addressed the molecular mechanism behind the toxicity of proteins like tau and  $\alpha$ -syn, it remains to be clarified whether a toxic gain-of-function, a loss-of-function or both is responsible for the degeneration of synapses and neurons in diseases like AD and PD. Future research unraveling the disease mechanisms will add to the present knowledge about the potential points of intervention, leading to the development of effective treatments.

The combined studies in this thesis demonstrate the impact of potentially toxic and misfolded proteins involved in neurodegenerative diseases on structural plasticity of synapses and on cortical network activity. Chronic two-photon imaging in live mice enables the study of brain tissue in a time-resolved manner during the progression of pathology. The present studies on spine dynamics in mouse models of alpha-synucleinopathy and tauopathy provide a link to the pathophysiology underlying dementia which is associated with both  $\alpha$ -synucleinopathies like Parkinson's disease and tauopathies like frontotemporal dementia or Alzheimer's disease. Especially in combination with site-directed seeding of pathogenic protein species, these chronic imaging studies enable both the study of disease progression and the evaluation of potential drug candidates and their impact on spine pathology *in vivo*.

In conclusion, studies in animal models as presented in this work can be of advantage for the understanding of the very complex facets of neurodegenerative diseases. Piece by piece, they create knowledge about the mechanisms of synaptic and neuronal death, which may translate to patients to improve clinical practice for better diagnosis and therapy.



# Bibliography

- [1] Blumenstock, S. *et al.* Seeding and transgenic overexpression of alpha-synuclein triggers dendritic spine pathology in the neocortex. *EMBO Molecular Medicine* **9**, 716–731 (2017).
- [2] Hoffmann, N. A., Dorostkar, M. M., Blumenstock, S., Goedert, M. & Herms, J. Impaired plasticity of cortical dendritic spines in P301S tau transgenic mice. *Acta neuropathologica communications* **1**, 1 (2013).
- [3] WHO. Active ageing: A policy framework. *The Aging Male* **5**, 1–37 (2002).
- [4] Forman, M. S., Trojanowski, J. Q. & Lee, V. M. Neurodegenerative diseases: A decade of discoveries paves the way for therapeutic breakthroughs. *Nature medicine* **10**, 1055–1063 (2004).
- [5] Parkinson, J. *An Essay on the Shaking Palsy* (Whittingham and Rowland, 1817). Google-Books-ID: 4ygSAAAAYAAJ.
- [6] De Lau, L. M. & Breteler, M. M. Epidemiology of Parkinson’s disease. *The Lancet Neurology* **5**, 525–535 (2006).
- [7] Meissner, W. G. *et al.* Priorities in Parkinson’s disease research. *Nature Reviews Drug Discovery* **10**, 377–393 (2011).
- [8] Koller, W. C. *et al.* Does a long preclinical period occur in Parkinson’s disease? *Neurology* **41**, 8–13 (1991).
- [9] Gonera, E. G., van’t Hof, M., Berger, H. J., van Weel, C. & Horstink, M. W. Symptoms and duration of the prodromal phase in Parkinson’s disease. *Movement Disorders: Official Journal of the Movement Disorder Society* **12**, 871–876 (1997).
- [10] Fearnley, J. M. & Lees, A. J. Ageing and Parkinson’s disease: Substantia nigra regional selectivity. *Brain: A Journal of Neurology* **114** ( Pt 5), 2283–2301 (1991).
- [11] Schiesling, C., Kieper, N., Seidel, K. & Krüger, R. Review: Familial Parkinson’s disease—genetics, clinical phenotype and neuropathology in relation to the common sporadic form of the disease. *Neuropathology and Applied Neurobiology* **34**, 255–271 (2008).
- [12] Farrer, M. J. Genetics of Parkinson disease: Paradigm shifts and future prospects. *Nature Reviews Genetics* **7**, 306–318 (2006).
- [13] Adler, C. H. Premotor Symptoms and Early Diagnosis of Parkinson’s Disease. *International Journal of Neuroscience* **121**, 3–8 (2011).
- [14] Raggi, A., Bella, R., Pennisi, G., Neri, W. & Ferri, R. Sleep disorders in Parkinson’s disease: A narrative review of the literature. *Reviews in the Neurosciences* **24** (2013).
- [15] Doty, R. L. Olfaction in Parkinson’s disease and related disorders. *Neurobiology of Disease* **46**, 527–552 (2012).
- [16] Starkstein, S. E., Brockman, S. & Hayhow, B. D. Psychiatric syndromes in Parkinson’s disease:.. *Current Opinion in Psychiatry* **25**, 468–472 (2012).

## BIBLIOGRAPHY

---

- [17] Pfeiffer, R. F. Gastrointestinal dysfunction in Parkinson's disease. *The Lancet Neurology* **2**, 107–116 (2003).
- [18] Aarsland D, Andersen K, Larsen JP & Lolk A. Prevalence and characteristics of dementia in parkinson disease: An 8-year prospective study. *Archives of Neurology* **60**, 387–392 (2003).
- [19] Halliday, G., Hely, M., Reid, W. & Morris, J. The progression of pathology in longitudinally followed patients with Parkinson's disease. *Acta Neuropathologica* **115**, 409–415 (2008).
- [20] Carlsson, A., Lindqvist, M. & Magnusson, T. 3,4-Dihydroxyphenylalanine and 5-hydroxytryptophan as reserpine antagonists. *Nature* **180**, 1200 (1957).
- [21] Carlsson, A., Lindqvist, M., Magnusson, T. & Waldeck, B. On the presence of 3-hydroxytyramine in brain. *Science (New York, N.Y.)* **127**, 471 (1958).
- [22] Cotzias, G. C., Papavasiliou, P. S. & Gellene, R. Modification of Parkinsonism—chronic treatment with L-dopa. *The New England Journal of Medicine* **280**, 337–345 (1969).
- [23] Andén, N. E., Dahlström, A., Fuxe, K. & Larsson, K. Mapping out of catecholamine and 5-hydroxytryptamine neurons innervating the telencephalon and diencephalon. *Life Sciences* **4**, 1275–1279 (1965).
- [24] Poirier, L. J. & Sourkes, T. L. INFLUENCE OF THE SUBSTANTIA NIGRA ON THE CATECHOLAMINE CONTENT OF THE STRIATUM. *Brain: A Journal of Neurology* **88**, 181–192 (1965).
- [25] Baba, M. *et al.* Aggregation of alpha-synuclein in Lewy bodies of sporadic Parkinson's disease and dementia with Lewy bodies. *The American Journal of Pathology* **152**, 879–884 (1998).
- [26] Spillantini, M. G. *et al.* Alpha-synuclein in Lewy bodies. *Nature* **388**, 839–840 (1997).
- [27] Lewy, F. & Forster, E. Paralysis agitans. In *Pathologische Anatomie. Lewandowsky's Handbuch Der Neurologie*, vol. 3. Band: Spez. Neurologie II of *Pathologische Anatomie*, 920–933 (Springer, Berlin, 1912).
- [28] Conway, K. A. *et al.* Acceleration of oligomerization, not fibrillization, is a shared property of both  $\alpha$ -synuclein mutations linked to early-onset Parkinson's disease: Implications for pathogenesis and therapy. *Proceedings of the National Academy of Sciences* **97**, 571–576 (2000).
- [29] Forman, M. S. *et al.* Tau and alpha-synuclein pathology in amygdala of Parkinsonism-dementia complex patients of Guam. *The American Journal of Pathology* **160**, 1725–1731 (2002).
- [30] Pappolla, M. A., Shank, D. L., Alzofon, J. & Dudley, A. W. Colloid (hyaline) inclusion bodies in the central nervous system: Their presence in the substantia nigra is diagnostic of Parkinson's disease. *Human Pathology* **19**, 27–31 (1988).
- [31] Redgrave, P. *et al.* Goal-directed and habitual control in the basal ganglia: Implications for Parkinson's disease. *Nature Reviews Neuroscience* **11**, 760–772 (2010).
- [32] Gerfen, C. R. *et al.* D1 and D2 dopamine receptor-regulated gene expression of striatonigral and striatopallidal neurons. *Science (New York, N.Y.)* **250**, 1429–1432 (1990).

- [33] McNaught, K. S. P. & Jenner, P. Proteasomal function is impaired in substantia nigra in Parkinson's disease. *Neuroscience letters* **297**, 191–194 (2001).
- [34] Friedman, A. & Galazka-Friedman, J. The current state of free radicals in Parkinson's disease. Nigral iron as a trigger of oxidative stress. *Advances in Neurology* **86**, 137–142 (2001).
- [35] Guo, J. L. & Lee, V. M. Y. Cell-to-cell transmission of pathogenic proteins in neurodegenerative diseases. *Nature Medicine* **20**, 130–138 (2014).
- [36] Prayson, R. A. *Neuropathology: A Volume in the Series: Foundations in Diagnostic Pathology* (Elsevier Health Sciences, 2011). Google-Books-ID: WN1fSy6qlzUC.
- [37] Dickson, D. W. Parkinson's Disease and Parkinsonism: Neuropathology. *Cold Spring Harbor Perspectives in Medicine* **2**, a009258–a009258 (2012).
- [38] Braak, H. *et al.* Staging of brain pathology related to sporadic Parkinson's disease. *Neurobiology of aging* **24**, 197–211 (2003).
- [39] Kramer, M. L. & Schulz-Schaeffer, W. J. Presynaptic  $\alpha$ -Synuclein Aggregates, Not Lewy Bodies, Cause Neurodegeneration in Dementia with Lewy Bodies. *Journal of Neuroscience* **27**, 1405–1410 (2007).
- [40] Lesage, S. *et al.* Loss of VPS13C Function in Autosomal-Recessive Parkinsonism Causes Mitochondrial Dysfunction and Increases PINK1/Parkin-Dependent Mitophagy. *American Journal of Human Genetics* **98**, 500–513 (2016).
- [41] Klein, C. & Westenberger, A. Genetics of Parkinson's Disease. *Cold Spring Harbor Perspectives in Medicine* **2**, a008888–a008888 (2012).
- [42] Maroteaux, L., Campanelli, J. T. & Scheller, R. H. Synuclein: A neuron-specific protein localized to the nucleus and presynaptic nerve terminal. *The Journal of Neuroscience* **8**, 2804–2815 (1988).
- [43] Iwai, A. *et al.* The precursor protein of non-A $\beta$  component of Alzheimer's disease amyloid is a presynaptic protein of the central nervous system. *Neuron* **14**, 467–475 (1995).
- [44] Jakes, R., Spillantini, M. G. & Goedert, M. Identification of two distinct synucleins from human brain. *FEBS letters* **345**, 27–32 (1994).
- [45] Stefanis, L.  $\alpha$ -Synuclein in Parkinson's Disease. *Cold Spring Harbor Perspectives in Medicine* **2**, a009399–a009399 (2012).
- [46] Beyer, K. Mechanistic aspects of Parkinson's disease:  $\alpha$ -synuclein and the biomembrane. *Cell Biochemistry and Biophysics* **47**, 285–299 (2007).
- [47] George, J. M. The synucleins. *Genome biology* **3**, reviews3002–1 (2001).
- [48] Moussaud, S. *et al.* Alpha-synuclein and tau: Teammates in neurodegeneration? *Molecular neurodegeneration* **9**, 43 (2014).
- [49] Weinreb, P. H., Zhen, W., Poon, A. W., Conway, K. A. & Lansbury, P. T. NACP, a protein implicated in Alzheimer's disease and learning, is natively unfolded. *Biochemistry* **35**, 13709–13715 (1996).
- [50] Davidson, W. S., Jonas, A., Clayton, D. F. & George, J. M. Stabilization of  $\alpha$ -synuclein secondary structure upon binding to synthetic membranes. *Journal of Biological Chemistry* **273**, 9443–9449 (1998).

## BIBLIOGRAPHY

---

- [51] Middleton, E. R. & Rhoades, E. Effects of Curvature and Composition on  $\alpha$ -Synuclein Binding to Lipid Vesicles. *Biophysical Journal* **99**, 2279–2288 (2010).
- [52] Bartels, T., Choi, J. G. & Selkoe, D. J.  $\alpha$ -Synuclein occurs physiologically as a helically folded tetramer that resists aggregation. *Nature* **477**, 107–110 (2011).
- [53] Conway, K. A., Harper, J. D. & Lansbury, P. T. Accelerated in vitro fibril formation by a mutant alpha-synuclein linked to early-onset Parkinson disease. *Nature Medicine* **4**, 1318–1320 (1998).
- [54] Withers, G. S., George, J. M., Banker, G. A. & Clayton, D. F. Delayed localization of synelfin (synuclein, NACP) to presynaptic terminals in cultured rat hippocampal neurons. *Developmental brain research* **99**, 87–94 (1997).
- [55] Kholodilov, N. G. *et al.* Increased expression of rat synuclein in the substantia nigra pars compacta identified by mRNA differential display in a model of developmental target injury. *Journal of neurochemistry* **73**, 2586–2599 (1999).
- [56] Vila, M. *et al.*  $\alpha$ -Synuclein Up-Regulation in Substantia Nigra Dopaminergic Neurons Following Administration of the Parkinsonian Toxin MPTP. *Journal of neurochemistry* **74**, 721–729 (2000).
- [57] Abeliovich, A. *et al.* Mice lacking  $\alpha$ -synuclein display functional deficits in the nigrostriatal dopamine system. *Neuron* **25**, 239–252 (2000).
- [58] Fortin, D. L. Neural Activity Controls the Synaptic Accumulation of  $\alpha$ -Synuclein. *Journal of Neuroscience* **25**, 10913–10921 (2005).
- [59] Murphy, D. D., Rueter, S. M., Trojanowski, J. Q. & Lee, V. M.-Y. Synucleins are developmentally expressed, and  $\alpha$ -synuclein regulates the size of the presynaptic vesicular pool in primary hippocampal neurons. *Journal of Neuroscience* **20**, 3214–3220 (2000).
- [60] Südhof, T. C. & Rothman, J. E. Membrane Fusion: Grappling with SNARE and SM Proteins. *Science* **323**, 474–477 (2009).
- [61] Burré, J. *et al.*  $\alpha$ -Synuclein promotes SNARE-complex assembly in vivo and in vitro. *Science* **329**, 1663–1667 (2010).
- [62] Burre, J., Sharma, M. & Südhof, T. C. Systematic Mutagenesis of  $\alpha$ -Synuclein Reveals Distinct Sequence Requirements for Physiological and Pathological Activities. *Journal of Neuroscience* **32**, 15227–15242 (2012).
- [63] Vargas, K. J. *et al.* Synucleins Regulate the Kinetics of Synaptic Vesicle Endocytosis. *Journal of Neuroscience* **34**, 9364–9376 (2014).
- [64] Chandra, S., Gallardo, G., Fernández-Chacón, R., Schlüter, O. M. & Südhof, T. C.  $\alpha$ -Synuclein Cooperates with CSP $\alpha$  in Preventing Neurodegeneration. *Cell* **123**, 383–396 (2005).
- [65] Benskey, M. J., Perez, R. G. & Manfredsson, F. P. The contribution of alpha synuclein to neuronal survival and function - Implications for Parkinson's disease. *Journal of Neurochemistry* **137**, 331–359 (2016).
- [66] Prince, M. & Jackson, J. World Alzheimer Report (2009).
- [67] Spires-Jones, T. L., Stoothoff, W. H., de Calignon, A., Jones, P. B. & Hyman, B. T. Tau pathophysiology in neurodegeneration: A tangled issue. *Trends in Neurosciences* **32**, 150–159 (2009).

- [68] Alzheimer, A. Über eine eigenartige Erkrankung der Hirnrinde. *Allg. Zeitschr. Psychiatr.* 146–148 (1907).
- [69] Sütterlin, S., Hossmann, I. & Klingholz, R. *Demenz-Report: Wie Sich Die Regionen in Deutschland, Österreich Und Der Schweiz Auf Die Alterung Der Gesellschaft Vorbereiten Können* (DEU, 2011).
- [70] Joachim, C. L., Morris, J. H., Kosik, K. S. & Selkoe, D. J. Tau antisera recognize neurofibrillary tangles in a range of neurodegenerative disorders. *Annals of Neurology* **22**, 514–520 (1987).
- [71] Braak, H. & Del Tredici, K. Potential Pathways of Abnormal Tau and  $\alpha$ -Synuclein Dissemination in Sporadic Alzheimer’s and Parkinson’s Diseases. *Cold Spring Harbor Perspectives in Biology* **8**, a023630 (2016).
- [72] Huang, Y. & Mucke, L. Alzheimer Mechanisms and Therapeutic Strategies. *Cell* **148**, 1204–1222 (2012).
- [73] Hof, P. R., Cox, K. & Morrison, J. H. Quantitative analysis of a vulnerable subset of pyramidal neurons in Alzheimer’s disease: I. Superior frontal and inferior temporal cortex. *The Journal of Comparative Neurology* **301**, 44–54 (1990).
- [74] Whitehouse, P. J. *et al.* Alzheimer’s disease and senile dementia: Loss of neurons in the basal forebrain. *Science (New York, N.Y.)* **215**, 1237–1239 (1982).
- [75] Gómez-Isla, T. *et al.* Profound loss of layer II entorhinal cortex neurons occurs in very mild Alzheimer’s disease. *The Journal of Neuroscience: The Official Journal of the Society for Neuroscience* **16**, 4491–4500 (1996).
- [76] Terry, R. D. *et al.* Physical basis of cognitive alterations in alzheimer’s disease: Synapse loss is the major correlate of cognitive impairment. *Annals of Neurology* **30**, 572–580 (1991).
- [77] Grutzendler, J., Helmin, K., Tsai, J. & Gan, W.-B. Various dendritic abnormalities are associated with fibrillar amyloid deposits in Alzheimer’s disease. *Annals of the New York Academy of Sciences* **1097**, 30–39 (2007).
- [78] Haass, C. & Selkoe, D. J. Cellular processing of  $\beta$ -amyloid precursor protein and the genesis of amyloid  $\beta$ -peptide. *Cell* **75**, 1039–1042 (1993).
- [79] Haass, C., Kaether, C., Thinakaran, G. & Sisodia, S. Trafficking and Proteolytic Processing of APP. *Cold Spring Harbor Perspectives in Medicine* **2**, a006270–a006270 (2012).
- [80] Hardy, J. A. & Higgins, G. A. Alzheimer’s disease: The amyloid cascade hypothesis. *Science (New York, N.Y.)* **256**, 184–185 (1992).
- [81] Hardy, J. The Amyloid Hypothesis of Alzheimer’s Disease: Progress and Problems on the Road to Therapeutics. *Science* **297**, 353–356 (2002).
- [82] Braak, H. & Braak, E. Neuropathological staging of Alzheimer-related changes. *Acta Neuropathologica* **82**, 239–259 (1991).
- [83] Braak, H. & Braak, E. Frequency of stages of Alzheimer-related lesions in different age categories. *Neurobiology of Aging* **18**, 351–357 (1997 Jul-Aug).
- [84] Lee, V. M., Goedert, M. & Trojanowski, J. Q. Neurodegenerative tauopathies. *Annual Review of Neuroscience* **24**, 1121–1159 (2001).

## BIBLIOGRAPHY

---

- [85] Nelson, P. T. *et al.* Correlation of Alzheimer disease neuropathologic changes with cognitive status: A review of the literature. *Journal of Neuropathology and Experimental Neurology* **71**, 362–381 (2012).
- [86] Binder, L. I., Frankfurter, A. & Rebhun, L. I. The distribution of tau in the mammalian central nervous system. *The Journal of cell biology* **101**, 1371–1378 (1985).
- [87] Neve, R. L., Harris, P., Kosik, K. S., Kurnit, D. M. & Donlon, T. A. Identification of cDNA clones for the human microtubule-associated protein tau and chromosomal localization of the genes for tau and microtubule-associated protein 2. *Brain Research* **387**, 271–280 (1986).
- [88] Goedert, M., Spillantini, M. G., Jakes, R., Rutherford, D. & Crowther, R. A. Multiple isoforms of human microtubule-associated protein tau: Sequences and localization in neurofibrillary tangles of Alzheimer's disease. *Neuron* **3**, 519–526 (1989).
- [89] Goedert, M. & Jakes, R. Expression of separate isoforms of human tau protein: Correlation with the tau pattern in brain and effects on tubulin polymerization. *The EMBO journal* **9**, 4225–4230 (1990).
- [90] Weingarten, M. D., Lockwood, A. H., Hwo, S. Y. & Kirschner, M. W. A protein factor essential for microtubule assembly. *Proceedings of the National Academy of Sciences of the United States of America* **72**, 1858–1862 (1975).
- [91] Butner, K. A. & Kirschner, M. W. Tau protein binds to microtubules through a flexible array of distributed weak sites. *The Journal of Cell Biology* **115**, 717–730 (1991).
- [92] Ballatore, C., Lee, V. M.-Y. & Trojanowski, J. Q. Tau-mediated neurodegeneration in Alzheimer's disease and related disorders. *Nature Reviews Neuroscience* **8**, 663–672 (2007).
- [93] Mazanetz, M. P. & Fischer, P. M. Untangling tau hyperphosphorylation in drug design for neurodegenerative diseases. *Nature Reviews Drug Discovery* **6**, 464–479 (2007).
- [94] Kampers, T., Pangalos, M., Geerts, H., Wiech, H. & Mandelkow, E. Assembly of paired helical filaments from mouse tau: Implications for the neurofibrillary pathology in transgenic mouse models for Alzheimer's disease. *FEBS letters* **451**, 39–44 (1999).
- [95] Takashima, A. *et al.* Presenilin 1 associates with glycogen synthase kinase-3 $\beta$  and its substrate tau. *Proceedings of the National Academy of Sciences of the United States of America* **95**, 9637–9641 (1998).
- [96] Brandt, R., Léger, J. & Lee, G. Interaction of tau with the neural plasma membrane mediated by tau's amino-terminal projection domain. *The Journal of Cell Biology* **131**, 1327–1340 (1995).
- [97] Kuret, J. *et al.* Evaluating triggers and enhancers of tau fibrillization. *Microscopy Research and Technique* **67**, 141–155 (2005).
- [98] Mandelkow, E.-M., Stamer, K., Vogel, R., Thies, E. & Mandelkow, E. Clogging of axons by tau, inhibition of axonal traffic and starvation of synapses. *Neurobiology of Aging* **24**, 1079–1085 (2003).
- [99] Thies, E. & Mandelkow, E.-M. Missorting of tau in neurons causes degeneration of synapses that can be rescued by the kinase MARK2/Par-1. *The Journal of Neuroscience: The Official Journal of the Society for Neuroscience* **27**, 2896–2907 (2007).

- 
- [100] Rubinsztein, D. C. The roles of intracellular protein-degradation pathways in neurodegeneration. *Nature* **443**, 780–786 (2006).
- [101] Krüger, R. *et al.* Ala30Pro mutation in the gene encoding alpha-synuclein in Parkinson's disease. *Nature Genetics* **18**, 106–108 (1998).
- [102] Zarranz, J. J. *et al.* The new mutation, E46K, of  $\alpha$ -synuclein causes parkinson and Lewy body dementia. *Annals of neurology* **55**, 164–173 (2004).
- [103] Appel-Cresswell, S. *et al.* Alpha-synuclein p.H50Q, a novel pathogenic mutation for Parkinson's disease. *Movement Disorders: Official Journal of the Movement Disorder Society* **28**, 811–813 (2013).
- [104] Lesage, S. *et al.* G51D  $\alpha$ -synuclein mutation causes a novel parkinsonian-pyramidal syndrome. *Annals of Neurology* **73**, 459–471 (2013).
- [105] Polymeropoulos, M. H. *et al.* Mutation in the alpha-synuclein gene identified in families with Parkinson's disease. *Science (New York, N.Y.)* **276**, 2045–2047 (1997).
- [106] Pasanen, P. *et al.* Novel  $\alpha$ -synuclein mutation A53E associated with atypical multiple system atrophy and Parkinson's disease-type pathology. *Neurobiology of Aging* **35**, 2180.e1–5 (2014).
- [107] Chartier-Harlin, M.-C. *et al.*  $\alpha$ -synuclein locus duplication as a cause of familial Parkinson's disease. *The Lancet* **364**, 1167–1169 (2004).
- [108] Singleton, A. B. *et al.* Alpha-Synuclein locus triplication causes Parkinson's disease. *Science (New York, N.Y.)* **302**, 841 (2003).
- [109] Uchiyama, T. & Giasson, B. I. Propagation of alpha-synuclein pathology: Hypotheses, discoveries, and yet unresolved questions from experimental and human brain studies. *Acta Neuropathologica* **131**, 49–73 (2016).
- [110] Choi, W. *et al.* Mutation E46K increases phospholipid binding and assembly into filaments of human alpha-synuclein. *FEBS letters* **576**, 363–368 (2004).
- [111] Ghosh, D. *et al.* The Parkinson's disease-associated H50Q mutation accelerates  $\alpha$ -Synuclein aggregation in vitro. *Biochemistry* **52**, 6925–6927 (2013).
- [112] Fortin, D. L. Lipid Rafts Mediate the Synaptic Localization of  $\alpha$ -Synuclein. *Journal of Neuroscience* **24**, 6715–6723 (2004).
- [113] Betarbet, R. *et al.* Chronic systemic pesticide exposure reproduces features of Parkinson's disease. *Nature Neuroscience* **3**, 1301–1306 (2000).
- [114] Fares, M.-B. *et al.* The novel Parkinson's disease linked mutation G51D attenuates in vitro aggregation and membrane binding of  $\alpha$ -synuclein, and enhances its secretion and nuclear localization in cells. *Human Molecular Genetics* **23**, 4491–4509 (2014).
- [115] Ghosh, D. *et al.* The newly discovered Parkinson's disease associated Finnish mutation (A53E) attenuates  $\alpha$ -synuclein aggregation and membrane binding. *Biochemistry* **53**, 6419–6421 (2014).
- [116] Hutton, M. *et al.* Association of missense and 5'-splice-site mutations in tau with the inherited dementia FTDP-17. *Nature* **393**, 702–705 (1998).
- [117] von Bergen, M. *et al.* Mutations of tau protein in frontotemporal dementia promote aggregation of paired helical filaments by enhancing local beta-structure. *The Journal of Biological Chemistry* **276**, 48165–48174 (2001).

## BIBLIOGRAPHY

---

- [118] Lippa, C. F. *et al.* Lewy bodies contain altered alpha-synuclein in brains of many familial Alzheimer's disease patients with mutations in presenilin and amyloid precursor protein genes. *The American Journal of Pathology* **153**, 1365–1370 (1998).
- [119] Iseki, E., Marui, W., Kosaka, K. & Uéda, K. Frequent coexistence of Lewy bodies and neurofibrillary tangles in the same neurons of patients with diffuse Lewy body disease. *Neuroscience letters* **265**, 9–12 (1999).
- [120] Arai, Y. *et al.* Alpha-synuclein-positive structures in cases with sporadic Alzheimer's disease: Morphology and its relationship to tau aggregation. *Brain Research* **888**, 287–296 (2001).
- [121] Burns, J. M., Galvin, J. E., Roe, C. M., Morris, J. C. & McKeel, D. W. The pathology of the substantia nigra in Alzheimer disease with extrapyramidal signs. *Neurology* **64**, 1397–1403 (2005).
- [122] Mori, H. *et al.* Lewy bodies in progressive supranuclear palsy. *Acta neuropathologica* **104**, 273–278 (2002).
- [123] Duda, J. E. *et al.* Concurrence of  $\alpha$ -synuclein and tau brain pathology in the Contursi kindred. *Acta Neuropathologica* **104**, 7–11 (2002).
- [124] Yamaguchi, K. *et al.* Abundant neuritic inclusions and microvacuolar changes in a case of diffuse Lewy body disease with the A53T mutation in the  $\alpha$ -synuclein gene. *Acta Neuropathologica* **110**, 298–305 (2005).
- [125] Yancopoulos, D., Xuereb, J. H., Crowther, R. A., Hodges, J. R. & Spillantini, M. G. Tau and alpha-synuclein inclusions in a case of familial frontotemporal dementia and progressive aphasia. *Journal of Neuropathology and Experimental Neurology* **64**, 245–253 (2005).
- [126] Kotzbauer, P. T. *et al.* Fibrillization of alpha-synuclein and tau in familial Parkinson's disease caused by the A53T alpha-synuclein mutation. *Experimental Neurology* **187**, 279–288 (2004).
- [127] Millicamps, S. & Julien, J.-P. Axonal transport deficits and neurodegenerative diseases. *Nature Reviews Neuroscience* **14**, 161–176 (2013).
- [128] Compta, Y. *et al.* Lewy- and Alzheimer-type pathologies in Parkinson's disease dementia: Which is more important? *Brain* **134**, 1493–1505 (2011).
- [129] Kordower, J. H., Freeman, T. B. & Olanow, C. W. Neuropathology of fetal nigral grafts in patients with Parkinson's disease. *Movement Disorders: Official Journal of the Movement Disorder Society* **13 Suppl 1**, 88–95 (1998).
- [130] Duyckaerts, C., Uchihara, T., Seilhean, D., He, Y. & Hauw, J. J. Dissociation of Alzheimer type pathology in a disconnected piece of cortex. *Acta Neuropathologica* **93**, 501–507 (1997).
- [131] Waxman, E. A. & Giasson, B. I. A Novel, High-Efficiency Cellular Model of Fibrillar  $\alpha$ -Synuclein Inclusions and the Examination of Mutations that Inhibit Amyloid Formation. *Journal of neurochemistry* **113**, 374–388 (2010).
- [132] Nonaka, T., Watanabe, S. T., Iwatsubo, T. & Hasegawa, M. Seeded Aggregation and Toxicity of  $\alpha$ -Synuclein and Tau. *The Journal of Biological Chemistry* **285**, 34885–34898 (2010).



- [133] Luk, K. C. *et al.* Exogenous  $\alpha$ -synuclein fibrils seed the formation of Lewy body-like intracellular inclusions in cultured cells. *Proceedings of the National Academy of Sciences* **106**, 20051–20056 (2009).
- [134] Volpicelli-Daley, L. A. *et al.* Exogenous  $\alpha$ -Synuclein Fibrils Induce Lewy Body Pathology Leading to Synaptic Dysfunction and Neuron Death. *Neuron* **72**, 57–71 (2011).
- [135] De Boni, U. & Crapper, D. R. Paired helical filaments of the Alzheimer type in cultured neurones. *Nature* **271**, 566–568 (1978).
- [136] Frost, B., Jacks, R. L. & Diamond, M. I. Propagation of Tau Misfolding from the Outside to the Inside of a Cell. *The Journal of Biological Chemistry* **284**, 12845–12852 (2009).
- [137] Guo, J. L. & Lee, V. M.-Y. Seeding of Normal Tau by Pathological Tau Conformers Drives Pathogenesis of Alzheimer-like Tangles. *Journal of Biological Chemistry* **286**, 15317–15331 (2011).
- [138] Guo, J. L. & Lee, V. M. Neurofibrillary tangle-like tau pathology induced by synthetic tau fibrils in primary neurons over-expressing mutant tau. *FEBS Letters* **587**, 717–723 (2013).
- [139] Bousset, L. *et al.* Structural and functional characterization of two alpha-synuclein strains. *Nature Communications* **4** (2013).
- [140] Peelaerts, W. *et al.*  $\alpha$ -Synuclein strains cause distinct synucleinopathies after local and systemic administration. *Nature* **522**, 340–344 (2015).
- [141] Sanders, D. W. *et al.* Distinct tau prion strains propagate in cells and mice and define different tauopathies. *Neuron* **82**, 1271–1288 (2014).
- [142] Williams, R. W. & Herrup, K. The control of neuron number. *Annual review of neuroscience* **11**, 423–453 (1988).
- [143] Nimchinsky, E. A., Sabatini, B. L. & Svoboda, K. Structure and Function of Dendritic Spines. *Annual Review of Physiology* **64**, 313–353 (2002).
- [144] Laßek, M., Weingarten, J. & Volkandt, W. The synaptic proteome. *Cell and Tissue Research* **359**, 255–265 (2015).
- [145] Volk, L., Chiu, S.-L., Sharma, K. & Haganir, R. L. Glutamate Synapses in Human Cognitive Disorders. *Annual Review of Neuroscience* **38**, 127–149 (2015).
- [146] Cajal, S. R. Estructura de los centros nerviosos de las aves. *Trim Histol Norm Patol* **1**, 1–10 (1888).
- [147] Harris, K. M. & Kater. Dendritic Spines: Cellular Specializations Imparting Both Stability and Flexibility to Synaptic Function. *Annual Review of Neuroscience* **17**, 341–371 (1994).
- [148] Gray, E. G. Axo-somatic and axo-dendritic synapses of the cerebral cortex: An electron microscope study. *Journal of anatomy* **93**, 420 (1959).
- [149] Rizo, J. & Südhof, T. C. The Membrane Fusion Enigma: SNAREs, Sec1/Munc18 Proteins, and Their Accomplices—Guilty as Charged? *Annual Review of Cell and Developmental Biology* **28**, 279–308 (2012).
- [150] Rochefort, N. L. & Konnerth, A. Dendritic spines: From structure to in vivo function. *EMBO reports* **13**, 699–708 (2012).

## BIBLIOGRAPHY

---

- [151] Fiala, J. C., Spacek, J. & Harris, K. M. Dendritic spine pathology: Cause or consequence of neurological disorders? *Brain research reviews* **39**, 29–54 (2002).
- [152] Fiala, J. C., Feinberg, M., Popov, V. & Harris, K. M. Synaptogenesis via dendritic filopodia in developing hippocampal area CA1. *The Journal of Neuroscience* **18**, 8900–8911 (1998).
- [153] Harris, K. M., Jensen, F. E. & Tsao, B. Three-dimensional structure of dendritic spines and synapses in rat hippocampus (CA1) at postnatal day 15 and adult ages: Implications for the maturation of synaptic physiology and long-term potentiation [published erratum appears in *J Neurosci* 1992 Aug; 12 (8): Following table of contents]. *The Journal of Neuroscience* **12**, 2685–2705 (1992).
- [154] Peters, A. & Kaiserman-Abramof, I. R. The small pyramidal neuron of the rat cerebral cortex. The perikaryon, dendrites and spines. *American Journal of Anatomy* **127**, 321–355 (1970).
- [155] Miller, M. & Peters, A. Maturation of rat visual cortex. II. A combined Golgi-electron microscope study of pyramidal neurons. *The Journal of Comparative Neurology* **203**, 555–573 (1981).
- [156] Parnass, Z., Tashiro, A. & Yuste, R. Analysis of spine morphological plasticity in developing hippocampal pyramidal neurons. *Hippocampus* **10**, 561–568 (2000).
- [157] Dunaevsky, A., Tashiro, A., Majewska, A., Mason, C. & Yuste, R. Developmental regulation of spine motility in the mammalian central nervous system. *Proceedings of the National Academy of Sciences* **96**, 13438–13443 (1999).
- [158] Nusser, Z. *et al.* Cell type and pathway dependence of synaptic AMPA receptor number and variability in the hippocampus. *Neuron* **21**, 545–559 (1998).
- [159] Schikorski, T. & Stevens, C. F. Quantitative ultrastructural analysis of hippocampal excitatory synapses. *The Journal of neuroscience* **17**, 5858–5867 (1997).
- [160] Matsuzaki, M., Honkura, N., Ellis-Davies, G. C. R. & Kasai, H. Structural basis of long-term potentiation in single dendritic spines. *Nature* **429**, 761–766 (2004).
- [161] Okamoto, K.-I., Nagai, T., Miyawaki, A. & Hayashi, Y. Rapid and persistent modulation of actin dynamics regulates postsynaptic reorganization underlying bidirectional plasticity. *Nature Neuroscience* **7**, 1104–1112 (2004).
- [162] Nägerl, U. V., Eberhorn, N., Cambridge, S. B. & Bonhoeffer, T. Bidirectional activity-dependent morphological plasticity in hippocampal neurons. *Neuron* **44**, 759–767 (2004).
- [163] Maletic-Savatic, M. Rapid Dendritic Morphogenesis in CA1 Hippocampal Dendrites Induced by Synaptic Activity. *Science* **283**, 1923–1927 (1999).
- [164] Engert, F. & Bonhoeffer, T. Dendritic spine changes associated with hippocampal long-term synaptic plasticity. *J. Physiol* **260**, C917–925 (1991).
- [165] Nägerl, U. V., Kostinger, G., Anderson, J. C., Martin, K. A. C. & Bonhoeffer, T. Protracted Synaptogenesis after Activity-Dependent Spinogenesis in Hippocampal Neurons. *Journal of Neuroscience* **27**, 8149–8156 (2007).
- [166] Zhou, Q., Homma, K. J. & Poo, M.-m. Shrinkage of Dendritic Spines Associated with Long-Term Depression of Hippocampal Synapses. *Neuron* **44**, 749–757 (2004).

- 
- [167] Fu, M. & Zuo, Y. Experience-dependent structural plasticity in the cortex. *Trends in Neurosciences* **34**, 177–187 (2011).
- [168] Hong, S. *et al.* Complement and microglia mediate early synapse loss in Alzheimer mouse models. *Science* **352**, 712–716 (2016).
- [169] Schulz-Schaeffer, W. Is Cell Death Primary or Secondary in the Pathophysiology of Idiopathic Parkinson’s Disease? *Biomolecules* **5**, 1467–1479 (2015).
- [170] Yuste, R. Fluorescence microscopy today. *Nature methods* **2**, 902–904 (2005).
- [171] Minsky, M. Microscopy apparatus (1961). US-Klassifikation 356/432, 359/389, 348/79, 250/215; Internationale Klassifikation G02B21/00; Unternehmensklassifikation G02B21/0024, G02B21/002; Europäische Klassifikation G02B21/00M4A, G02B21/00M4.
- [172] Conchello, J.-A. & Lichtman, J. W. Optical sectioning microscopy. *Nature Methods* **2**, 920–931 (2005).
- [173] Chalfie, M., Tu, Y., Euskirchen, G., Ward, W. W. & Prasher, D. C. Green fluorescent protein as a marker for gene expression. *Science* **263**, 802–805 (1994).
- [174] Tsien, R. Y. The green fluorescent protein. *Annual review of biochemistry* **67**, 509–544 (1998).
- [175] Denk, W., Strickler, J. H. & Webb, W. W. Two-photon laser scanning fluorescence microscopy. *Science (New York, N.Y.)* **248**, 73–76 (1990).
- [176] Göppert-Mayer, M. Über elementarakte mit zwei quantensprüngen. *Annalen der Physik* **401**, 273–294 (1931).
- [177] Göppert-Mayer, M. Elementary processes with two quantum transitions. *Annalen der Physik* **18**, 466–479 (2009).
- [178] Denk, W. & Svoboda, K. Photon upmanship: Why multiphoton imaging is more than a gimmick. *Neuron* **18**, 351–357 (1997).
- [179] Kaiser, W. & Garrett, C. G. B. Two-Photon Excitation in CaF<sub>2</sub>:Eu<sup>2+</sup>. *Physical Review Letters* **7**, 229–231 (1961).
- [180] Helmchen, F. & Denk, W. Deep tissue two-photon microscopy. *Nature Methods* **2**, 932–940 (2005).
- [181] Curley, P. F., Ferguson, A. I., White, J. G. & Amos, W. B. Application of a femtosecond self-sustaining mode-locked Ti: Sapphire laser to the field of laser scanning confocal microscopy. *Optical and quantum electronics* **24**, 851–859 (1992).
- [182] Svoboda, K. & Yasuda, R. Principles of Two-Photon Excitation Microscopy and Its Applications to Neuroscience. *Neuron* **50**, 823–839 (2006).
- [183] Patterson, G. H., Knobel, S. M., Arkhammar, P., Thastrup, O. & Piston, D. W. Separation of the glucose-stimulated cytoplasmic and mitochondrial NAD(P)H responses in pancreatic islet beta cells. *Proceedings of the National Academy of Sciences of the United States of America* **97**, 5203–5207 (2000).
- [184] Huang, S., Heikal, A. A. & Webb, W. W. Two-photon fluorescence spectroscopy and microscopy of NAD(P)H and flavoprotein. *Biophysical Journal* **82**, 2811–2825 (2002).

## BIBLIOGRAPHY

---

- [185] Maiti, S., Shear, J. B., Williams, R. M., Zipfel, W. R. & Webb, W. W. Measuring serotonin distribution in live cells with three-photon excitation. *Science (New York, N.Y.)* **275**, 530–532 (1997).
- [186] Fine, S. & Hansen, W. P. Optical second harmonic generation in biological systems. *Applied Optics* **10**, 2350–2353 (1971).
- [187] Freund, I., Deutsch, M. & Sprecher, A. Connective tissue polarity. Optical second-harmonic microscopy, crossed-beam summation, and small-angle scattering in rat-tail tendon. *Biophysical Journal* **50**, 693–712 (1986).
- [188] Zipfel, W. R. *et al.* Live tissue intrinsic emission microscopy using multiphoton-excited native fluorescence and second harmonic generation. *Proceedings of the National Academy of Sciences* **100**, 7075–7080 (2003).
- [189] Kleinfeld, D., Mitra, P. P., Helmchen, F. & Denk, W. Fluctuations and stimulus-induced changes in blood flow observed in individual capillaries in layers 2 through 4 of rat neocortex. *Proceedings of the National Academy of Sciences of the United States of America* **95**, 15741–15746 (1998).
- [190] de Calignon, A., Spire-Jones, T. L., Pitstick, R., Carlson, G. A. & Hyman, B. T. Tangle-Bearing Neurons Survive Despite Disruption of Membrane Integrity in a Mouse Model of Tauopathy. *Journal of Neuropathology & Experimental Neurology* **68**, 757–761 (2009).
- [191] Velasco, A. *et al.* Detection of filamentous tau inclusions by the fluorescent Congo red derivative FSB [(trans,trans)-1-fluoro-2,5-bis(3-hydroxycarbonyl-4-hydroxy)styrylbenzene]. *FEBS Letters* **582**, 901–906 (2008).
- [192] Shimomura, O., Johnson, F. H. & Saiga, Y. Extraction, purification and properties of aequorin, a bioluminescent protein from the luminous hydromedusan, *Aequorea*. *Journal of Cellular and Comparative Physiology* **59**, 223–239 (1962).
- [193] Inouye, S. & Tsuji, F. I. *Aequorea* green fluorescent protein. Expression of the gene and fluorescence characteristics of the recombinant protein. *FEBS letters* **341**, 277–280 (1994).
- [194] Shaner, N. C., Steinbach, P. A. & Tsien, R. Y. A guide to choosing fluorescent proteins. *Nature Methods* **2**, 905–909 (2005).
- [195] Feng, G. *et al.* Imaging neuronal subsets in transgenic mice expressing multiple spectral variants of GFP. *Neuron* **28**, 41–51 (2000).
- [196] Grienberger, C. & Konnerth, A. Imaging Calcium in Neurons. *Neuron* **73**, 862–885 (2012).
- [197] Grynkiewicz, G., Poenie, M. & Tsien, R. Y. A new generation of Ca<sup>2+</sup> indicators with greatly improved fluorescence properties. *The Journal of Biological Chemistry* **260**, 3440–3450 (1985).
- [198] Tsien, R. Y. New calcium indicators and buffers with high selectivity against magnesium and protons: Design, synthesis, and properties of prototype structures. *Biochemistry* **19**, 2396–2404 (1980).
- [199] Nagai, T., Sawano, A., Park, E. S. & Miyawaki, A. Circularly permuted green fluorescent proteins engineered to sense Ca<sup>2+</sup>. *Proceedings of the National Academy of Sciences of the United States of America* **98**, 3197–3202 (2001).

- [200] Nakai, J., Ohkura, M. & Imoto, K. A high signal-to-noise Ca(2+) probe composed of a single green fluorescent protein. *Nature Biotechnology* **19**, 137–141 (2001).
- [201] Holtmaat, A. *et al.* Long-term, high-resolution imaging in the mouse neocortex through a chronic cranial window. *Nature Protocols* **4**, 1128–1144 (2009).
- [202] Fuhrmann, M., Mitteregger, G., Kretschmar, H. & Herms, J. Dendritic Pathology in Prion Disease Starts at the Synaptic Spine. *Journal of Neuroscience* **27**, 6224–6233 (2007).
- [203] Christie, R. H. *et al.* Growth Arrest of Individual Senile Plaques in a Model of Alzheimer’s Disease Observed by In Vivo Multiphoton Microscopy. *Journal of Neuroscience* **21**, 858–864 (2001).
- [204] Grutzendler, J., Narayanan, K. & Gan, W.-B. Long-term dendritic spine stability in the adult cortex. *Nature* **420**, 810–812 (2002).
- [205] Yang, G., Pan, F., Parkhurst, C. N., Grutzendler, J. & Gan, W.-B. Thinned-skull cranial window technique for long-term imaging of the cortex in live mice. *Nature Protocols* **5**, 201–208 (2010).
- [206] Sperling, R. A., Karlawish, J. & Johnson, K. A. Preclinical Alzheimer disease—the challenges ahead. *Nature Reviews Neurology* **9**, 54–58 (2012).
- [207] Götz, J. & Ittner, L. M. Animal models of Alzheimer’s disease and frontotemporal dementia. *Nature Reviews Neuroscience* **9**, 532–544 (2008).
- [208] Landel, C. P., Chen, S. Z. & Evans, G. A. Reverse genetics using transgenic mice. *Annual Review of Physiology* **52**, 841–851 (1990).
- [209] Capecchi, M. R. The new mouse genetics: Altering the genome by gene targeting. *Trends in genetics: TIG* **5**, 70–76 (1989).
- [210] Lee, Y., Dawson, V. L. & Dawson, T. M. Animal Models of Parkinson’s Disease: Vertebrate Genetics. *Cold Spring Harbor Perspectives in Medicine* **2**, a009324–a009324 (2012).
- [211] Visanji, N. P. *et al.*  $\alpha$ -Synuclein-Based Animal Models of Parkinson’s Disease: Challenges and Opportunities in a New Era. *Trends in Neurosciences* (2016).
- [212] Masliah, E. Dopaminergic Loss and Inclusion Body Formation in  $\alpha$ -Synuclein Mice: Implications for Neurodegenerative Disorders. *Science* **287**, 1265–1269 (2000).
- [213] Sperfeld, A. D. *et al.* FTDP-17: An early-onset phenotype with parkinsonism and epileptic seizures caused by a novel mutation. *Annals of Neurology* **46**, 708–715 (1999).
- [214] Allen, B. *et al.* Abundant tau filaments and nonapoptotic neurodegeneration in transgenic mice expressing human P301S tau protein. *The journal of neuroscience* **22**, 9340–9351 (2002).
- [215] Watts, J. C. *et al.* Transmission of multiple system atrophy prions to transgenic mice. *Proceedings of the National Academy of Sciences of the United States of America* **110**, 19555–19560 (2013).
- [216] Mougenot, A.-L. *et al.* Prion-like acceleration of  $\alpha$ -synucleinopathy in a transgenic mouse model. *Neurobiology of Aging* **33**, 2225–2228 (2012).

## BIBLIOGRAPHY

---

- [217] Luk, K. C. *et al.* Intracerebral inoculation of pathological  $\alpha$ -synuclein initiates a rapidly progressive neurodegenerative  $\alpha$ -synucleinopathy in mice. *Journal of Experimental Medicine* **209**, 975–986 (2012).
- [218] Sacino, A. N. *et al.* Amyloidogenic  $\alpha$ -synuclein seeds do not invariably induce rapid, widespread pathology in mice. *Acta Neuropathologica* **127**, 645–665 (2014).
- [219] Bétemps, D. *et al.* Alpha-synuclein spreading in M83 mice brain revealed by detection of pathological  $\alpha$ -synuclein by enhanced ELISA. *Acta Neuropathologica Communications* **2**, 29 (2014).
- [220] Sacino, A. N. *et al.* Intramuscular injection of  $\alpha$ -synuclein induces CNS  $\alpha$ -synuclein pathology and a rapid-onset motor phenotype in transgenic mice. *Proceedings of the National Academy of Sciences of the United States of America* **111**, 10732–10737 (2014).
- [221] Recasens, A. *et al.* Lewy body extracts from Parkinson disease brains trigger  $\alpha$ -synuclein pathology and neurodegeneration in mice and monkeys: LB-Induced Pathology. *Annals of Neurology* **75**, 351–362 (2014).
- [222] Masuda-Suzukake, M. *et al.* Prion-like spreading of pathological  $\alpha$ -synuclein in brain. *Brain* **136**, 1128–1138 (2013).
- [223] Luk, K. C. *et al.* Pathological  $\alpha$ -Synuclein Transmission Initiates Parkinson-like Neurodegeneration in Nontransgenic Mice. *Science* **338**, 949–953 (2012).
- [224] Clavaguera, F. *et al.* Transmission and spreading of tauopathy in transgenic mouse brain. *Nature Cell Biology* **11**, 909–913 (2009).
- [225] Clavaguera, F. *et al.* Brain homogenates from human tauopathies induce tau inclusions in mouse brain. *Proceedings of the National Academy of Sciences* **110**, 9535–9540 (2013).
- [226] Guo, J. L. *et al.* Unique pathological tau conformers from Alzheimer’s brains transmit tau pathology in nontransgenic mice. *The Journal of Experimental Medicine* jem.20160833 (2016).
- [227] Iba, M. *et al.* Synthetic Tau Fibrils Mediate Transmission of Neurofibrillary Tangles in a Transgenic Mouse Model of Alzheimer’s-Like Tauopathy. *Journal of Neuroscience* **33**, 1024–1037 (2013).
- [228] Stancu, I.-C. *et al.* Templated misfolding of Tau by prion-like seeding along neuronal connections impairs neuronal network function and associated behavioral outcomes in Tau transgenic mice. *Acta Neuropathologica* (2015).
- [229] Peeraer, E. *et al.* Intracerebral injection of preformed synthetic tau fibrils initiates widespread tauopathy and neuronal loss in the brains of tau transgenic mice. *Neurobiology of disease* **73**, 83–95 (2015).
- [230] Rocher, A. B. *et al.* Structural and functional changes in tau mutant mice neurons are not linked to the presence of NFTs. *Experimental Neurology* **223**, 385–393 (2010).
- [231] de Calignon, A. *et al.* Caspase activation precedes and leads to tangles. *Nature* **464**, 1201–1204 (2010).
- [232] Kuchibhotla, K. V. *et al.* Neurofibrillary tangle-bearing neurons are functionally integrated in cortical circuits in vivo. *Proceedings of the National Academy of Sciences of the United States of America* **111**, 510–514 (2014).

- [233] Guo, Z. V. *et al.* Procedures for behavioral experiments in head-fixed mice. *PloS One* **9**, e88678 (2014).
- [234] Schön, C. *et al.* Long-Term In Vivo Imaging of Fibrillar Tau in the Retina of P301S Transgenic Mice. *PLoS ONE* **7**, e53547 (2012).
- [235] Guizar-Sicairos, M., Thurman, S. T. & Fienup, J. R. Efficient subpixel image registration algorithms. *Optics letters* **33**, 156–158 (2008).
- [236] Rose, T., Jaepel, J., Hübener, M. & Bonhoeffer, T. Cell-specific restoration of stimulus preference after monocular deprivation in the visual cortex. *Science (New York, N.Y.)* **352**, 1319–1322 (2016).
- [237] Kerr, J. N. D. & Denk, W. Imaging in vivo: Watching the brain in action. *Nature Reviews. Neuroscience* **9**, 195–205 (2008).
- [238] Menkes-Caspi, N. *et al.* Pathological Tau Disrupts Ongoing Network Activity. *Neuron* **85**, 959–966 (2015).
- [239] Kopeikina, K. J., Hyman, B. T. & Spires-Jones, T. L. Soluble forms of tau are toxic in Alzheimer’s disease. *Translational Neuroscience* **3**, 223–233 (2012).
- [240] Institute, A. ISH Data :: Allen Brain Atlas: Mouse Brain. <http://mouse.brain-map.org/>.
- [241] Mizrahi, A., Crowley, J. C., Shtoyerman, E. & Katz, L. C. High-Resolution In Vivo Imaging of Hippocampal Dendrites and Spines. *Journal of Neuroscience* **24**, 3147–3151 (2004).
- [242] Gu, L. *et al.* Long-Term In Vivo Imaging of Dendritic Spines in the Hippocampus Reveals Structural Plasticity. *Journal of Neuroscience* **34**, 13948–13953 (2014).
- [243] Liu, R.-J. & Aghajanian, G. K. Stress blunts serotonin- and hypocretin-evoked EPSCs in prefrontal cortex: Role of corticosterone-mediated apical dendritic atrophy. *Proceedings of the National Academy of Sciences of the United States of America* **105**, 359–364 (2008).
- [244] Duman, R. S. & Li, N. A neurotrophic hypothesis of depression: Role of synaptogenesis in the actions of NMDA receptor antagonists. *Philosophical Transactions of the Royal Society of London. Series B, Biological Sciences* **367**, 2475–2484 (2012).
- [245] Vutskits, L., Gascon, E., Tassonyi, E. & Kiss, J. Z. Effect of ketamine on dendritic arbor development and survival of immature GABAergic neurons in vitro. *Toxicological Sciences: An Official Journal of the Society of Toxicology* **91**, 540–549 (2006).
- [246] Dong, Y., Wu, X., Xu, Z., Zhang, Y. & Xie, Z. Anesthetic Isoflurane Increases Phosphorylated Tau Levels Mediated by Caspase Activation and A $\beta$  Generation. *PLOS ONE* **7**, e39386 (2012).
- [247] Perucho, J. *et al.* Anesthesia with isoflurane increases amyloid pathology in mice models of Alzheimer’s disease. *Journal of Alzheimer’s disease: JAD* **19**, 1245–1257 (2010).
- [248] Yang, G., Chang, P. C., Bekker, A., Blanck, T. J. J. & Gan, W.-B. Transient effects of anesthetics on dendritic spines and filopodia in the living mouse cortex. *Anesthesiology* **115**, 718–726 (2011).

## BIBLIOGRAPHY

---

- [249] Arendt, T. *et al.* Reversible paired helical filament-like phosphorylation of tau is an adaptive process associated with neuronal plasticity in hibernating animals. *The Journal of Neuroscience: The Official Journal of the Society for Neuroscience* **23**, 6972–6981 (2003).
- [250] Planel, E. *et al.* Anesthesia leads to tau hyperphosphorylation through inhibition of phosphatase activity by hypothermia. *The Journal of Neuroscience: The Official Journal of the Society for Neuroscience* **27**, 3090–3097 (2007).
- [251] Conway, K. A., Harper, J. D. & Lansbury, P. T. Fibrils Formed in Vitro from  $\alpha$ -Synuclein and Two Mutant Forms Linked to Parkinson's Disease are Typical Amyloid  $\dagger$ . *Biochemistry* **39**, 2552–2563 (2000).
- [252] Lewis, J. & Dickson, D. W. Propagation of tau pathology: Hypotheses, discoveries, and yet unresolved questions from experimental and human brain studies. *Acta Neuropathologica* **131**, 27–48 (2016).
- [253] Volpicelli-Daley, L. A., Luk, K. C. & Lee, V. M.-Y. Addition of exogenous  $\alpha$ -synuclein preformed fibrils to primary neuronal cultures to seed recruitment of endogenous  $\alpha$ -synuclein to Lewy body and Lewy neurite-like aggregates. *Nature Protocols* **9**, 2135–2146 (2014).
- [254] Tsigelny, I. F. *et al.* Role of  $\alpha$ -synuclein penetration into the membrane in the mechanisms of oligomer pore formation. *The FEBS journal* **279**, 1000–1013 (2012).
- [255] Lee, H.-J. *et al.* Assembly-dependent endocytosis and clearance of extracellular alpha-synuclein. *The International Journal of Biochemistry & Cell Biology* **40**, 1835–1849 (2008).
- [256] Emmanouilidou, E. *et al.* Cell-Produced  $\alpha$ -Synuclein Is Secreted in a Calcium-Dependent Manner by Exosomes and Impacts Neuronal Survival. *The Journal of Neuroscience* **30**, 6838–6851 (2010).
- [257] Danzer, K. M. *et al.* Heat-shock protein 70 modulates toxic extracellular  $\alpha$ -synuclein oligomers and rescues trans-synaptic toxicity. *The FASEB Journal* **25**, 326–336 (2011).
- [258] Freundt, E. C. *et al.* Neuron-to-neuron transmission of  $\alpha$ -synuclein fibrils through axonal transport. *Annals of neurology* **72**, 517–524 (2012).
- [259] Shepherd, G. M. G. Corticostriatal connectivity and its role in disease. *Nature Reviews Neuroscience* **14**, 278–291 (2013).
- [260] Osterberg, V. R. *et al.* Progressive Aggregation of Alpha-Synuclein and Selective Degeneration of Lewy Inclusion-Bearing Neurons in a Mouse Model of Parkinsonism. *Cell Reports* **10**, 1252–1260 (2015).
- [261] Pan, W. X., Mao, T. & Dudman, J. T. Inputs to the Dorsal Striatum of the Mouse Reflect the Parallel Circuit Architecture of the Forebrain. *Frontiers in Neuroanatomy* **4** (2010).
- [262] Fujiwara, H. *et al.*  $\alpha$ -Synuclein is phosphorylated in synucleinopathy lesions. *Nature Cell Biology* **4**, 160–164 (2002).
- [263] Hasegawa, M. *et al.* Phosphorylated  $\alpha$ -Synuclein Is Ubiquitinated in  $\alpha$ -Synucleinopathy Lesions. *Journal of Biological Chemistry* **277**, 49071–49076 (2002).



- [264] Wu, J. W. *et al.* Small Misfolded Tau Species Are Internalized via Bulk Endocytosis and Anterogradely and Retrogradely Transported in Neurons. *The Journal of Biological Chemistry* **288**, 1856–1870 (2013).
- [265] Calafate, S. *et al.* Synaptic Contacts Enhance Cell-to-Cell Tau Pathology Propagation. *Cell Reports* **11**, 1176–1183 (2015).
- [266] Kfoury, N., Holmes, B. B., Jiang, H., Holtzman, D. M. & Diamond, M. I. Trans-cellular Propagation of Tau Aggregation by Fibrillar Species. *The Journal of Biological Chemistry* **287**, 19440–19451 (2012).
- [267] Saman, S. *et al.* Exosome-associated Tau Is Secreted in Tauopathy Models and Is Selectively Phosphorylated in Cerebrospinal Fluid in Early Alzheimer Disease. *The Journal of Biological Chemistry* **287**, 3842–3849 (2012).
- [268] Wang, Y. *et al.* The release and trans-synaptic transmission of Tau via exosomes. *Molecular Neurodegeneration* **12** (2017).
- [269] Goedert, M., Jakes, R. & Vanmechelen, E. Monoclonal antibody AT8 recognises tau protein phosphorylated at both serine 202 and threonine 205. *Neuroscience Letters* **189**, 167–169 (1995).
- [270] Sampson, T. R. *et al.* Gut Microbiota Regulate Motor Deficits and Neuroinflammation in a Model of Parkinson’s Disease. *Cell* **167**, 1469–1480.e12 (2016).
- [271] Asai, H. *et al.* Depletion of microglia and inhibition of exosome synthesis halt tau propagation. *Nature Neuroscience* **18**, 1584–1593 (2015).
- [272] Giasson, B. I., Murray, I. V. J., Trojanowski, J. Q. & Lee, V. M.-Y. A Hydrophobic Stretch of 12 Amino Acid Residues in the Middle of  $\alpha$ -Synuclein Is Essential for Filament Assembly. *Journal of Biological Chemistry* **276**, 2380–2386 (2001).
- [273] Giasson, B. I. Initiation and Synergistic Fibrillization of Tau and Alpha-Synuclein. *Science* **300**, 636–640 (2003).
- [274] Badiola, N. *et al.* Tau Enhances  $\alpha$ -Synuclein Aggregation and Toxicity in Cellular Models of Synucleinopathy. *PLoS ONE* **6**, e26609 (2011).
- [275] Trachtenberg, J. T. *et al.* Long-term in vivo imaging of experience-dependent synaptic plasticity in adult cortex. *Nature* **420**, 788–794 (2002).
- [276] Testa, I. *et al.* Nanoscopy of Living Brain Slices with Low Light Levels. *Neuron* **75**, 992–1000 (2012).
- [277] Villalba, R. M., Lee, H. & Smith, Y. Dopaminergic denervation and spine loss in the striatum of MPTP-treated monkeys. *Experimental Neurology* **215**, 220–227 (2009).
- [278] Ingham, C. A., Hood, S. H. & Arbuthnott, G. W. Spine density on neostriatal neurones changes with 6-hydroxydopamine lesions and with age. *Brain Research* **503**, 334–338 (1989).
- [279] Day, M. *et al.* Selective elimination of glutamatergic synapses on striatopallidal neurons in Parkinson disease models. *Nature Neuroscience* **9**, 251–259 (2006).
- [280] Suárez, L. M. *et al.* L-DOPA Treatment Selectively Restores Spine Density in Dopamine Receptor D2-Expressing Projection Neurons in Dyskinetic Mice. *Biological Psychiatry* **75**, 711–722 (2014).

## BIBLIOGRAPHY

---

- [281] Finkelstein, D. I. *et al.* Clioquinol Improves Cognitive, Motor Function, and Microanatomy of the Alpha-Synuclein hA53T Transgenic Mice. *ACS Chemical Neuroscience* **7**, 119–129 (2016).
- [282] Oaks, A. W., Frankfurt, M., Finkelstein, D. I. & Sidhu, A. Age-Dependent Effects of A53T Alpha-Synuclein on Behavior and Dopaminergic Function. *PLoS ONE* **8**, e60378 (2013).
- [283] Winner, B. *et al.* Role of  $\alpha$ -Synuclein in Adult Neurogenesis and Neuronal Maturation in the Dentate Gyrus. *Journal of Neuroscience* **32**, 16906–16916 (2012).
- [284] Neuner, J. *et al.* Pathological  $\alpha$ -synuclein impairs adult-born granule cell development and functional integration in the olfactory bulb. *Nature Communications* **5**, 3915 (2014).
- [285] Zaja-Milatovic, S. *et al.* Selective dendritic degeneration of medium spiny neurons in dementia with Lewy bodies. *Neurology* **66**, 1591–1593 (2006).
- [286] Zaja-Milatovic, S. *et al.* Dendritic degeneration in neostriatal medium spiny neurons in Parkinson disease. *Neurology* **64**, 545–547 (2005).
- [287] Kopeikina, K. J. *et al.* Synaptic alterations in the rTg4510 mouse model of tauopathy. *The Journal of comparative neurology* **521**, 1334–1353 (2013).
- [288] Yoshiyama, Y. *et al.* Synapse Loss and Microglial Activation Precede Tangles in a P301S Tauopathy Mouse Model. *Neuron* **53**, 337–351 (2007).
- [289] Dickstein, D. L., Brautigam, H., Stockton, S. D., Schmeidler, J. & Hof, P. R. Changes in dendritic complexity and spine morphology in transgenic mice expressing human wild-type tau. *Brain Structure and Function* **214**, 161–179 (2010).
- [290] Kremer, A. *et al.* Early Improved and Late Defective Cognition Is Reflected by Dendritic Spines in Tau.P301L Mice. *Journal of Neuroscience* **31**, 18036–18047 (2011).
- [291] Arellano, J. I., Espinosa, A., Fairén, A., Yuste, R. & DeFelipe, J. Non-synaptic dendritic spines in neocortex. *Neuroscience* **145**, 464–469 (2007).
- [292] Holtmaat, A. J. *et al.* Transient and Persistent Dendritic Spines in the Neocortex In Vivo. *Neuron* **45**, 279–291 (2005).
- [293] Oueslati, A., Ximerakis, M. & Vekrellis, K. Protein Transmission, Seeding and Degradation: Key Steps for  $\alpha$ -Synuclein Prion-Like Propagation. *Experimental Neurobiology* **23**, 324 (2014).
- [294] Bittner, T. *et al.* Multiple Events Lead to Dendritic Spine Loss in Triple Transgenic Alzheimer’s Disease Mice. *PLoS ONE* **5**, e15477 (2010).
- [295] Rockenstein, E. *et al.* Lysosomal pathology associated with  $\alpha$ -synuclein accumulation in transgenic models using an eGFP fusion protein. *Journal of Neuroscience Research* **80**, 247–259 (2005).
- [296] Nemani, V. M. *et al.* Increased Expression of  $\alpha$ -Synuclein Reduces Neurotransmitter Release by Inhibiting Synaptic Vesicle Reclustering after Endocytosis. *Neuron* **65**, 66–79 (2010).
- [297] Burre, J., Sharma, M. & Sudhof, T. C. Definition of a Molecular Pathway Mediating  $\alpha$ -Synuclein Neurotoxicity. *Journal of Neuroscience* **35**, 5221–5232 (2015).

- [298] Garcia-Reitböck, P. *et al.* SNARE protein redistribution and synaptic failure in a transgenic mouse model of Parkinson's disease. *Brain* **133**, 2032–2044 (2010).
- [299] Sousa, V. L. *et al.*  $\alpha$ -Synuclein and its A30P mutant affect actin cytoskeletal structure and dynamics. *Molecular biology of the cell* **20**, 3725–3739 (2009).
- [300] Tsaneva-Atanasova, K., Burgo, A., Galli, T. & Holcman, D. Quantifying Neurite Growth Mediated by Interactions among Secretory Vesicles, Microtubules, and Actin Networks. *Biophysical Journal* **96**, 840–857 (2009).
- [301] Diogenes, M. J. *et al.* Extracellular Alpha-Synuclein Oligomers Modulate Synaptic Transmission and Impair LTP Via NMDA-Receptor Activation. *Journal of Neuroscience* **32**, 11750–11762 (2012).
- [302] Yuste, R. & Bonhoeffer, T. Morphological changes in dendritic spines associated with long-term synaptic plasticity. *Annual review of neuroscience* **24**, 1071–1089 (2001).
- [303] Harris, J. A. *et al.* Human P301L-Mutant Tau Expression in Mouse Entorhinal-Hippocampal Network Causes Tau Aggregation and Presynaptic Pathology but No Cognitive Deficits. *PLoS ONE* **7** (2012).
- [304] Merino-Serrais, P. *et al.* The influence of phospho-tau on dendritic spines of cortical pyramidal neurons in patients with Alzheimer's disease. *Brain* **136**, 1913–1928 (2013).
- [305] Blazquez-Llorca, L., Garcia-Marin, V., Merino-Serrais, P., Ávila, J. & DeFelipe, J. Abnormal Tau Phosphorylation in the Thorny Excrescences of CA3 Hippocampal Neurons in Patients with Alzheimer's Disease. *Journal of Alzheimer's Disease* **26**, 683–698 (2011).
- [306] Sorra, K. E. & Harris, K. M. Overview on the structure, composition, function, development, and plasticity of hippocampal dendritic spines. *Hippocampus* **10**, 501–511 (2000).
- [307] Kahle, P. J.  $\alpha$ -Synucleinopathy models and human neuropathology: Similarities and differences. *Acta Neuropathologica* **115**, 87–95 (2007).
- [308] Spittaels, K. *et al.* Prominent axonopathy in the brain and spinal cord of transgenic mice overexpressing four-repeat human tau protein. *The American Journal of Pathology* **155**, 2153–2165 (1999).
- [309] Higuchi, M., Lee, V. M. Y. & Trojanowski, J. Q. Tau and axonopathy in neurodegenerative disorders. *Neuromolecular Medicine* **2**, 131–150 (2002).
- [310] Leroy, K. *et al.* Early Axonopathy Preceding Neurofibrillary Tangles in Mutant Tau Transgenic Mice. *The American Journal of Pathology* **171**, 976–992 (2007).
- [311] Gasparini, L. *et al.* Tau inclusions in retinal ganglion cells of human P301S tau transgenic mice: Effects on axonal viability. *Neurobiology of Aging* **32**, 419–433 (2011).
- [312] Hampton, D. W. *et al.* Cell-mediated neuroprotection in a mouse model of human tauopathy. *The Journal of Neuroscience: The Official Journal of the Society for Neuroscience* **30**, 9973–9983 (2010).
- [313] Tang, Y. & Le, W. Differential Roles of M1 and M2 Microglia in Neurodegenerative Diseases. *Molecular Neurobiology* **53**, 1181–1194 (2016).
- [314] Hanisch, U.-K. & Kettenmann, H. Microglia: Active sensor and versatile effector cells in the normal and pathologic brain. *Nature Neuroscience* **10**, 1387–1394 (2007).

## BIBLIOGRAPHY

---

- [315] Miyamoto, A. *et al.* Microglia contact induces synapse formation in developing somatosensory cortex. *Nature Communications* **7**, 12540 (2016).
- [316] Cowan, C. M. & Mudher, A. Are Tau Aggregates Toxic or Protective in Tauopathies? *Frontiers in Neurology* **4** (2013).
- [317] Lashuel, H. A., Overk, C. R., Oueslati, A. & Masliah, E. The many faces of  $\alpha$ -synuclein: From structure and toxicity to therapeutic target. *Nature Reviews Neuroscience* **14**, 38–48 (2012).
- [318] Fredenburg, R. A. *et al.* The Impact of the E46K Mutation on the Properties of  $\alpha$ -Synuclein in Its Monomeric and Oligomeric States <sup>†</sup>. *Biochemistry* **46**, 7107–7118 (2007).
- [319] Karpinar, D. P. *et al.* Pre-fibrillar  $\alpha$ -synuclein variants with impaired  $\beta$ -structure increase neurotoxicity in Parkinson's disease models. *The EMBO journal* **28**, 3256–3268 (2009).
- [320] Winner, B. *et al.* In vivo demonstration that  $\alpha$ -synuclein oligomers are toxic. *Proceedings of the National Academy of Sciences* **108**, 4194–4199 (2011).
- [321] Danzer, K. M. *et al.* Different species of alpha-synuclein oligomers induce calcium influx and seeding. *The Journal of Neuroscience: The Official Journal of the Society for Neuroscience* **27**, 9220–9232 (2007).
- [322] Alim, M. A. *et al.* Demonstration of a role for alpha-synuclein as a functional microtubule-associated protein. *Journal of Alzheimer's disease: JAD* **6**, 435–442; discussion 443–449 (2004).
- [323] Hsu, L. J. *et al.*  $\alpha$ -Synuclein Promotes Mitochondrial Deficit and Oxidative Stress. *The American Journal of Pathology* **157**, 401–410 (2000).
- [324] Hashimoto, M. *et al.* The Role of alpha-synuclein assembly and metabolism in the pathogenesis of Lewy body disease. *Journal of molecular neuroscience: MN* **24**, 343–352 (2004).
- [325] de Calignon, A. *et al.* Propagation of Tau Pathology in a Model of Early Alzheimer's Disease. *Neuron* **73**, 685–697 (2012).
- [326] SantaCruz, K. *et al.* Tau Suppression in a Neurodegenerative Mouse Model Improves Memory Function. *Science (New York, N.Y.)* **309**, 476–481 (2005).
- [327] Shahani, N., Subramaniam, S., Wolf, T., Tackenberg, C. & Brandt, R. Tau aggregation and progressive neuronal degeneration in the absence of changes in spine density and morphology after targeted expression of Alzheimer's disease-relevant tau constructs in organotypic hippocampal slices. *The Journal of Neuroscience: The Official Journal of the Society for Neuroscience* **26**, 6103–6114 (2006).
- [328] Kopeikina, K. J. *et al.* Tau accumulation causes mitochondrial distribution deficits in neurons in a mouse model of tauopathy and in human Alzheimer's disease brain. *The American Journal of Pathology* **179**, 2071–2082 (2011).
- [329] Patterson, K. R. *et al.* Characterization of Prefibrillar Tau Oligomers in Vitro and in Alzheimer Disease. *The Journal of Biological Chemistry* **286**, 23063–23076 (2011).
- [330] Lasagna-Reeves, C. A. *et al.* Alzheimer brain-derived tau oligomers propagate pathology from endogenous tau. *Scientific Reports* **2** (2012).

# Acknowledgements

I would like to thank Prof. Jochen Herms, for his lasting support and for affording me many possibilities to work on this fascinating project and to develop scientifically. I would particularly like to acknowledge the possibilities to present my work at international conferences and the work with international collaborators.

I furthermore want to cordially thank Prof. Barbara Conradt, who readily agreed to represent this dissertation at the faculty for biology.

Thank you also to all second readers of this thesis for your time and interest in this work.

My appreciation goes to the people who have contributed to my success by experimenting and publishing with me and by giving their consent to include those studies into this dissertation. I particularly would like to thank the first authors Nadine Hoffmann and Petar Marinković.

Several collaborators have provided me with material or the possibility to share thoughts and learn. I want to highlight Prof. Virginia Lee, Dr. Kelvin Luk, Prof. Armin Giese, Prof. Ilse Dewachter, Ilie-Cosmin Stancu, Dr. Etienne Herzog and Dr. Maria-Florencia Angelo, to whom I am very thankful. I furthermore want to acknowledge the excellent technical support provided by Pati, Ela, Eric, Kathi, Sarah and Nadine.

To all colleagues, who have created a stimulating and enjoyable atmosphere in the lab and for their help whenever needed. Thank you especially to Sophie, Finn, Severin, Tanja, Manu, Carmelo, Eva, Steffen and Hanna. To Julia, Martin, Daniel and Viktoria, thank you for delightful break times. To Felix, I am deeply grateful for help, sharing and for being a wonderful friend. I would also like to thank all people who proof-read this dissertation, including my friend Arden Moscati.

Last but not least, to my parents, to Petra and to Stefan, who have been my support always, I thank you with all my heart.